SOIL WATER FLOW AND IRRIGATED SOIL WATER BALANCE IN RESPONSE TO POWDER RIVER BASIN COALBED METHANE PRODUCT WATER

by

Margaret MacNeill Buchanan

A thesis submitted in partial fulfillment of the requirements for the degree

of

Master of Science

in

Land Resources and Environmental Sciences

MONTANA STATE UNIVERSITY Bozeman, Montana

April 2005

© COPYRIGHT

by

Margaret MacNeill Buchanan

2005

All Rights Reserved

APPROVAL

of a thesis submitted by

Margaret MacNeill Buchanan

The thesis has been read by each member of the thesis committee and has been found to be satisfactory regarding content, English usage, format, citations, bibliographic style, and consistency, and is ready for submission to the College of Graduate Studies.

Dr. Jon M. Wraith

April 15, 2005

Approved for the Department of Land Resources and Environmental Sciences

Dr. Jon M. Wraith

April 15, 2005

Approved for the College of Graduate Studies

Dr. Bruce R. McLeod

April 18, 2005

iii

STATEMENT OF PERMISSION TO USE

In presenting this thesis in partial fulfillment of the requirements for a master's

degree at Montana State University, I agree that the Library shall make it available to

borrowers under rules of the Library.

If I have indicated my intention to copyright this thesis by including a copyright notice

page, copying is allowable only for scholarly purposes, consistent with "fair use" as

prescribed in the U.S. Copyright Law. Requests for permission for extended quotation from

or reproduction of this thesis in whole or in parts may be granted only by the copyright

holder.

Margaret M. Buchanan

April 15, 2005

ACKNOWLEDGEMENTS

I would like to thank my graduate adviser, Dr. Jon Wraith, and the members of my graduate committee, Dr. James Bauder and Dr. David Brown, for their support and assistance. My thanks also goes to Dr. Tom Keck for field soils expertise, Dr. Cathy Zabinski for statistical guidance, and Dr. Paolo Castiglione for modeling help. I am indebted to Mike Elmose, the Swenson family, and Bill Ott for allowing me access to their land and soils, and to the LRES administrative staff for lots of help along the way. I would also like to express gratitude to the students and staff in the Wraith and Bauder labs for their help with many and varied aspects of the research, and for their good humor and friendship. Finally, I would like to acknowledge my appreciation for the U.S. Department of Energy, which provided the financial support for this project.

TABLE OF CONTENTS

	Page
LIST OF TABLES	ix
LIST OF FIGURES	xi
ABSTRACT	ix xi xiii 1 ted with Production of Coalbed Methane asin 1 coalbed Methane Resources 4 ity and Sodicity 6 for Salt and Sodium 9 ptivity 11 Sodic Water 13 ic Function under Saline, Sodic Conditions 16 coalbed methane Solic Function under Saline, Sodic Conductivity 19 for Hydraulic Conductivity Measurement 20 apacts of Saline, Sodic Water on Soils 24 Experiment 26 Experiment 27 Experime
1. INTRODUCTION	1
Background	1
Soil Concerns Associated with Production of Coalbed Methane	1
in the Powder River Basin	1
Powder River Basin Coalbed Methane Resources	
Literature Review.	
Overview of Soil Salinity and Sodicity	
Soil Hydraulic Conductivity	
Soil Clay Response to Sodic Water	
Studies of Soil Hydraulic Function under Saline, Sodic Conditions	
The van Genuchten Equation for Soil Hydraulic Conductivity	
Tension Infiltrometers for Hydraulic Conductivity Measurement	
Modeling Hydraulic Impacts of Saline, Sodic Water on Soils	
The Hydrus-1D Model	
References	
2. INFILTRATION WATER FLUX IN THREE MONTANA SOILS TREATED WITH SIMULATED COALBED METHANE, POWDER RIVER, AND RAIN WATERS	36
Today doubles	26
Objectives	
Hypothesis 2	
LIVIOHIESIS /) I

	Page
Hypothesis 3	51
Hypothesis 4	
Discussion	
References	63
3. SIMULATION OF SOIL PROFILE WATER BALANCE IN RESPONSE IRRIGATION WITH COALBED METHANE AND POWDER RIVER WATERS	
Introduction	67
Objectives	
Methods	
The Hydrus-1D Model	
Soil Water Balance Simulations	
Results	
Fine Sandy Loam Soil under Sprinkler Irrigation	
Fine Sandy Loam Soil under Flood Irrigation	
Silt Loam Soil under Sprinkler Irrigation.	
Silt Loam Soil under Flood Irrigation.	86
Silty Clay Loam Soil under Sprinkler Irrigation	87.
Silty Clay Loam Soil under Flood Irrigation.	87
Silty Clay Soil under Sprinkler Irrigation.	88
Silty Clay Soil under Flood Irrigation.	
Discussion	101
References	109
SUMMARY AND CONCLUSIONS	112
APPENDICES	117
APPENDIX A: FIELD SOIL DESCRIPTIONS,	
SOIL COLUMN STUDY	118
APPENDIX B: X-RAY DIFFRACTION CLAY MINERALOGY RESULTS, SOIL COLUMN STUDY	120
APPENDIX C: BASELINE AND TREATED SOIL CHEMISTRY, SOIL COLUMN STUDY	129

	Page
APPENDIX D: STATISTICAL TABLES FROM SPSS,	
SOIL COLUMN STUDY	138
APPENDIX E: HYDRUS INPUT DATA, MODEL	
SIMULATION STUDY	145

LIST OF TABLES

Ta	ble	Page
1.	EC and SAR values from PRB coal seam waters compared to values acceptable for irrigation waters	3
2.	Montana Board of Environmental Review EC and SAR standards for irrigation season (March 2 – October 31). Means with maxima in parentheses.	5
3.	Soil borrow sites: geographic location and land use	39
4.	Soil series as mapped in USDA-NRCS Gallatin County Soil Survey for soil borrow sites (GCSS Map Series), and soil series in Powder River Basin used for irrigated agriculture (PRB Target Series)	41
5.	Mean sand, silt, and clay percentages, bulk density, textural class and specific surface area (SA) for clay, silt, and sandy loam soils (n=3 for each horizon).	42
6.	Soil mineralogy (XRD analysis, indicates presence only) (n=1). K is kaolinite, Ch is chlorite, I is illite, S is smectite, Q is quartz, F is feldspar, C is calcite.	42
7.	Baseline and treated soil chemistries: EC, SAR, CEC, and pH. (n=3) Analyses performed by MDS Harris Laboratories (Lincoln, NE)	43
8.	Salt concentrations used for synthesized CBM and PR water	44
9.	Mean laboratory test results for synthesized CBM and PR water and DI water used in the soil column experiments.	44
C1	Soil organic matter and cation composition, baseline and treated (CBM or PR water) samples.	131
C2	2. Soluble soil nutrients, baseline samples	132
C3	3. Soluble soil nutrients, pre-treated samples	135
D1	1. ANOVA results for water flux measured using pre-treatment quality (CBM or PR) water for a) sandy loam b) silt loam c) clay loam soils	139

Tabl	le	Page
D2.	ANOVA results for mean relative decrease in water flux measured using pre-treatment (CBM or PR) and DI water for a) sandy loam, b) silt loam, c) clay loam soils.	140
D3.	Multiple comparisons results mean relative decrease in water flux measured using pre-treatment (CBM or PR) and DI water, by horizon-pre-treatment water quality pair in the clay loam	142
D4.	ANOVA results among soils comparing mean relative decrease in water flux measured using pre-treatment (CBM or PR) and DI water	142
D5.	Jonckheere-Terpstra non-parametric test results comparing mean relative decrease in water flux measurements by soil type	143
D6.	Jonckheere-Terpstra non-parametric test results comparing mean relative decrease in water flux measurements by soil type, by pre-treatment water quality interaction.	143
D 7.	Means and standard errors for relative mean infiltration flux (cm/h) for clay loam, silt loam, and sandy loam soils. Statistics are for untransformed measurements.	144
D 8.	Means and standard errors for relative mean infiltration flux (cm/h) for clay loam, silt loam and sandy loam soils at four soil-supply pressures. Statistics are for untransformed measurements	144
E1.	Soil hydraulic parameter values (van Genuchten 1980) used for Hydrus-1D simulations	146
E 2.	Simulated water balance components for baseline soil conditions and for five scenarios of increasing sodicity, for four different soils. All values, excluding the RWU/ET ratio, are in cm.	147

LIST OF FIGURES

Fi	gure	Page
1.	Design for a negative pressure tension infiltrometer (Perroux and White 1988)	21
2.	Soil borrow sites in southwest Montana: a) clay loam, b) silt loam, c) sandy loam.	42
3.	Difference in mean infiltration flux measurements using pre-treatment waters for soils pre-treated with CBM and PR water. Letters above columns indicate significant differences within soil type. Error bars are standard error of mean differences (n=5)	50
4.	Mean relative decrease in infiltration flux measurements using DI water, by soil and pre-treatment water quality. Values were calculated as (pre-treatment water flux-DI water flux)/pre-treatment water flux. Letters above columns indicate significant differences within soil type. Error bars are standard error of mean differences (n=5)	52
5.	Mean relative decrease in soil sodium adsorption ratio (SAR) for A and B horizons after pre-treatment with CBM or PR water compared with baseline soil SAR, by soil, horizon and pre-treatment water quality. Values were calculated as (pre-treated SAR-baseline SAR)/baseline SAR Error bars are standard error of mean differences (n=3)	52
6.	Mean relative decrease in infiltration flux measurements using DI water, by soil and horizon. Values were calculated as (pre-treatment water flux-DI water flux)/pre-treatment water flux. Letters above columns indicate significant differences within soil type. Error bars are standard error of mean differences (n=5)	54
7.	Mean relative decrease in infiltration flux measurements using DI water, by soil, horizon, and pre-treatment water quality. Values were calculated as (pre-treatment water flux-DI water flux)/pre-treatment water flux. No significant differences were observed within soils. Error bars are standard error of mean differences (n=5)	525
8.	Mean relative decrease in infiltration flux measurements using DI water, by soil. Values were calculated as (pre-treatment water flux-DI water flux)/pre-treatment water flux. No significant differences were observed among soil types. Error bars are standard error of mean differences (n=5)	56

Fig	gure	Page
9.	Mean relative decrease in infiltration flux measurements using DI water, by soil and pre-treatment water quality. Values were calculated as (pre-treatment water flux-DI water flux)/pre-treatment water flux. No significant differences were observed among soil types. Error bars are standard error of mean differences (n=5)	56
10.	Water retention functions $\theta[h]$ used as input for baseline and progressively sodic water quality simulations. Functions are for a) fine sandy loam, b) silt loam, c) silty clay loam, d) silty clay soils	75
11.	Hydraulic conductivity functions used as input for baseline and progressively sodic water quality simulations. Functions are for a) fine sandy loam, b) silt loam, c) silty clay loam, d) silty clay soils	77
12.	Hydrus 1-D graphical input screen for initial pressure head distribution by depth in the soil profile.	79
13.	Relative depth density of simulated alfalfa roots in the soil profile	82
14.	Hydrus-1D simulation results: Cumulative water distribution by soil and irrigation method for basline and progressively sodic irrigation water qualities. Results are for a) fine sandy loam, b) silt loam, c) silty clay loam, d)silty clay soils	90
15.	Ratio of root water uptake (transpiration) to total evapotranspiration (RWU/ET) by soil and irrigation method for baseline and progressively sodic irrigation water qualities. Results are for a) fine sandy loam, b) silty loam, c) silty clay loam, d) silty clay soils.	94
16.	Cumulative infiltration by soil and irrigation method for baseline and progressively sodic irrigation water qualities. Results are for a) silt loam, b) silty clay loam, c) silty clay soils	98
17.	Root zone pressure head for silt loam soil under sprinkler irrigation, for baseline and progressively sodic irrigation water qualities. Critical upper bound pressure head for maximum alfalfa root extraction of soil water is -25 cm.	100
18.	Root zone pressure head for silty clay soil under sprinkler irrigation, for baseline and increasingly sodic irrigation water qualities. Critical upper and lower bound pressure heads for alfalfa root extraction of soil water are -10 cm and -8000 cm.	100

ABSTRACT

A repacked soil columns experiment and a series of computer soil water balance simulations were conducted to examine potential impacts of coalbed methane (CBM) water from Montana's Powder River Basin (PRB) on soil water flow and water balance in PRB soils. CBM water is often high in sodium, which may separate soil clay particles, particularly after soil exposure to low-salinity rainfall or snowmelt, and when soils contain expansible smectite clay minerals. Aggregates in soils exposed to sodic water may swell and slake, and clays and other fine particles may disperse, clogging soil pores and slowing or preventing soil water flow.

In the soil columns experiment, A and B horizon materials from sandy loam, silt loam, and clay loam soils were pre-treated with water having salinity and sodicity typical of PRB CBM water or of Powder River (PR) water currently used for irrigation in the basin. Tension infiltrometer measurements were used to determine infiltration flux, first using pre-treatment water, and subsequently deionized (DI) water, simulating rainwater. Measurements were compared by pre-treatment water, horizon, and soil type. Under pre-treatment water testing, the sandy loam and clay loam soils pre-treated with CBM water exhibited smaller infiltration flux values than when pre-treated with PR water. Only the sandy loam soil showed a greater decrease in infiltration flux with DI water on soils pre-treated with CBM relative to PR water pre-treated soils. There was no difference in infiltration flux decrease with DI water between A and B horizon soils, or between smectite and non-smectite soils.

The soil water balance numerical simulations modeled potential effects of sodic irrigation waters on sandy loam, silt loam, clay loam and silty clay PRB soils under sprinkler or flood irrigation, during one growing season. Baseline soil water retention functions were constructed for the five soils, and adjusted via trends identified in the literature to create five additional functions for each soil, simulating exposure to five increasingly sodic irrigation waters. Simulation results showed greater impact of sodic irrigation under flood than sprinkler irrigation. The fine sandy loam and silty clay loam soils exhibited the fewest changes in water balance partitioning, while the silt loam and silty clay soils showed the greatest changes, especially in increased runoff and reduced transpiration.

CHAPTER 1

INTRODUCTION

Background

Soil Concerns Associated with Production of Coalbed Methane in the Powder River Basin

The development of coalbed methane (CBM) reserves in the Powder River Basin (PRB) of Wyoming and Montana has increased dramatically since 1997 and is forecast to expand significantly over the next decade (U.S. Bureau of Land Management (BLM) and State of Montana 2002, Wheaton and Olsen 2001). The final environmental impact statement (EIS) for CBM development in Montana (BLM et al. 2003) allows for potential development of up to 26,000 new CBM wells in the state, and the Wyoming final EIS accommodates potentially 51,000 new wells (Berman 2003).

Methane extraction from shallow coal seams involves the removal of large volumes of groundwater. This water often contains high levels of dissolved solids, particularly sodium (Na) (Nuccio 2002). A 2003 federal appeals court decision ruled CBM water to be a pollutant and subject to Clean Water Act permitting even when discharged into ephemeral water channels (Gable 2003). Economically feasible disposition of CBM water presents a major challenge to methane producers and is a concern for local landowners and environmental regulators (Coalbed methane in Montana 2001, The orderly development of coalbed methane 2001). Because this groundwater product represents a potentially

significant water resource in a semi-arid agricultural region, its use for irrigation has been proposed and is being attempted in some areas in the PRB (Steward 2001, Hemmer 2001). The agricultural use of CBM water involves exposing soils to potential chemical and physical changes that could significantly affect soil structure and function. Addition of saline and/or sodic waters to these soils could reduce their capacities both to drain and to retain plant-available water, particularly in the case of high-montmorillonite clay fraction soils found in some irrigated acreage in the PRB (Bauder 2001).

Primary soil concerns related to CBM water are the water's salinity, often expressed either as total dissolved solids (TDS) or electrical conductivity (EC), and its sodicity, usually expressed as the sodium adsorption ratio (SAR), the concentration of Na relative to concentrations of calcium (Ca) and magnesium (Mg). High soil sodicity may cause reduced water infiltration when that soil is exposed to low-salinity water, such as snowmelt or rainfall (Hansen et al. 1999, Ayers and Wescott 1985). Sodic water may promote swelling of layered clay minerals and dispersion of soil aggregates, slowing or even preventing water movement through the soil (Ayers and Wescott 1985). Salinization and sodication of soils may result in increased runoff and erosion, and subsequent loss of agricultural soils, as well as salt and sediment contamination of surface waters and aquifers (Sumner et al. 1998). Soil colloids suspended in runoff may sorb and mobilize metals, soil nutrients, pesticides and other organic contaminants (Sumner et al. 1998).

In a study of PRB CBM water quality in 83 wells in the Wyoming portion of the basin where CBM extraction has been active for several years, Rice et al. (2002) found an increase in SAR and TDS (due to higher Na and bicarbonate (HCO₃) contents) to the north and west,

toward the Montana portion of the basin. The Water Resources Technical Report, a supplement to the Draft Montana Statewide Oil & Gas Environmental Impact Statement for CBM in Montana (ALL Consulting and CH2M HILL 2001), includes mean EC and SAR values measured by the Montana Department of Environmental Quality at the CX Ranch CBM production area in Decker, MT. These Montana values exceeded those reported in Rice et al. (2002) for the northernmost wellsites tested in the Wyoming study. EC and SAR values from both studies are summarized in Table 1, as are ranges of values generally considered as appropriate (zero to moderate restriction on use) for irrigation waters (Ayers and Wescott 1985). It appears from these studies that CBM water in the PRB is generally within accepted limits for irrigation water salinity, but high in sodicity compared with accepted values.

Table 1. EC and SAR values from PRB coal seam waters compared to values acceptable for irrigation waters.

	EC		SAR	
	dS/m			
	Range	Mean	Range	Mean
Wyoming PRB	0.4-4.3	1.3	5-68.7	12
Montana PRB	NR	2.2	NR	47
Acceptable for irrigation	0.7-3.1		3-9	

NR=not reported

With the increasing use of saline, sodic waters for irrigation in many parts of the world, and the prospect of CBM product water use on Montana agricultural lands, more information is needed concerning specific physical responses of different soil types to different water qualities (Oster 1994). Although reclamation of Na-affected soils is possible, it may be

prohibitively expensive. New water sources and water qualities may require new agricultural management practices, and studies such as the one reported here may contribute to a knowledge base that will aid landowners in taking advantage of available water sources without damaging their soils (Oster and Shainberg 2001).

Powder River Basin Coalbed Methane Resources

The PRB is located in southeast Montana and northeast Wyoming and trends approximately southeast to northwest across the border between those states. The Tongue River Basin constitutes a sub-basin of the PRB (Wyoming State Water Plan n.d.). The Powder and Tongue Rivers originate in Wyoming and are two of three (with the Bighorn River) major tributaries to the lower Yellowstone River. Under the Yellowstone River Compact of 1950, Wyoming is entitled to 40% of Tongue and 42% of Powder River flows, and Montana is entitled to the remainder (Wyoming State Water Plan n.d.).

Water from the Powder River (PR) is used to irrigate approximately 4,500 ha in Montana (Bauder and Brock 2001). Low precipitation ,along with marine sediment constituents of basin geology, have already contributed to high EC and SAR water in that channel, and to salinization of surface water-irrigated PRB soils (Bauder and Brock 2001, Lowry and Wilson 1986).

Coals in the PRB are assumed to be of biogenic origin, created via microbial reduction of carbon dioxide (Rice et al. 2002, Nuccio 2002). PRB coals are also subbituminous, yielding a relatively high volume, about 20.097 J/kg (8,700 Btu/lb), of methane (Flores et al. 2001). In 2002 the U.S. Department of Energy estimated PRB recoverable

CBM reserves at 0.82 trillion m³ (29 trillion ft³), stating that in that year, PRB CBM wells were producing about 20% of the nation's coalbed methane. That study estimated economically-recoverable gas as dependent on cost-variable waste disposal methods and found production would vary between the 0.82 trillion m³ estimate with no restrictions on surface disposal down to 0.5-0.6 trillion m³ under a requirement to reduce water salinity by reverse osmosis treatment (U.S. Department of Energy 2002).

The quantity of water produced in conjunction with CBM extraction varies nationally with basin-to-basin differences in deposition, depth, and type of coal (USGS 2000). Water volumes are typically greatest during the first, dewatering, phase of methane removal, and decrease sharply before the peak, or stable, methane production phase (Nuccio 2002). The 2002 Draft Montana Statewide Oil and Gas Environmental Impact Statement estimates, based on data from the CX Ranch CBM extraction site near Decker, Montana, put the initial per-well discharge rate at an average 0.945 L/s (15 gpm), with some wells discharging 1.26-1.575 L/s (20-25 gpm), and with a 20 year estimated average of 0.1575 L/s (2.5 gpm) (U.S. BLM and State of Montana 2002).

Because the PRB channels water flow from Wyoming into Montana, irrigators in Montana are concerned with CBM water management across the interstate border as well as within the state. In March 2003, the Montana Board of Environmental Review adopted numeric EC and SAR standards for the Powder, Tongue and Little Powder Rivers, Rosebud Creek, and tributaries (Montana Board of Environmental Review 2003). Thirty day averages and maxima for the irrigation season (March 2 – October 31) are as follows:

Table 2. Montana Board of Environmental Review EC and SAR standards for irrigation season (March 2 – October 31). Means with maxima in parentheses.

	Powder River	Little Powder River	Tongue River	Rosebud Creek
EC (dS/m)	2.0 (2.5)	2.0 (2.5)	1.0 (1.5)	1.0 (1.5)
SAR	4.0 (6.0)	5.0 (7.5)	3.0 (4.5)	3.0 (4.5)

The Montana final EIS on CBM development (U.S. BLM et al. 2003) was issued in January 2003, with Records of Decision issued by the Montana Department of Environmental Quality and Board of Oil and Gas Conservation later that year. The final EIS recommends the use of impoundments (infiltration and evaporation ponds) as the primary means of managing CBM water, but allows for beneficial use of produced water, including irrigation. The final EIS also anticipates no adverse impacts to soils from CBM product water.

Literature Review

Overview of Soil Salinity and Sodicity

Soil salinity may be expressed as electrical conductivity (EC), which is approximately related to salt concentration (total dissolved solids, TDS, or molar concentration, C) depending on the salt, by the following ratios (Essington 2004):

TDS (mg L⁻¹)
$$\approx$$
 640 x EC (dS m⁻¹) for dilute solutions [1]

or

C (mmol L⁻¹)
$$\approx 10 \text{ x EC (dS m}^{-1})$$
 [2]

EC is usually measured by preparing a saturated paste extract or by preparing a solution in some ratio of soil to distilled or deionized water. The soil water is then extracted via vacuum filtration, and a conductivity cell placed in the solution to measure electrical current flowing, via dissolved salts, between the electrodes in the cell (Essington 2004).

In general, a soil is considered to be at least moderately saline when it has a saturated paste extract EC of greater than 4.0 dS/m (Keren 1999, California Fertilizer Association 1998). High salinity levels in irrigation water are generally more of a problem for plants than for soils. Salinity can decrease water availability to plants when they must absorb water against an increased osmotic gradient. Toxicity to some plant species of salts or specific ions (e.g. boron, chloride), and adverse influences on early stage plant growth are other hazards (Hansen et al. 1999).

Soil sodicity is commonly expressed as one of two ratios, ESP or SAR. Exchangeable sodium percentage (ESP) is defined by the U.S. Salinity Laboratory Staff (1954) in terms of the exchangeable sodium ratio (ESR) as:

$$ESP = 100 \times ESR/(1+ESR).$$
[3]

ESR is derived from the Gapon equation, which expresses reactions on soil exchange surfaces (negatively-charged surfaces of clay and organic matter) in terms of the molar concentrations of involved cations, in this case Na⁺, Ca²⁺, and Mg²⁺. ESP is measured through replacement of the soil exchange cations with the cations in an applied solution (usually ammonium, NH₄⁺) and measurement of replaced cation concentrations (Page et al. 1982).

SAR is the sodium adsorption ratio, the ratio of the molar concentration of Na⁺ to concentrations of Ca²⁺, and Mg²⁺ in a soil solution or in irrigation or other water to which soil is exposed:

$$SAR = [Na^{+}]/\{([Ca^{2+}] + [Mg^{2+}])/2\}^{0.5}$$
 [4]

with units of mmol^{0.5} (or meq^{0.5})/L^{0.5} (Essington 2004).

SAR is related and approximately equal to ESP with the 0-30% ESP range, and is often used to estimate the ESP of a soil (Essington 2004) as:

$$SAR \approx ESR/0.01 \approx ESP$$
 [5]

with 0.01 being a value approximately equivalent to the Gapon selectivity coefficient under conditions where ESP is less than 25-30% (Essington 2004).

Although SAR is measured via analysis of the saturation paste extract and is therefore primarily a property of the soil solution and not of the soil exchange, an equilibrium between the soil exchange and solution is assumed and SAR is currently in more common use than ESP because it is more easily determined (Essington 2004) and because there are complications associated with the required pH and with salt and cation measurements (Sumner 1995).

Suarez (1981) developed an alternative SAR calculation to account for the presence of calcium carbonate solid in the soil, which controls [Ca²⁺] in solution. This equation considers the partial pressure of carbon dioxide (pCO₂) and the ratio of HCO₃ to Ca, as these factors mediate the rate of precipitation and dissolution of Ca. This method of calculation results in what is sometimes referred to as the "true SAR", as distinguished from the "practical SAR" calculated in equation [4] (Essington 2004). Suarez (1981) points out,

however, that under saline conditions, such as those present in both PR and CBM water, SAR is not particularly sensitive to Ca concentrations. For this reason, in addition to ease of calculation, the practical SAR is used here.

Soil Hydraulic Effects of Salt and Sodium

High salinity and sodicity of CBM waters are concerns where the water is spread onto land or into existing water channels for storage, infiltration, evaporation, dilution, or irrigation purposes. Soils containing significant percentages of fine particles, particularly Na-montmorillonite clays, are vulnerable to reductions in hydraulic conductivity and infiltration rates when Na⁺ replaces other cations on the soil exchange complex (McNeal et al. 1968). Soils in arid regions such as the PRB often contain a high ESP before irrigation or other water is applied, so the sodium content of applied water is a particular issue in these dry landscapes (Ouirk and Schofield 1955). Sodium may cause reduced soil permeability as a result of two related processes: swelling of the clay lattice that blocks larger pores essential to soil drainage and causes failure of soil aggregates, and dispersion of clay particles because of platelet deflocculation, with resulting clogging of smaller soil pores (Quirk and Schofield 1955). The swelling process has been shown to be largely a reversible one; dispersion is believed to be nonreversible (Levy 1999). Swelling is the predominant factor in hydraulic conductivity reduction in soils with significant percentages of swelling clays, while dispersion and pore-clogging are the main mechanisms in silts and loams (Sumner 1995). Smectites such as montmorillonite contribute to swelling, while illite clay minerals are more apt to create dispersive conditions (Churchman et al. 1995). In sandy (low clay percentage)

soils, application of high sodicity (ESP=20) water may initially reduce the saturated hydraulic conductivity (Ks) as clays are dispersed, but Ks is often recovered with continued leaching as those clays are removed from the system (Sumner 1995).

Because sodic effects on soil depend to a large degree on soil texture (primarily clay percentage) and clay mineralogy, and on the EC of the water being used for irrigation, there is no single SAR or ESP value in broad use as a threshold to define sodic soils, although ESPs between 5 and 20 have been proposed (Levy 1999). The U.S. Department of Agriculture's handbook on saline and sodic soils (U.S. Soil Salinity Laboratory 1954) and the Western Fertilizer Handbook (California Fertilizer Association 1998) define a sodic soil as having an EC less than 4.0 dS/m and an ESP greater than 15, and a saline-sodic soil as having an EC greater than 4.0 dS/m and an ESP greater than 15. SAR threshold values of 12-15 have been suggested as defining sodic soil conditions in North America (Shainberg and Letey 1984).

Low salinity water may create problems when it is applied to high SAR soils, as the presence of salts in solution tends to counter clay swelling and dispersion. Quirk and Schofield (1955) defined a threshold electrolyte concentration (TEC) of applied water as that below which the water will cause a 10-15% decrease in permeability of a soil. The TEC varies with soil texture and mineralogy, and with soil and water chemistry. Soils higher in 2:1 layered clays, especially the montmorillonites common in arid regions of North America, display more significant decreases in hydraulic conductivity with higher SAR and lower EC of applied water than do soils high in kaolinite, sesquioxides or amorphous minerals (McNeal and Coleman 1966). The presence of iron or aluminum oxides or organic matter in soils

may help to bind clays together, aiding in structural maintenance and ameliorating the swelling and dispersive effects of sodium (Churchman et al. 1993, McNeal et al. 1968), but may also, under some circumstances, increase dispersion (Churchman et al. 1995). The effects of an applied water quality on hydraulic conductivity cannot be predicted solely by identifying soil type (Malik et al. 1992) or by characterizing the salinity or sodicity of the applied water, but occur in response to a particular combination of soil and water characteristics (McNeal and Coleman 1966).

Soil Hydraulic Conductivity

Hydraulic conductivity (K) quantifies the rate of water movement through the soil matrix along a given hydraulic gradient, the distribution of water's potential energy over a distance of soil (Hillel 1998). It is expressed as a flux, the distance of flow per unit time of a volume of water across an area of soil, most often in units of L/t, and with magnitudes ordinarily between 10⁻⁴ and 10⁻⁹ m/s (Hillel 1998). The hydraulic conductivity of a given soil varies with its texture and structure (pore size distribution, pore geometry and pore connectivity) and with its wetness. Hydraulic conductivity increases dramatically, over several orders of magnitude, as soil wetness increases.

Saturated hydraulic conductivity, Ks, quantifies the rate of water movement in a saturated soil, through water-filled pores of all sizes, in response to a positive pressure gradient. In an unsaturated soil, the gradient is one of negative (below atmospheric) pressures in the soil matrix, and water flows only through pores small enough to remain undrained, from areas of higher to lower (more negative) matric potential (Hillel 1998). A

wetter soil will have a higher matric potential than will a drier soil. The hydraulic conductivity function describes rates of soil water movement over a range of matric potentials, K[h], or moisture contents, $K[\theta]$.

The K[h] relationship varies significantly with soil texture and structure. When saturated, coarser soils, having larger and more continuous pores, generally have greater hydraulic conductivity than saturated finer soils. Under unsaturated conditions, a finer-textured soil, with smaller pores that remain water-filled, will often conduct water faster than will a coarser-textured soil at the same matric potential.

Hydraulic conductivity is an extremely variable soil property. Measurements of Ks and K[h] can vary spatially and temporally over four orders of magnitude within a short distance on the same soil (Radcliffe and Rasmussen 2001). Different measurement techniques can also result in large variability (Radcliffe and Rasmussen 2001).

Hydraulic conductivity may be distinguished from infiltration rate (IR), which is the flux (volume per time) per unit surface area of water entering the soil profile (i.e., crossing the upper soil boundary) (Levy 2000). The salinity of water applied to soil affects both K[h] and IR, although IR may be more sensitive, decreasing even in low Na, high Ca soils, both conditions under which K[h] responds less to total electrolyte content of the applied water (Levy 1999, Shainberg and Letey 1984). In arid and semi-arid regions, many soils contain Ca and Mg minerals that dissolve and add these cations to the soil solution, acting to counter the Na effect (Sumner 1995).

Soil Clay Response to Sodic Water

The clay fraction of soils, because of its large surface area and negative charges, is the primary determinant of soil physical behavior (Levy 1999). Clay minerals with a higher surface area, such as montmorillonite, which has a specific surface area of approximately 750 m² g⁻¹ (Shainberg and Letey 1984), have a greater interaction with chemicals in the soil solution and are therefore generally more reactive than are clays with a lower specific surface area. This reactivity also depends on which cations are present in the soil solution and on their concentration (Shainberg and Letey 1984).

In clays, a diffuse double layer consisting of a negatively-charged clay platelet surface and counter ions (cations) from the soil solution is formed as the cations are simultaneously attracted by van der Waal's, ion correlation, and other forces to the negatively charged surface of the particle and pushed back into solution by the ion concentration (diffusion) gradient and other repulsive forces (Shainberg and Letey 1984). Divalent ions such as Ca²⁺ and Mg²⁺ are attracted to the clay surface at twice the force as are monovalent ions such as Na⁺. The Na⁺ hydrated radius is also larger than hydrated radii of Ca²⁺ and Mg²⁺, and the hydration energy of Na⁺ is lower than for the other two cations (Norrish 1954), which increases the distance between clay platelets. As Na⁺ attracts bipolar water molecules between adjacent clay particles, the diffuse double layer tends to expand, moving clay particles farther apart (Levy 1999) and potentially deflocculating clay platelets.

The salt concentration of the soil water determines the direction and strength of the osmotic pressure acting either to admit cations into spaces between clay layers or to withdraw them into solution (Quirk and Murray 1991). In a more saline soil solution, there is

less osmotic pressure on cations to move away from the clay surface and clay particles remain in floccules (Shainberg and Letey 1984). In low-salt solutions, water molecules move into the interlamellar spaces, hydrating Na⁺ ions and creating an additional layer of water molecules, and clay particles tend to disperse (Quirk 1986).

Studies on leaching of soils with rain or distilled water show surface sealing from clay dispersion, even in soils with relatively low clay contents but with significant silt (Levy et al. 1998). Sealing may also occur deeper in the soil profile. Shaw et al. (1998) proposed a model for sodic clay soil function whereby the A horizon is exposed to rainfall, dispersing clays in that layer and leaving coarser particles at the surface. The B horizon, often finer-textured than the A, receives dispersed clays from above, clogging pores and leaving a layer of reduced permeability at the top of that horizon.

Rhoades (1972) reviewed guidelines and specific considerations for managing irrigation with high salt and sodium irrigation waters. He stated the importance of assessing local conditions, including the rate of evapotranspiration that can concentrate salts in soil water, crop tolerance for specific ions, soil texture and compaction (potentially leading to matric stress in plants), soil mineral weathering, and irrigation method. These may all affect the impacts of saline, sodic water on crops and soil permeability.

Oster (1994), in another review, pointed to the importance of leaching with low-salinity water as the primary means of managing irrigation with high-salinity waters, and to the hazard posed to soil physical properties, hydraulic conductivity in particular, by the high sodium levels often present in recycled waste or agricultural drainage waters. In cases such as many areas in the PRB where there is an inadequate freshwater supply, amendments of

sulfuric acid, elemental sulfur, or gypsum to soils may be required to maintain adequate levels of hydraulic activity (Oster 1994).

So and Aylmore (1995) discussed potential mechanisms for destruction of soil physical condition by sodicity and questioned the use of the ESP (or SAR) concept, developed under controlled laboratory conditions (using homoionic pure clays, for example), when considering the complex soils on the landscape. In lab studies, it appears that Na⁺ adsorbs to the outer surfaces of clay domains (platelet clusters) until a threshold ESP of 7-20% is reached, following which Na⁺ enters spaces in the domain interior, and swelling occurs. In field soils, ESP values in that range are not strongly correlated with properties such as crusting or hard-setting of soil surfaces, available soil water holding capacity, or soil strength and workability (So and Aylmore 1995).

Sumner (1995) added to this the observation that even low levels of exchangeable sodium can cause measurable deterioration of soil physical properties and that threshold SAR values in use for land use decision-making are fairly arbitrary and are based on laboratory studies conducted under conditions not representative of field soil conditions. He noted that double-layer theory predictably describes the behavior of clay particles in pure Namontmorillonite clays, but becomes problematic in Ca- and mixed-cation clays where calcium promotes aggregation of clay particles into domains, reducing the surface area on which Na⁺ can act. Sumner (1995) also pointed to studies indicating that the presence of illite, magnesium, potassium, and organic matter may each contribute to increases in clay dispersion under certain conditions of ion composition or pH. He reiterated that the presence

of swelling clays or high SARs are not required for soil damage to occur, particularly with low-EC water application or precipitation.

Studies of Soil Hydraulic Function under Saline, Sodic Conditions

McNeal and Coleman (1968) examined hydraulic conductivity effects of applied solutions in a range of sodicities on soils with varying clay mineralogy. They found a greater decrease in hydraulic conductivity with increased SAR of applied water in soils with a greater percentage of 2:1 layer silicates, especially montmorillonite, and more stable values in soils containing greater amounts of kaolinite, sesquioxides, and amorphous minerals. Their attempts to restore hydraulic function through leaching with high-EC, high-Ca solutions were unsuccessful, except in those soils with a whole-soil montmorillonite percentage over 10%. This, they believed, may have been because the decrease in K in montmorillonitic soils was due primarily to clay swelling and macropore reduction, which is believed to be reversible, rather than to dispersion of soil fines and pore blockage, which is thought to be nonreversible.

Minhas and Sharma (1986) measured Ks and degree of clay dispersion in a sandy loam and a clay loam soil leached with waters in a range of SAR (5-45) and electrolyte concentrations (EC of 0.5-50 dS/m), and again after application of distilled water (simulated rainwater). They observed large decreases in Ks and increases in dispersion after distilled water application even after leaching with the low SAR water, and found greater effects in the sandy loam than the clay loam soil. Saturated hyraulic conductivity was not improved by re-leaching with saline water. The authors hypothesized that clay dispersion and resultant

soil pore clogging was the primary Ks reduction mechanisim in the sandy loam, while surface sealing was the main effect in the clay loam.

Evans et al. (1990) conducted a furrow infiltrometer study with application waters of various NaCl concentrations on saline, sodic, smectic clay Australian red-brown earth soils. Infiltration rates in that study were higher for very high (9.2 dS/m) salinity, high sodicity applied waters. The authors pointed out that any increase in leaching and in groundwater replenishment with higher-salt irrigation waters is countered by adverse effects of salinity on soil structure and crop growth.

Singh et al. (1992) tested effects of irrigation water on illite clay soils in a range of EC-SAR combinations on infiltration rate, clay dispersion, and leaching displacement of salts, as well as on crop yield. They found greater reductions in infiltration rate with increased EC at the same SAR, and decreased salt displacement and increased dispersion with increased SAR. Their study found EC and SAR distribution declining with depth in the soil profile (to 1.2 m), but increasing below that depth after monsoon rains, and increasing with increased SAR of applied water, even with similar EC, after 6 years of irrigation. They also found a greater SAR effect on all three measured parameters (infiltration rate, clay dispersion, and leaching displacement of salts) in soils affected by monsoon rains.

Chaudhari (2001), in a laboratory permeameter study of 24 water quality combinations (TDS=5-50 meq L⁻¹ or EC range 0.5-5 dS m⁻¹, SAR range 2.5-30) on clay, clay loam, and silt loam soils, found a reduction in the saturated hydraulic conductivity in all soil textures after equilibration with a solution of higher SAR and lower TDS. The silt loam soil exhibited the greatest reduction in Ks after equilibration, perhaps because the higher-clay soils had a

greater percent base saturation and higher buffering capacity. The greatest dispersion was observed in the silt loam and the greatest swelling was observed in the clay. In a related 2003 study, Chaudhari and Somawanshi looked at effects on K[h], wetting front advancement, and diffusivity with the same soils and irrigation water qualities. K[h] increased at a given SAR with increasing EC, and decreased at a given EC with increasing SAR. The silt loam exhibited a greater K[h] decline between Ks and K measurements taken at negative water potentials. The authors attributed this to the silt loam's greater macroporosity. Most of the larger pores were evacuated at high suction, and dispersion of silt and clay particles reduced the average pore size more dramatically than in the finer-textured soils.

Bethune and Batey (2002) conducted a study of the effects of irrigation with low-salinity water on Australian clay soils made saline-sodic with the 10-year-long use of recycled irrigation water. Their results showed no adverse growing-season effect of low-salinity winter precipitation infiltrating into the soils (measurements were not taken during winter months). The study did show reductions in steady-state surface infiltration (loam, top 0.3 m depth) with reduction in EC of irrigation water. Water balance-measured infiltration did not decrease, which they attributed to crack formation with soil drying. They anticipated that further leaching would cause soil structure deterioration. In their study, 14 months of leaching with low-salinity water did not appear to cause a reduction in subsoil (heavy clay, >0.3 m depth) salinity sufficient to cause a decline in permeability, as measured by post-irrigation rate of decline in perched water table depth.

Levy et al. (2002) studied effects of irrigation water salinity and sodicity on bulk density and hydraulic conductivity in three soils during furrow irrigation with interrupted flow. They did not find a correlation between EC or ESP of water and changes in bulk density, but did see a decrease in hydraulic conductivity with decreased EC and increased ESP.

The van Genuchten Equation for Soil Hydraulic Conductivity

Van Genuchten (1980) proposed a closed-form equation for the K[h] function, based on agreement with experimental data. The equation is derived from a theory developed by Mualem (1976) to model hydraulic conductivity based on soil-water retention measurements. The Mualem-van Genuchten equation for hydraulic conductivity, called the van Genuchten equation here, may be stated as:

$$K[h] = Ks\{1-(\alpha h)^{n-1} [1+(\alpha h)^n]^{-m}\}^2 / [1+(\alpha h)^n]^{m/2}$$
 [6]

where α is a fitting parameter (L⁻¹) inversely related to the bubbling pressure (the matric potential required to empty the largest soil pore of water, n is a unitless parameter related to pore connectivity and tortuosity, and m is equal to 1-1/n and is unitless (Radcliffe and Rasmussen 2002).

The related water retention function is:

$$\theta [h] = \theta r + (\theta s - \theta r) [1/1 + (\alpha |h|)^n]^m$$
 [7]

where θ is the volumetric water content of the soil, θr is the residual water content, and θs is the water content at saturation (Hillel 1998).

Tension Infiltrometers for Hydraulic Conductivity Measurement

In 1988, Perroux and White introduced a pair of designs for disc permeameters (called tension infiltrometers, or TIs, here) to measure soil hydraulic properties under both positive and negative water pressures (Fig. 1). Their intent was to refine an apparatus for taking these measurements under conditions of macropore or other preferential flow. A TI allows precise control of water supply pressures (h) at values less than zero soil matric potential at the soil surface. Under capillarity theory, the more negative the water pressure, the smaller the soil pores that will remain water-filled and thus conduct water (Perroux and White 1988). This relationship is described by the capillary rise equation:

$$h_c = 2\gamma \cos\alpha / rg\rho_w$$
 [8]

where h_c is the height of capillary rise [L], γ is the surface tension between water and air [m/t²], α is the contact angle between the water and the pore wall, r is the pore or capillary radius (equivalent to the matric potential) [L], g is gravitational acceleration [L²/t], and ρ_w is the density of water [m/v] (Hillel 1998).

Ankeny et al. (1991) presented a method for field determination of Ks and K[h] using a sequence of TI measurements taken at steady-state water flow at different descending (0 to progressively more negative) tensions on the same soil surface. From Wooding's (1968) solution for steady-state infiltration from a shallow circular pond (soil surface area), they derived linear functions for the fluxes measured at each pressure head. They then used a numerical approximation of K[h] based on an average matric flux potential curve, to build a piecewise K[h] function from the differences in K between pressure heads.

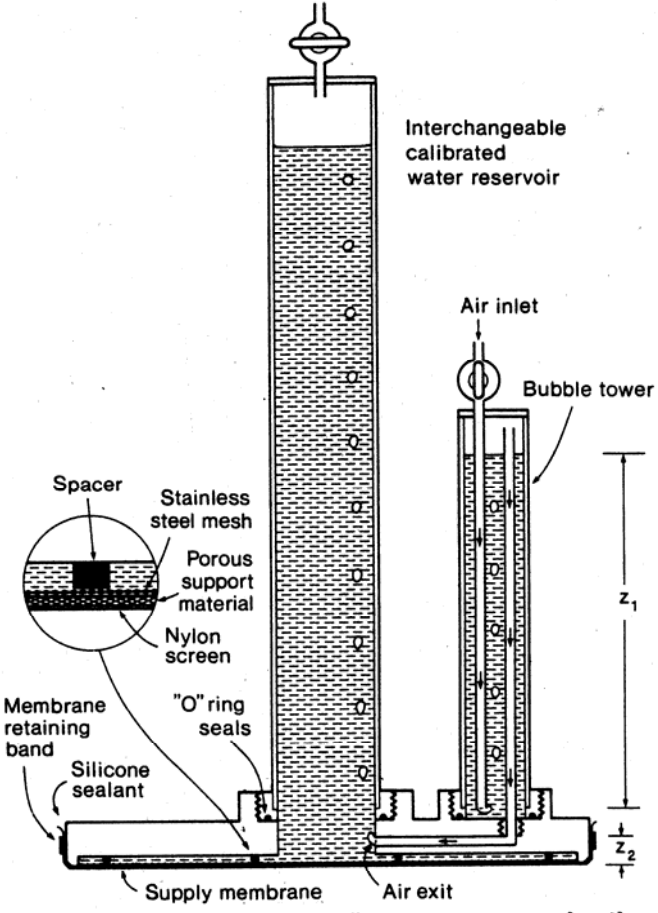


Fig. 1. Disc permeameter for supplying water at pressures less than or equal to zero. Reservoirs of varying diameters may be interchanged. Arrows show direction of air flow.

Fig. 1. Design for a negative pressure tension infiltrometer (Perroux and White 1988).

Reynolds and Elrick (1991) described an alternative analysis to derive K[h] from multi-tension, steady-state TI measurements on a single surface. They combined Wooding's (1968) equation with Gardner's (1958) exponential relationship between K[h] and Ks to come up with a piecewise linear solution for each pair of supply pressures and flow rates measured. Reynolds and Elrick (1991) advised using an ascending (drier to wetter) set of matric potentials in order to avoid the hysteresis effect likely when a descending set of

measurements is taken with resultant drainage near the soil surface and wetting at the infiltration front between successive measurements.

Logsdon and Jaynes (1993) developed a nonlinear regression technique for estimating the K[h] function from TI measurements made at steady-state during ponded infiltration, then at two or more negative supply pressures. They used Wooding's (1968) equation to fit optimal values for Ks and the α parameter. These fitted values were then substituted back into the Gardner (1958) equation to derive the K[h] function for the soil in question. They cited as advantages to their method the physical and mathematical ease of use and the close agreement found between K[h] measured via excavation of a one-dimensional soil column and K[h] as determined by the nonlinear regression method. These authors used a descending (wetter to drier) sequence of tensions in their measurements, citing previous studies in which this was done to reduce time to reach steady-state. They discouraged use of ponded infiltration measurements combined with negative pressure measurements in soils with macropores.

Reynolds et al. (2000) compared estimates of Ks extrapolated from TI measurements in sandy, loamy and clay loam soils under 2 tillage conditions with those measured using a pressure infiltrometer or undisturbed soil cores. These authors stressed the variability of Ks under differing soil types and conditions, and the impact of soil characteristics on the appropriateness of any Ks measurement method. They used the Reynolds and Elrick (1991) three-dimensional field TI procedure and found a lack of correlation between mean, minimum and maximum Ks values for the TI, pressure infiltrometer and undisturbed soil core methods, as well as smaller Ks values at higher permeabilities (>10⁻⁴ m s⁻¹, as with the

cracking clay loam) from the TI method than from the 2 other methods. Their study confirmed previous work that found Ks to have a high degree of sensitivity to differences in soil and measurement techniques.

White et al. (1992) compared TI with other measurement techniques to measure surface soil hydraulic properties. They cited as the TI's primary limitation the assumptions behind the analysis used to model hydraulic properties from measured data. The main assumption is that the soil is homogeneous and isotropic, although most field soils vary in bulk density, water content, and texture, as well as other properties affecting hydraulic function, near the soil surface. Problematic characteristics of some soils, most notably swelling clays or hydrophobic soils, also present violations of the mathematical assumptions underlying commonly-used analyses. Time to true steady-state flow, which is estimated to be several hours in many soils, presents another problem for practical measurement of steady-state hydraulic properties. The need for contact material between the TI membrane and the actual (uneven) soil surface, which may skew or dominate water flow, may be another weakness, although less of a problem at steady- or near-steady-state than in early-stage transient flow measurements.

Unequivocably evaluating the K[h] and other soil hydraulic properties is highly problematic (Hillel 1998). However, TI has evolved as a flexible measurement approach for use in intact and fairly large soil volumes. Although we may never know what a "true" K[h] is for a given soil, due to dependence on measurement conditions, careful use of individual methods can illustrate the level of changes in response to specific soil or water conditions (Klute and Dirksen 1986).

Modeling Hydraulic Impacts of Saline, Sodic Water on Soils

Modeling provides environmental scientists with a means of examining specific relationships among selected variables operating within systems that are extremely large, long-term, multicomponent, noncontrollable, multiscale, multidisciplinary, mulltivariate, nonlinear, and complex (Mulligan and Wainwright 2004). In combination with insight gained through scientific field and laboratory study, a model's abstraction and isolation of processes can aid inquiry by testing variables over an otherwise non-testable temporal or spatial scale, by testing a range of parameter values not practically tested in physical experiments, and by facilitating comparisons between different data sets used with the same model for simulations (Mulligan and Wainwright 2004).

Oreskes et al. (1994) explain that verifying whether or not a model is accurately representing relationships within a natural system is logically impossible because natural systems and the models used to represent them are open systems. Models include variables not completely known, and variables that depend on non-verifiable assumptions, so their results cannot be truly verified. Additionally, because the full extent of interactions between natural system components are not known, the convergence of model results with results of field or laboratory studies does not establish their validity.

Feyen et al. (1998) reviewed basic types of water flow and solute transport models in unsaturated, heterogeneous soils. They pointed out weaknesses inherent in traditional mathematical models for soil-water flow based on the Richards (1954) equation because of those models' inability to describe micro- and macro-level variation in soil porosity. It is therefore difficult, they said, to accurately model both the rate and direction of local water

movement in soil with preferential flow paths, and to use local-scale model-input hydraulic parameters to estimate field scale flow (Feyen et al. 1998). The authors also discuss alternative model types that better account for heterogeneity, but note the paucity of research providing field validation of any of these models over a range of soils and conditions.

Measuring or estimating the soil geometrical properties necessary for parameterization of the models presents other difficulties.

Cai et al. (1994) used Hydrus-1D to model water and salt storage and movement in a saline Australian red-brown earth (high clay soil) that was fallow in winter and ponded over three years during the summer with low-salinity groundwater. Their study was calibrated with data from a field study conducted earlier on the same soil. They concluded that low water content and low saturated hydraulic conductivity (Ks) were associated with greater soil water storage, that infiltration rate depended more on Ks than on water table depth (at water table depths greater than 1.5 m), and that a higher Ks promoted summer (saline water) recharge and winter (precipitation) leaching of salts from the profile.

Feng et al. (2003a, 2003b) constructed a model, ENVIRO-GRO, to examine plant growth, soil matric and osmotic pressure changes, salt distribution and rooting pattern effects with varying irrigation water volume, application frequency, and salinity on crop yield. They used data from an earlier study of corn yield as input to build the simulation and to compare measured with simulated results. They found good agreement between modeled and field-measured values for plant growth, pressure head changes and root growth effects, but less agreement for salt distribution. The authors cited their model's lack of need for curve-fitting parameters (for hydraulic conductivity, water retention and root water uptake functions) as an

advantage, but its inability to separate evaporation and transpiration as a weakness, particularly with regard to salt distribution estimation.

Tedeschi and Menenti (2002) used measurements made in a vegetable crop field experiment to build simulations using the SWAP (Soil-Water-Atmosphere-Plant) model to examine long-term (4 year) effects from irrigation at varying frequencies with sodic and fresh water on soil structure and on salt and water balance. They measured soil hydraulic property changes by constructing van Genuchten (1980) relationships for hydraulic conductivity as a function of water content ($K[\theta]$) and matric potential (K[h]) and by using van Genuchten parameters derived from treatment data to represent irrigation frequency and water salinity. They found that water retention curves were well-correlated with applied water sodicity, and that estimated parameters used in the model had a strong influence on results, even aside from inputs of water quality and initial soil conditions.

The Hydrus-1D Model

Hydrus-1D (ver. 2 1998, Simunek et al. 1998) is a model developed by the U.S. Salinity Laboratory to analyze water and solute flow through soils and other variably saturated porous media. The software provides routines for tracking water movement and root uptake, using the Richards (1954) equation [9] for water flow in variably saturated soils, with the addition of a sink term, *S*, for root water uptake.

$$\delta\theta/\delta t = \delta/\delta x \left[K \delta h / x + \cos \alpha \right] - S$$
 [9]
where *h* is water pressure head [L], θ is the volumetric water content [L³/L³], *t* is time,

x is the vertical spatial coordinate with positive values upward [L], and S is the root uptake sink term $[L^3/L^2t)$ (Simunek et al. 1998).

The Feddes et al. (1978) model for root water uptake as a function of soil matric potential is one option in Hydrus-1D for defining the *S* term

$$S(h) = \alpha(h)S_p \tag{10}$$

where $\alpha(h)$ is a function of the soil matric potential $(0 \le \alpha \ge 1)$ [dimensionless], and S_p is the potential water uptake rate [1/t] (Simunek et al. 1998).

Hydrus-1D solves the nonlinear Richards (1954) equation via numeric iteration with user-defined discretization of the soil profile into spatial nodes (depths) at which hydraulic properties (hydraulic capacity, hydraulic conductivity, and water content) are evaluated. Time discretizations for numerical computation solution intervals are also set by the user. Solutions are checked via water balance error calculated at prescribed times for selected regions within the flow domain. Water volume computed by water contents is compared with inflow minus outflow for each region (Simunek et al. 1998).

The Hydrus-1D model uses upper and lower boundary conditions (matric head, drainage, flux), weather (precipitation, evaporation, transpiration), and soil texture-dependent hydraulic properties as the primary variables controlling soil-water flow, and root density distribution and vegetation type as the controls on root uptake (Simunek et al. 1998). The van Genuchten model (Eq. [6] and [7]) is one option used to define the soil hydraulic conductivity and water retention functions. Hydraulic parameters are defined either directly by the user, or by the Rosetta Dynamically Linked Library (Schaap 2001) which uses pedotransfer functions with a neural network program to assign van Genuchten parameters to

soil textural classes or to specific particle size distribution and bulk density combinations (Hydrus-1D software help 1998).

Hydrus-1D output consists of matric head and water content readings over time at user-defined observation points in the profile; matric head, hydraulic properties, flux and root uptake over depth at specified times; boundary and root zone water fluxes and matric heads over time; and graphical representations of the K[h] and θ [h] functions. This output allows users to monitor hydraulic status at critical times during a simulation run, or at points of interest in the profile.

REFERENCES

ALL Consulting and CH2M HILL. 2001. Water resources technical report. Montana statewide oil and gas environmental impact statement and amendment of the Powder River and Billings resource management plans. Prepared for the U.S. Dept. of Interior, Bureau of Land Management, Miles City Field Office. Miles City, MT.

Ankeny, M.D., M. Ahmed, T.C. Kaspar, and R. Horton. 1991. Simple field method for determining unsaturated hydraulic conductivity. Soil Sci. Soc. Am. J. 55-467-470.

Ayers, R.S., and D.W. Wescott. 1985. Water quality for agriculture. FAO Irrigation and Drainage Paper 29, rev. 1. Food and Agriculture Organization of the United Nations, Rome.

Bauder, J.W. 2001. Recommended in-stream standards, thresholds, and criteria for irrigation or water spreading to soils of alluvial channels, ephemeral streams, floodplains, and potentially irrigable parcels of land within the boundaries of the Northern Cheyenne Reservation: Final report (unpublished). Montana State University, Bozeman.

Bauder, J.W., and T.A. Brock. 2001. Irrigation water quality, soil amendment, and crop effects on sodium leaching. Arid Land Res. Manage. 15:101-113.

Berman, D. 2003. BLM endorses water holding ponds in Powder River Basin EIS. Land Letter 10(9), 16 January 2003. (Available at http://web.lexis-exis.com/universe)(Verified 5 Aug. 2004).

Bethune, M.G., and T.J. Batey. 2002. Impact on soil hydraulic properties resulting from irrigating saline-sodic soils with low salinity water. Aust. J. Exp Agric. 42:273-279.

Cai, L., S.A. Prathapar, and H.G. Beecher. 1994. Modelling leaching and recharge in a bare transitional red-brown earth ponded with low salinity water in summer. Aust. J. Exp. Agric. 24:1085-1092.

California Fertilizer Association, Soil Improvement Committee. 1998. Using amendments to correct soil and growing-media problems. p. 229-241. *In* Western Fertilizer Handbook, 2nd Horticultural ed. Interstate Publishers, Danville, IL.

Chaudhari, S.K. 2001. Saturated hydraulic conductivity, dispersion, swelling, and exchangeable sodium percentage of different textured soils as influenced by water quality. Commun. Soil Sci. Plant Anal. 32:2439-2455.

Chaudhari, S.K., and R.B. Somawanshi. 2003. Unsaturated flow of different quality irrigation waters through clay, clay loam and silt loam soils and its dependence on soil and solution parameters. Agric. Water Manage. 64:69-90.

Churchman, G.J., J.O. Skjemstad, and J.M. Oades. 1993. Influence of clay minerals and organic matter on effects of sodicity on soils. Aust. J. Soil Res. 31:779-800.

Coalbed methane development in Montana: Hearing, U.S. Senate, Committee on Appropriations, March 10, 2001. Hearing before a Subcommittee of the Committee on Appropriations. S.Hrg. 107-104 (Available online at http://www.access.gpo.gov/congress/senate) (Verified 6 Sept. 2004).

Essington, M.E. 2004. Soil and water chemistry: An Integrative Approach. CRC Press, Boca Raton.

Evans, R.G., C.J. Smith, J.D. Oster, and B.A. Myers. 1990. Saline water application effects on furrow infiltration of red-brown earths. ASAE Trans. 33:1563-1572.

Feng, G.L., A, Meiri, and J. Letey. 2003a. Evaluation of a model for irrigation management under saline conditions. I. Effects on plant growth. Soil Sci. Soc. Am. J. 67:71-76.

Feyen, J., D. Jacques, A. Timmerman, and J. Vanderborght. 1998. Modelling water flow and solute transport in heterogeneous soils: a review of recent approaches. J. Agric. Eng. Res. 70:231-256.

Flores, R.M., G.D. Stricker, J.F. Meyer, T. Doll, P.H. Norton, Jr., R.J. Livingston, and M.C. Jennings. 2001. A field conference on impacts of coalbed methane development in the Powder River Basin, Wyoming. U.S. Geol. Surv. Open File Report 01-126. (Available online at http://geology.cr.usgs.gov/energy/OF01-126/text_OF01-126.pdf) (Verified 5 Aug. 2004).

Gable, E. 2003. Powder River Basin development proceeds despite lawsuits. Land Letter 10, May 8. (Available online at: http://web.lexis-nexis.com/universe). (Verified 21 Oct. 2004).

Gardner, W.R. 1958. Some steady-state solutions of the unsaturated moisture flow equation with application to evaporation from a water table. Soil Sci. 85:244-249.

Hanson, B., S.R. Grattan, and A. Fulton. 1999. Agricultural salinity and drainage. University of California Irrigation Program, Davis, CA.

Hemmer, D. 2001. Testimony. p. 55-58. *In* The orderly development of coalbed methane resources from public lands: oversight hearing, U.S. House of Representatives, Committee on Resources, Subcommittee on Energy and Mineral Resources. Sept. 6. Serial No. 107-58. (Available online at http://www.access.gpo.gov/congress/house/house12ch107.html) (Verified 5 Aug. 2004).

Hillel, D. 1998. Environmental soil physics. Academic Press, San Diego, CA.

- Jarvis, N.J., and I. Messing. 1995. Near-saturated hydraulic conductivity in soils of contrasting texture measured by tension infiltrometers. Soil Sci. Soc. Am. J. 59:27-34.
- Klute, A. and C. Dirksen. 1986. Hydraulic conductivity and diffusivity: Laboratory methods. p. 687-734. In Klute. A., ed. Methods of soil analysis, part 1: Physical and mineralogical methods, 2nd ed. ASA, Madison, WI.
- Knudsen, D., G.A. Peterson, and P.F. Pratt. 1982. Lithium, sodium, and potassium. P. 225-245. *In* Page, A.L., et al. (ed.) Methods of Soil Analysis, part 2: Chemical and Microbiological Properties. 2nd ed. American Society of Agronomy, Inc. Madison, WI.
- Levy, G.J. 1999. Sodicity. p. G27-G64. *In* Sumner, M.E. (ed.). Handbook of soil science. CRC Press, Boca Raton.
- Levy, G.J., I. Shainberg, and W.P. Miller. 1998. Physical properties of sodic soils. p. 77-94. *In* Sumner, M.E., and R. Naidu (ed.). Sodic soils: distribution, properties, management, and environmental consequences. Oxford University Press, New York.
- Levy, G.J., N. Sharshekeev, and G.L. Zhuravskaya. 2002. Water quality and sodicity effects on soil bulk density and conductivity in interrupted flow. Soil Sci. 167:692-700.
- Logsdon, S.D. and D.B. Jaynes. 1993. Methodology for determining hydraulic conductivity with tension infiltrometers. Soil Sci. Am J. 57:142-1431.
- Lowry, M.E., and J.F. Wilson, Jr. 1986. Hydrology of area 50, northern Great Plains and Rocky Mountain coal provinces, Wyoming and Montana. U.S. Geological Survey Water Resources Investigations, 83-545. Cheyenne, WY.
- Malik, M., M.A. Mustafa, and J. Letey. 1992. Effect of mixed Na/Ca solutions on swelling, dispersion and transient water flow in unsaturated montmorillonitic soils. Geoderma 52:17-28.
- McNeal, B.L., and N.T. Coleman. 1966. Effect of solution composition on soil hydraulic conductivity. Soil Sci. Soc. Am. Proc. 30:308-312.
- McNeal, B.L., D.A. Layfield, W.A. Norvell, and J.D. Rhoades. 1968. Factors influencing hydraulic conductivity of soils in the presence of mixed-salt solutions. Soil Sci. Soc. Am. Proc. 32:187-192.
- Minhas, P.S., and D.R. Sharma. 1986. Hydraulic conductivity and clay dispersion as affected by application sequence of saline and simulated rain water. Irrig. Sci. 7:159-167.

Montana Board of Environmental Review March 2003. Coalbed methane discharge standards. Available at: http://waterquality.montana.edu/docs/methane/cbmstandards.shtml. (Verified 7 Sept. 2004).

Mualem, Y. 1976. A new model for predicting the hydraulic conductivity of unsaturated porous media. Water Resour. Res. 12:513-522.

Mulligan, M., and J. Wainwright. 2004. Modelling and model building. p. 7-73. *In* Wainwright, J., and M. Mulligan (eds.). Environmental modeling: finding simplicity in complexity. John Wiley & Sons Ltd., West Sussex, England.

Norrish, K. 1954. The swelling of montmorillonite. Discuss. Faraday Soc. 18:120-134.

Nuccio, V.F. 2002. Coalbed methane – What is it? Where is it? And why all the fuss? p. 1-6. *In* Schwochow, S.D., and V.F. Nuccio (ed.) Coalbed methane of North America, II. Rocky Mountain Association of Geologists, [n.l.].

The Orderly development of coalbed methane resources from public lands, September 6, 2001. Oversight hearing before the Subcommittee on Mineral and Energy Resources, Committee on Resources, U.S. House of Representatives. Serial No. 107-58. (Available online at http://www.access.gpo.gov/congress/house) (Verified 6 Sept. 2004).

Oster, J.D. 1994. Irrigation with poor quality water. Agric. Water Manage. 25:271-297.

Oster, J.D., and I. Shainberg. 2001. Soil responses to sodicity and salinity: Challenges and opportunities. Aust. J. Soil Res. 39:1219-1224.

Perroux, K.M., and I. White. Designs for disc permeameters. Soil Sci. Soc. Am. J. 52: 1205-1215.

Quirk, J.P. 1986. Soil permeability in relation to sodicity and salinity. Philos. Trans. R. Soc. London Ser. A. 316:297-315.

Quirk, J.P., and R.K. Schofield. 1955. The effect of electrolyte concentration on soil permeability. J. Soil Sci. 6:163-178.

Quirk, J.P., and R.S. Murray. 1991. Towards a model for soil structural behaviour. Aust. J. Soil Res. 29: 829-867.

Radcliffe, D.E., and T.C. Rasmussen. 2001. Soil water movement. p. 85-126. *In* Warrick, A.W. (ed.) Soil physics companion. CRC Press, Boca Raton.

Reynolds, W.D., and D.E. Elrick. 1991. Determination of hydraulic conductivity using a tension infiltrometer. Soil Sci. Soc. Am. J. 55:633-639.

Reynolds, W.D., B.T. Bowman, R.R. Brunke, C.F. Drury, and C.S. Tan. 2000. Comparison of tension infiltrometer, pressure infiltrometer, and soil core estimates of saturated hydraulic conductivity. Soil Sci.Soc. Am J. 64:478-484.

Rhoades, J.D. 1972. Quality of water for irrigation. Soil Sci.113:277-284.

Rice, C.A., T.T. Bartos, and M.S. Ellis. 2002. Chemical and isotopic composition of water in the Fort Union and Wasatch formations of the Powder River Basin, Wyoming and Montana: Implications for coalbed methane development. *In* S.D. Schwochow and V.F. Nuccio (eds.) Coalbed methane of North America – II. Rocky Mountain Association of Geologists.

Schaap, M.G. 2001. ROSETTA: a computer program for estimating soil hydraulic parameters with hierarchical pedotransfer functions. J. Hydrol. 251:163-176.

Shainberg, I., and J. Letey. 1984. Response of soils to sodic and saline conditions. Hilgardia 52:1-57.

Shaw, R.J., K.J. Coughlan, and L.C. Bell. 1998. Root zone sodicity. p. 96-106. *In* Sumner, M.E., and R. Naidu (ed.). Sodic soils: distribution, properties, management, and environmental consequences. Oxford University Press, New York.

Simunek, J., K. Huang, M. Sejna, and M.Th. van Genuchten. 1998. Hydrus 1-D for Windows. U.S. Salinity Laboratory, Riverside, CA. Available at: http://www.ussl.ars.usda.gov/MODELS/HYDR1D1.HTM (Verified 4 Nov. 2004).

Singh, R.B., C.P.S. Chauhan, and R.K. Gupta. 1992. Effect of high salinity and SAR waters on salinization, sodication, and yields of pearl-millet and wheat. Agric. Water Manage. 21:92-105.

So, H.B., and L.A.G. Aylemore. 1995. *In* Naidu, R., M.E. Sumner, and P. Rengasamy, eds. Australian sodic soils: distribution, properties and management. CSIRO, East Melbourne, Victoria.

Steward, D.G.M. 2001. Testimony. p. 18-37. *In* The orderly development of coalbed methane resources from public lands: oversight hearing, U.S. House of Representatives, Committee on Resources, Subcommittee on Energy and Mineral Resources. Sept. 6. Serial No. 107-58. (Available online at

http://www.access.gpo.gov/congress/house/house12ch107.html) (Verified 27 Oct. 2004).

Suarez, D.L. 1981. Relation between pH_c and sodium adsorption ratio (SAR) and an alternative method of estimating SAR of soil or drainage waters. Soil Sci. Soc. Am. J. 45:469-475.

- Sumner, M.E. 1995. Sodic soils: New perspectives. p. 1-33. In Naidu, R., M.E. Sumner, and P. Rengasamy, eds. Australian sodic soils: distribution, properties and management. CSIRO, East Melbourne, Victoria.
- Sumner, M.E., W.P. Miller, R.S. Kookana, and P. Hazelton. 1998. Sodicity, dispersion, and environmental quality. p. 149-172. *In* Sumner, M.E., and R. Naidu (ed.). Australian sodic soils: distribution, properties, and management. CSIRO, East Melbourne, Victoria.
- Tedeschi, A., and M. Menenti. 2002. Simulation studies of long-term saline water use: model validation and evaluation of schedules. Agric. Water Manage. 54:123-157.
- U.S. Bureau of Land Management, and State of Montana. 2002. Draft statewide oil and gas environmental impact statement (EIS) and amendment of the Powder River and Billings Resource Management Plans (RMPs). U.S. Bureau of Land Management, Miles City, MT. (Available online at http://www.deq.state.mt.us/CoalBedMethane/EIS.asp). (Verified 5 Aug. 2004).
- U.S. Bureau of Land Management, Buffalo Field Office. 2003. Final environmental impact statement and proposed plan amendment for the Powder River Basin Oil and Gas Project. WY-070.02-065. (Available online at http://www.wy.blm.gov/nepa/prb-feis/index.htm) (Verified 7 Sept. 2004).
- U.S. Dept. of Energy. 2002. DOE Study raises estimates of coalbed methane potential in Powder River Basin: Actual production will hinge on water disposal method. Available online at:
- http://www.netl.doe.gov/publications/press/2002/tl_cbm_powderriver.html (Verified 15 Nov. 2004).
- U.S. Geological Survey. 2000. Water produced with coal-bed methane. USGS Fact Sheet FS-156-00. Denver, Co. (Available at http://search.usgs.gov/) (Verified 27 Oct. 2004).
- U.S. Geological Survey. n.d. Water resources of Montana [online]. (Available at http://mt.water.usgs.gov/) (Verified 5 Apr. 2005).
- U.S. Salinity Laboratory Staff. 1954. Diagnosis and improvement of saline and sodic soils. Agric. Handb. 60 U.S. Gov. Print. Office, Washington, D.C.
- van Genuchten, M.Th.. 1980. A closed-form equation for predicting the hydraulic conductivity of unsaturated soils. Sci. Soc. Am. J. 44:892-898.
- Wheaton, J.R., and J.L. Olson. 2001. Overview of coal-bed methane development and a discussion of Montana impacts. p. 210-218. *In* Vincent, R. et al. (ed.) Land Reclamation a Different Approach. Proc. Annual Meeting of the American Society for Surface Mining and Reclamation, 18th. Vol. 1. ASSMR.

White, I., M.J. Sully, and K.M. Perroux. 1992. Measurement of surface-soil hydraulic properties: Disk permeameters, tension infiltrometers, and other techniques. *In* Topp, G. C., W.D. Reynolds, and R.E. Green (ed). Advances in Measurement of Soil Physical Properties: Bringing Theory into Practice, San Antonio, TX, 21-26 October 1990. SSSA Spec. Pub. No. 30. SSSA, Madison.

Whitney, G. 2001. Testimony. p. 5-14. *In* The orderly development of coalbed methane resources from public lands: oversight hearing, U.S. House of Representatives, Committee on Resources, Subcommittee on Energy and Mineral Resources. Sept. 6. (Available online at http://www.access.gpo.gov/congress/house/house12ch107.html) (Verified 5 Aug. 2004).

Wooding, R.A. 1968. Steady infiltration from a shallow circular pond. Water Resour. Res. 4:1259-1273.

Wyoming State Water Plan. Tongue/Powder River Basin overview. [n.d.] Statewide data inventory [online]. Available at: http://waterplan.state.wy.us/sdi/TP/TP-over.html (Verified 5 Aug. 2004).

CHAPTER 2

INFILTRATION WATER FLUX IN THREE MONTANA SOILS TREATED WITH SIMULATED COALBED METHANE, POWDER RIVER, AND RAIN WATERS

Introduction

The Powder River Basin (PRB), which straddles northeast Wyoming and southeast Montana, is a current site for development of an estimated 0.82 trillion m³ (29 trillion ft³) coalbed methane (CBM) resource (U.S. Dept. of Energy 2002). In Montana, the state's final environmental impact statement (EIS) for CBM development in the region (U.S. BLM 2003) allows for drilling of up to 26,000 new wells. This EIS ended a 4-year statewide moratorium on CBM development while federal and state agencies investigated environmental concerns associated with CBM extraction (Gable 2003). Among these concerns are potential effects on soil permeability of the often saline and sodic water co-produced with methane. Large volumes of this water are pumped to the land surface, especially in the well's early production stages, when hydrostatic pressure is reduced to allow gas release from coal surfaces (Flores et al. 2001). Use of this water for irrigation is one management option that has been proposed and implemented in some areas (The orderly development of coalbed methane resources 2001, Coalbed methane development in Montana 2001).

Sodic irrigation waters may reduce a soil's capacity to drain or to retain plant-available water by breaking down soil structure (Rengasamy and Olssen 1991, Levy et al. 1998). This is true especially when soils contain high-smectite clay fractions, as do many

montmorillonitic soils on irrigated acreage in the PRB (Meshnick 1977). Reductions in infiltration may occur when soil made sodic by application of high-sodium (Na) waters is exposed to low-salinity water such as rainfall or snowmelt. Monovalent Na⁺ has a low charge and large hydrated radius, and is less strongly attracted to negatively charged clay platelets than are smaller, divalent cations such as calcium (Ca²⁺) and magnesium (Mg²⁺). Clay platelets may separate with hydration of Na⁺ cations on the soil exchange, causing swelling and slaking of soil aggregates and dispersion of clays (Quirk and Schoffeld 1955, Sumner 1995). Even in soils without a significant clay fraction, dispersion of fines or organic matter due to sodicity may cause decreases in infiltration or in hydraulic conductivity (Sumner 1995, Chaudhari 2001).

The hydraulic conductivity (K) quantifies water flow through soils along a hydraulic gradient, from higher to lower potential energy (Hillel 1998). Water may flow through soils under positive pressure, such as when the soil is saturated and the soil surface is ponded, or in response to the negative potential energy exerted by drier areas in the soil matrix (Hillel 1998). The hydraulic conductivity function describes rates of soil water flow as a function of matric potential, K[h], or water content, $K[\theta]$.

The rate of soil water flow varies significantly with soil texture and structure (pore size distribution, pore geometry, pore connectivity) and with soil wetness. Coarser-textured or more highly structured soils generally have larger and more continuous pores, and have greater water flow rates under saturated conditions than soils with finer particles. Under some unsaturated (drier) conditions, a finer-textured or disaggregated soil, with smaller, but

still water-coated pores, will have a higher hydraulic conductivity than a coarser-textured soil (Hillel 1998).

Hydraulic conductivity is an extremely variable soil property. Measurements of Ks, the hydraulic conductivity at saturation water content, can vary spatially and temporally over four orders of magnitude within a short distance on the same soil, and different measurement techniques can also result in large measured variability (Radcliffe and Rasmussen 2001). The K[h] can easily vary over eight or more orders of magnitude across the range of field soil water contents.

The tension infiltrometer is a commonly used method for measuring the rate of water flow into soils (Hopmans et al. 2002). Perroux and White (1988) designed disc permeameters (also called tension infiltrometers, or TIs, here) to measure soil hydraulic properties under a range of positive and negative water supply potentials (h) in soils with macropore or other preferential flow conditions. Logsdon and Jaynes (1993) developed a nonlinear fitting technique using Wooding's (1968) equation to obtain optimal values for Ks and the α shape parameter, then substituting Ks and α into Gardner's (1958) equation to derive the K[h] function. K[h] estimates derived by this method agreed reasonably well with measurements taken by excavation of a one-dimensional soil column (Logsdon and Jaynes 1991).

Objectives

A repacked soils column study was conducted to examine the effects of CBM water application on hydraulic conductivity in three soils representative of irrigable soils in Montana's PRB. The sandy loam, silt loam, and clay loam soils were pre-treated with water

having a salinity and sodicity typical of CBM water in the Montana portion of the PRB, or with water typical in salinity and sodicity to the Powder River, currently a primary irrigation water source.

The study objective was to compare the effects of application of simulated CBM- and PR-quality waters on the infiltration flux rates at four water supply pressures (h). Comparisons were made to examine the effect of the two water qualities on soils with different textures and presence or absence of smectite clay minerals, and on the A and B horizons of each soil. Comparisons also examined effects of rainfall- or snowmelt-quality water (simulated using deionized, DI, water) on soils pre-treated with CBM or PR water.

Hypotheses were:

- Soils pre-treated with CBM water will exhibit a smaller infiltration flux when tested using CBM water compared with the same soils pre-treated and tested using PR water.
- Soils pre-treated with CBM water will exhibit a greater relative decrease in infiltration flux after DI water application, using DI test water, compared with soils pre-treated with PR water.
- B horizon soils will exhibit a greater relative decrease in infiltration flux after DI water application, using DI test water, compared with A horizon soils. B horizon soils pre-treated with CBM water will demonstrate a larger relative decrease in flux under DI water treatment than will the same soils pre-treated with PR water.

4) Soils with higher smectite clay mineral fraction will exhibit a greater relative decrease in infiltration flux after DI water application, using DI test water, compared with soils having lower smectite clay percentages. Smectite mineral-containing soils pre-treated with CBM water will show a greater relative decrease in flux under DI water treatment than will soils pre-treated with PR water.

Materials and Methods

Soils

Gallatin County, western Montana soil series matching the texture, basic mineralogy, and moisture regime of targeted soil series commonly used for irrigated agriculture in the Powder River Basin (Robinson 2003) were identified during the summer of 2003 with the assistance of Dr. Thomas Keck of the USDA Natural Resources Conservation Service (Whitehall, MT). The experiment was to be conducted in Gallatin County and therefore local soils were chosen for logistical reasons. Potential sites for these soils were located (Table 2) through the use of the Gallatin County Soil Survey (Brooker 2002) and data from the Montana Natural Resources Information System website (USDA NRCS Montana 2004). Soils used for the study were described in the field (Appendix A). Matching soils were located and landowner permission was secured, and samples of A and B horizon soils for the clay and silt loam sites were obtained in November, 2003, and for the sandy loam site in March, 2004 (Table 3, 4, Fig. 2).

Table 3. Soil borrow sites: geographic location and land use.

Soil	Sect, Twn, Rng	Geog. Coord.	Land Use
Clay loam	S11 T1N R1E	111° 33' W", 45° 51' 30 N	Range
Silt loam	S31 T1S R4E	111° 16' W, 45° 42' 30" N	Crop
Sandy loam	S26 T1N R1E	111° 26′ 30″ W, 45° 42′ 30″ N	Range

Baseline and treated soil samples were analyzed (MDS Harris Laboratories, Lincoln, NE) for sand, silt, and clay fractions and bulk density (Table 5). Specific surface area measurements were made by the Montana State University Soil Environmental Physics Laboratory using the EGME retention method (Pennell 2002, Table 5). MDS Harris also tested for cation exchange capacity (CEC), saturation extract electrical conductivity (EC, 1:1 soil:water), sodium adsorption ratio (SAR), and pH (Table 7), and for organic matter, exchangeable cations, and soil nutrients (Appendix C, Tables C1 and C2). Baseline soil samples were also tested (North Dakota State University Soil and Water Environmental Laboratory, Fargo, ND) for x-ray diffraction (XRD) analysis of mineralogy for particles <2um (Table 6). XRD output is included in Appendix B. The clay loam soil was the only</p> soil in which smectite minerals tested as present in the XRD analysis. Based on typical montmorillonite surface area estimates of 600 to 800 m²/g, and average surface areas for other clay minerals (Hillel 1998), smectite percentages for the clay loam soil were estimated as 23-32% for the A horizon, and 25-36% for the B horizon. This calculation excludes surface area contributions attributable to organic matter (approximately 3% mass fraction for the clay loam in both horizons).

a.



b.



c.



Fig. 2. Soil borrow sites in southwest Montana: a) sandy loam, b) silt loam, c) clay loam.

Table 4. Soil series as mapped in USDA-NRCS Gallatin County Soil Survey for soil borrow sites (GCSS Map Series), and soil series in Powder River Basin used for irrigated agriculture (PRB Target Series).

Soil	GCSS Map Soil Series	PRB Target Soil Series
Clay loam	Varney CL	Cherry, Spinekop, Thurlow SiCL
Silt loam	Amsterdam-Quagle SiL	Brushton, Lonna, Haverlon, Haverson SiL
Sandy loam	Chinook FSL	Glendive, Trembles, Glenburg FSL

GCSS = Gallatin County, MT Soil Survey (Brooker 2002)

PRB = Powder River Basin, MT

Table 5. Mean sand, silt, and clay percentages, bulk density, textural class and specific surface area (SA) for clay loam, silt loam, and sandy loam soils (n=3 for each horizon).

Soil	Horizon	Sand	Silt	Clay	Bulk Density	Specific SA
		(%)	(%)	(%)	(g/cm ³)	(m^2/g)
Clay Loam	A	40	30	30	1.2	192
	В	44	26	30	1.2	209
Silt Loam	A	16	62	22	1.2	84
	В	14	66	20	1.3	114
Sandy Loam	A	48	50	2	1.3	69
	В	52	44	4	1.3	75

Table 6. Soil mineralogy (XRD analysis, indicates presence only) (n=1). K is kaolinite, Ch is chlorite, I is illite, S is smectite, Q is quartz, F is feldspar, C is calcite.

Soil	Horizon	Clay Minerals	Other Minerals	
Clay Loam	A	K, Ch, I, S	Q, F, C	
	В	K, Ch, I, S	Q, F, C	
Silt Loam	A	K, I	Q, F, C	
	В	K, I	Q, F, C	
Sandy Loam	A	K, I	Q, F, C	
	В	K, I	Q, F, C	

Table 7. Baseline and treated soil chemistries: saturated paste EC, SAR, CEC, and pH (n=3). Analyses performed by MDS Harris Laboratories (Lincoln, NE).

Soil	Horizon	Status	EC	SAR	CEC	рН
			(dS/m)		(mmol _c /kg)	
Clay Loam	A	Baseline	0.78	2.28	32.3	8.2
		CBM	3.22	11.00	41.8	7.9
		PR	1.33	2.56	45.8	8.2
	В	Baseline	2.34	4.73	33.3	8.2
		CBM	3.85	11.16	45.4	8.6
		PR	1.53	3.11	42.2	8.0
Silt Loam	A	Baseline	2.90	0.35	26.5	7.4
		CBM	2.00	6.14	33.8	8.3
		PR	2.41	3.69	29.7	8.0
	В	Baseline	1.08	0.68	26.0	8.0
		CBM	2.79	8.46	31.0	8.1
		PR	1.76	2.18	29.3	8.2
Sandy Loam	A	Baseline	0.76	0.14	29.3	7.9
		CBM	2.31	11.45	23.7	8.6
		PR	1.04	2.37	24.9	8.4
	В	Baseline	0.57	0.15	22.0	8.1
		CBM	2.74	11.86	26.7	9.0
		PR	1.11	2.32	25.0	8.5

Soil Columns

The experiment was conducted between March and July 2004 in a glasshouse at the Montana State University Plant Growth Center. Five replicate 25 cm ID, 36 cm high PVC columns were prepared for A and B horizons of the three soils, and for two water quality treatments (CBM or PR water), for a total of 60 columns. Soils were sieved through 1.25 cm

grating to exclude large rocks and aggregates, and packed to 30 cm height in each column. Nylon mosquito netting and aluminum mesh window screen were secured to the bottom of each column to prevent loss of soil materials during handling and measurements. Columns were placed on a 35 cm deep masonry sand bed, capped with 0.5 cm of 0.28-0.34 mm diameter silica sand to promote hydraulic continuity from the bottoms of the soil columns.

Water Qualities

Target salinity and sodicity values for synthesized PR and CBM waters were set at 1.5 dS/m EC with an SAR of 4, and 3 dS/m EC with an SAR of 30, respectively. Target values for PR water were based on mean EC and SAR values from the U.S. Geological Survey monitoring station on the Powder River on the Montana-Wyoming border at Moorhead, MT (U.S. Geological Survey n.d.). Target values for CBM water were typical of EC and SAR measured in CBM wells in the northern Wyoming and southern Montana portion of the PRB (Rice et al. 2001, ALL Consulting and CH2M Hill 2001).

Synthesized CBM and PR waters were prepared in 20-L batches by mixing Bozeman, MT tapwater (Bozeman, Montana Water Quality Report 2003) with dry salts in appropriate ratios (Table 8). Deionized water was Bozeman, MT tapwater (Montana Water Quality Report 2003) passed through an ion exchange tank. Water quality was monitored throughout the study by submitting samples for laboratory analyses of Ca, Mg, and Na concentration, EC, and pH (AgVise, Northwood, ND, Table 10). The SAR was calculated using the measured Ca, Mg, and Na concentration values (Essington 2004). Mean values from laboratory test results are presented in Table 9.

Table 8. Salt concentrations used for synthesized CBM and PR water.

Salt	CBM	PR
	(g/L)	(g/L)
NaHCO ₃	0.9	0.4
K_2SO_4	0.05	0.2
NaCl	0.9	0.1
$MgSO_4$		0.1
CaCO ₃		0.1
CaCl		0.1

Table 9. Mean laboratory test results for DI and synthesized CBM and PR waters used in the soil columns experiments.

		CBM			PR			DI	
	EC	SAR	рН	EC	SAR	рН	EC	SAR	рН
	(dS/m)			(dS/m)			(dS/m)		_
Mean	3.03	30.72	8.49	1.59	4.91	8.29	0.04	0.03	7.72
SEM	0.09	1.28	0.04	0.06	0.16	0.02	0.01	0.01	0.35
n	10	10	10	22	22	22	5	5	5

CBM or DI Water Pre-treatments, DI Water Treatment, and Testing

The sequence of pre-treatments and testing was as follows:

1. Pre-treatment with either CBM or PR quality water. Half of the columns (30) were treated with 2-3 pore volumes (average 22 L) of CBM water. The other 30 columns were treated with the same amount of PR water. It was assumed that this volume would be sufficient to induce substantial change in infiltration flux response to the two water qualities. CBM or PR pre-treatment waters were administered every 1 or 2 days, over a period of 8-16 days. Water was administered from a watering can with disperser nozzle and ponded to the 5 cm depth allowed by the column lip extending

above the soil surface. After pre-treatment, columns were allowed to drain for 3 to 10 days before testing began. Soil surfaces were leveled and 2-3 mm depth of fine silica sand was applied to ensure complete contact between the infiltrometer disk membrane and the soil surface.

- 2. Testing with pre-treatment water. Infiltration flux was measured for all soil columns pre-treated with CBM water, using CBM water in the infiltrometer (CBM-CBM), and all columns pre-treated with PR water were similarly tested using PR water in the infiltrometer (PR-PR).
- 3. Treatment with DI water. All soil columns were then treated with 1 L DI water. DI water treatment was administered from a watering can with a disperser nozzle in a single application and columns drained for 1 to 5 days before testing began with DI water in the infiltrometer.
- 4. Testing with DI water. All 60 columns were tested with DI water in the infiltrometer (CBM-DI or PR-DI).

Tension Infiltrometer Measurements

Tension infiltrometer (TI) procedures followed a modified version of Logsdon and Jaynes (1993). Two tension infiltrometers (Vadose Zone Equipment Co., Amarillo, TX, and Soil Measurement Systems, Tucson, AZ) were used to measure two columns simultaneously. Columns were tested at four ascending supply pressures (-12, -6, -2, and -0.5 cm) with pretreatment water (CBM or PR water) and, subsequently, with DI water at the same supply pressures. Before quasi-steady-state infiltration flux measurements were taken, TI flow rates

were equilibrated on soils for a minimum of 1.25 h for the -12 cm supply pressure, 1 h for the -6 cm supply pressure, and 0.75 h for the -2 and -0.5 cm supply pressures. A minimum of ten incremental measurements of water level decline in the TI supply reservoir vs. time were taken at each supply pressure, at intervals of 10 min for the -12 and -6 cm supply pressures, and 5 min for the -2 and -0.5 cm supply pressures.

Measurements of water level decline in the TI supply reservoir through time were entered into MS Excel[®], and used along with radii of the TI supply tower and the disk membrane, to calculate mean infiltration fluxes (volume of water flowing through the soil area per unit time, cm/h) for each supply pressure on each soil column. A quasi-steady state flux rate measurement was thereby generated for each of the four supply pressures for each of the 60 columns as tested with pre-treatment water (CBM-CBM or PR-PR), and another set of four flux rates generated for each column as tested with DI water (CBM-DI or PR-DI).

Data Analysis

ANOVA and multiple comparisons testing (SPSS, ver. 13.0, 2004) were used to evaluate statistical significance (P<0.10) in differences among means in the two response factors of interest. These response factors were the pre-treatment water flux (CBM-CBM or PR-PR) and the relative flux decrease using DI water (CBM-DI or PR-DI). Relative flux decrease was calculated as the difference between pre-treatment water and DI water flux, divided by the pre-treatment water flux for each column, e.g. [(CBM-CBM) – (CBM-DI)] / (CBM-CBM). Pre-treatment water flux data were natural log-transformed. Relative flux

decrease data were transformed by adding 2 (to make all values positive) and taking the reciprocal.

Main factors in the ANOVA were soil, horizon, pre-treatment water quality, and supply pressure. Separate data columns incorporating multiple factors (e.g., horizon and pre-treatment water quality) were prepared to allow post-hoc testing in SPSS of main factor interaction effects.

Because variances were substantially greater in the clay and silt loams than in the sandy loam, statistical evaluations were completed within soils, except for a single ANOVA among soils to address Hypothesis 4. This latter evaluation was checked with a non-parametric Jonckheere-Terpstra test (SPSS, 2004). Also because of the non-homogeneity of variance among soils, multiple comparisons were completed using the Tamhane T2 test, a conservative means comparison based on pairwise t-tests.

Results

Hypothesis 1:

Soils pre-treated with CBM water will exhibit a smaller infiltration flux when tested using CBM water (CBM-CBM) compared with the same soils pre-treated and tested using PR water (PR-PR).

ANOVA results comparing differences in mean flux measurements taken for CBM-CBM or PR-PR columns, for each soil, are presented in Table D1, Appendix D.

Hypothesis 1 was validated for the sandy and clay loam soils, in which pre-treatment water quality was a significant factor in variation between mean infiltration flux rates

measured using pre-treatment water (PreTreatmentWaterQuality, P<0.001 for both soils). For the sandy loam soil, mean flux values were 0.60 and 0.81 cm/h for CBM-CBM and PR-PR columns, respectively. For the clay loam, mean flux values for CBM-CBM and PR-PR columns were 0.26 and 0.59 cm/h, respectively.

The hypothesis was not validated for the silt loam soil, in which pre-treatment water quality did not result in significant differences in infiltration flux measurements between CBM-CBM and PR-PR columns (PreTreatmentWaterQuality, P=0.595). For the silt loam soil, mean flux values for CBM-CBM and PR-PR columns were 0.46 and 0.56 cm/h, respectively (Fig. 3).

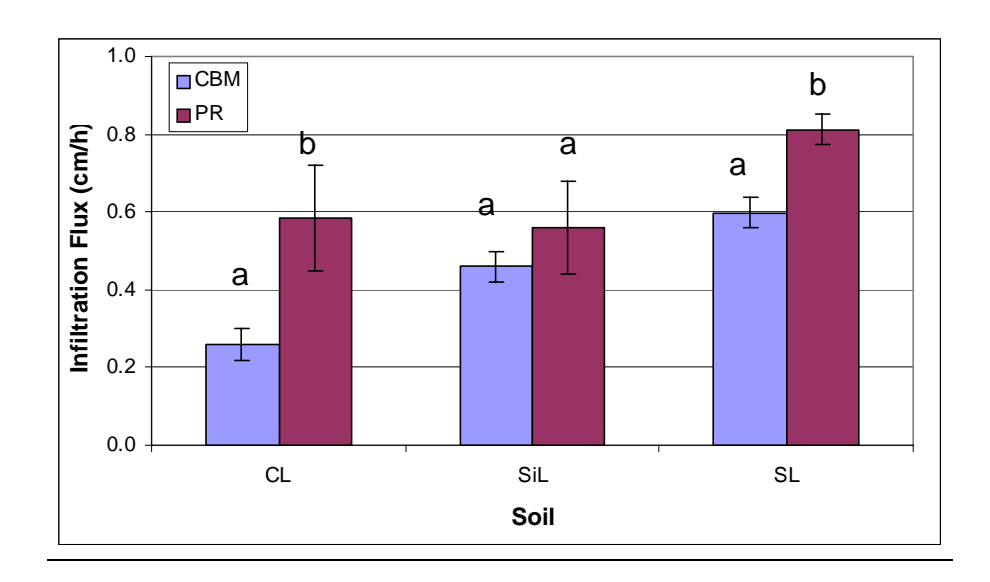


Fig. 3. Mean infiltration flux measurements using pre-treatment waters for soils pre-treated with CBM and PR water. Letters above columns indicate significant differences within soil type. Error bars are standard error of mean differences (n=5).

Hypothesis 2:

Soils pre-treated with CBM water will exhibit a greater relative decrease in infiltration flux after DI water application, using DI test water [(CBM-CBM) – (CBM-DI)] / (CBM-CBM), compared with soils pre-treated with PR water [(PR-PR) – (PR-DI)] / (PR-PR).

ANOVA results comparing mean relative flux decreases with DI water, for each soil, are presented in Table D2, Appendix D.

There were no significant effects of pre-treatment water quality (PreTreatmentWaterQuality) on relative flux decrease for the silt loam (P=0.529) or clay loam (P=0.621) soils, but there was a greater relative decrease in flux for CBM-pre-treated than for PR-pre-treated soils for the sandy loam soil (P<0.001). Relative decreases in flux for CBM-DI and PR-DI were 0.29 and 0.28 for the clay loam soil, 0.21 and 0.30 for the silt loam soil, and 0.46 and 0.38 for the sandy loam soil (Fig. 4). Laboratory test results indicated a greater change in SAR between baseline and CBM pre-treated soils for the sandy loam than for the silt loam or clay loam soils (Fig. 5).

Hypothesis 3:

B horizon soils will exhibit a greater relative decrease in infiltration flux after DI water application, using DI test water, compared with A horizon soils. B horizon soils pre-treated with CBM water (CBM-DI) will demonstrate a larger relative decrease in flux in under DI water treatment than will the same soils pre-treated with PR water (PR-DI).

ANOVA results comparing mean relative flux decrease with DI water, for each soil, are presented in Table D2, Appendix D.

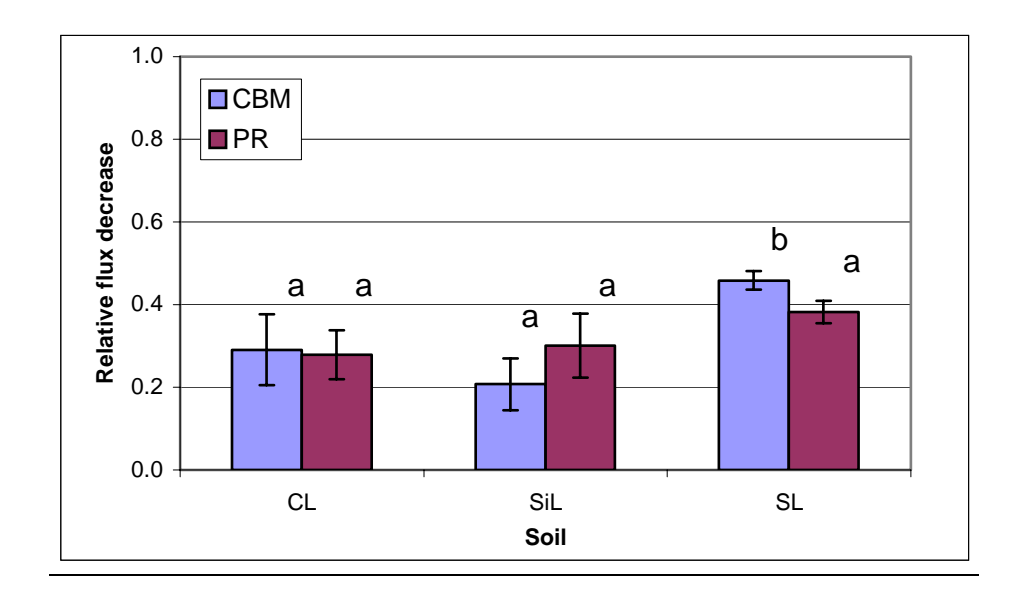


Fig. 4. Mean relative decrease in infiltration flux measurements using DI water, by soil and pre-treatment water quality. Values were calculated as (pre-treatment water flux - DI water flux)/pre-treatment water flux. Letters above columns indicate significant differences within soil type. Error bars are standard error of mean differences (n=5).

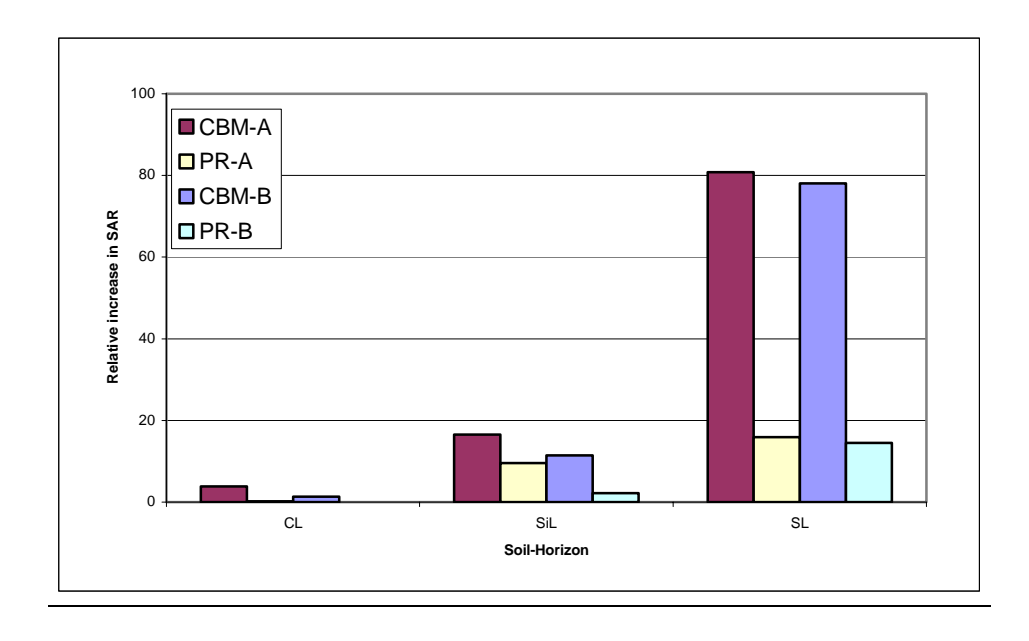


Fig. 5. Mean relative increase in soil sodium adsorption ratio (SAR) for A and B horizons after pre-treatment with CBM or PR water compared with baseline soil SAR, by soil, horizon and pre-treatment water quality. Values were calculated as mean (pre-treated SAR - baseline SAR)/baseline SAR. Error bars are standard error of mean differences (n=3).

Multiple comparison test results to examine mean relative flux decreases between horizon by pre-treatment water quality pairs, for the clay loam soil, are presented in Table D3, Appendix D.

The A and B horizons showed significantly different relative flux decreases of 0.31 and 0.53, respectively, in the sandy loam soil (Horizon, P<0.001). No effect of horizon was observed for the silt loam or clay loam soils (Horizon, P=0.137, P=0.403, respectively). Mean relative flux differences were 0.145 and 0.363 for the A and B horizons in the silt loam, and 0.317 and 0.253 for the A and B horizons in the clay loam (Fig. 6).

A significant horizon by pre-treatment water quality interaction was observed only in the clay loam (Horizon*PreTreatmentWQ, P=0.012), indicating a difference in trend between the two horizons for pre-treatment water quality influence on soil response to DI water treatment (Fig. 7). In the sandy and clay loams, the horizon by pre-treatment water quality interaction was not significant (P=0.667 and P=0.527, for the sandy and clay loams, respectively). Multiple comparison tests to examine relationships between horizon by pre-treatment water quality pairs in the clay loam soil indicated no significant differences between any horizon by pre-treatment water quality pairs.

Hypothesis 4:

Soils with higher smectite clay mineral fraction will exhibit a greater relative decrease in infiltration flux after DI water application, using DI test water, compared with soils having lower smectite clay percentages. Smectite mineral-containing soils pre-treated with CBM

water will show a greater relative decrease in flux under DI water treatment than will soils pre-treated with PR water.

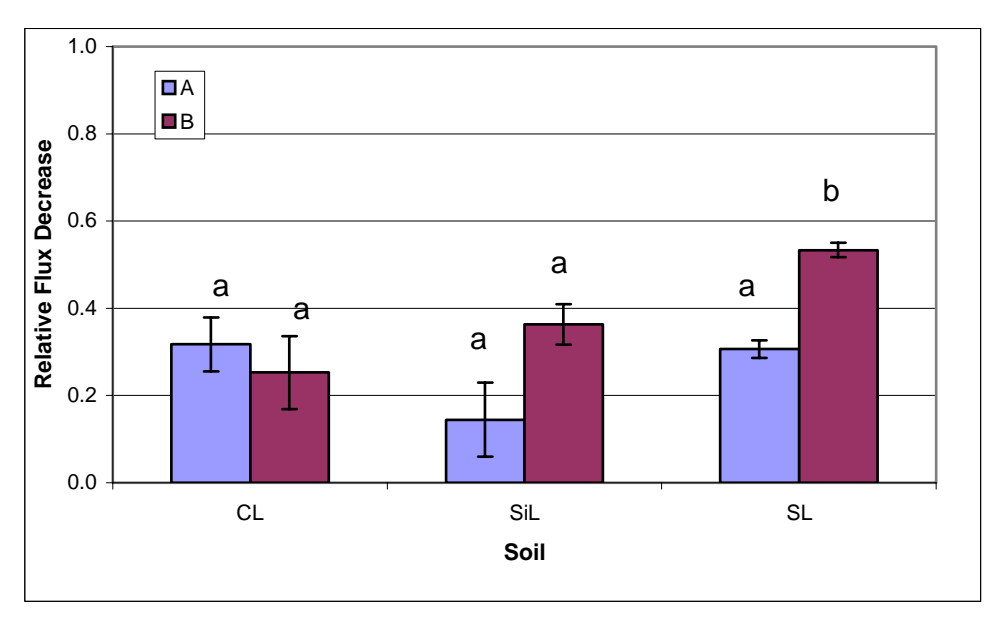


Fig. 6. Mean relative decrease in infiltration flux measurements using DI water, by soil and horizon. Values were calculated as (pre-treatment water flux - DI water flux)/pre-treatment water flux. Letters above columns indicate significant differences within soil type. Error bars are standard error of mean differences (n=5).

ANOVA results comparing mean relative flux decreases among soils are presented in Table D4, Appendix D. Results of the non-parametric Jonckheere-Terpstra non-parametric tests on the same data are in Tables D5 and D6, Appendix D.

No significant effect of soil (Soil, P=0.114, Fig. 8) or of the soil by pre-treatment water quality interaction (Soil*PreTreatmentWQ, P=0.631, Fig. 9) were observed, although the former was close to the selected significance value of P=0.10.

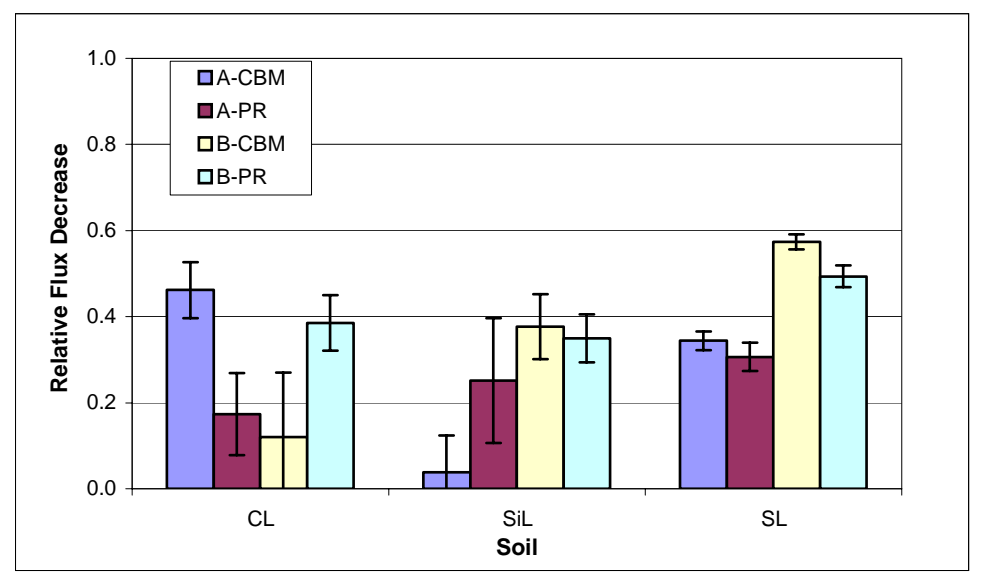


Fig. 7. Mean relative decrease in infiltration flux measurements using DI water, by soil, horizon, and pre-treatment water quality. Values were calculated as (pre-treatment water flux - DI water flux)/pre-treatment water flux. No significant differences were observed within soils. Error bars are standard error of mean differences (n=5).

Because the measured data set used for this ANOVA failed Levene's test for homogeneity of variance between soils, non-parametric Jonckheere-Terpstra tests were also completed to evaluate any effect on variation among soils or for the soil by pre-treatment water quality interaction. These tests indicated no effect of soil (P=0.150), but a marginally significant effect of the soil by pre-treatment water quality interaction (P=0.099).

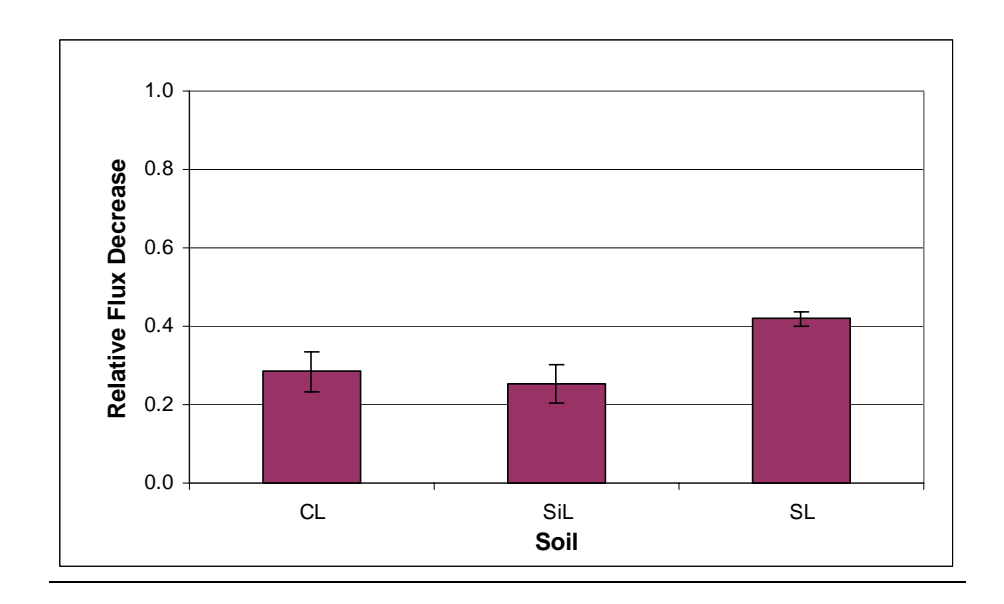


Fig. 8. Mean relative decrease in infiltration flux measurements using DI water, by soil. Values were calculated as (pre-treatment water flux - DI water flux)/pre-treatment water flux. No significant differences were observed among soil types. Error bars are standard error of mean differences (n=5).

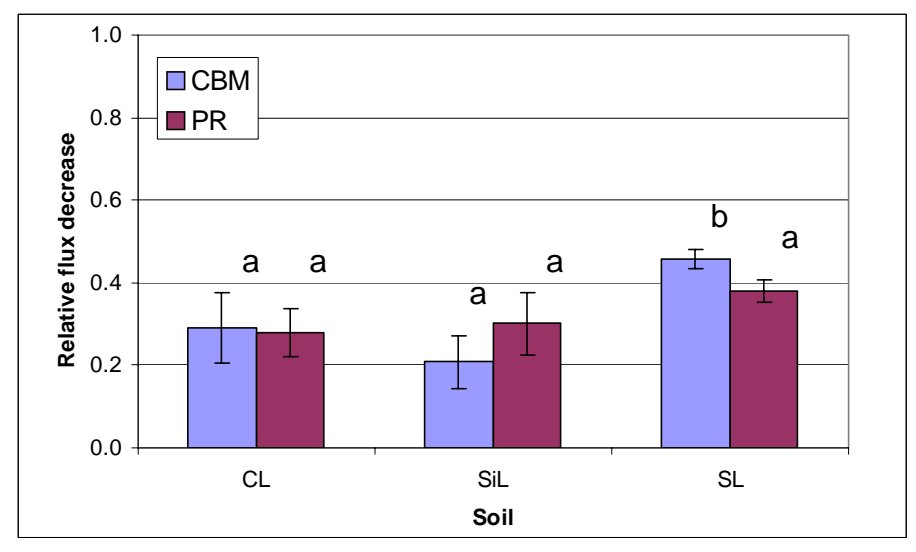


Fig. 9. Mean relative decrease in infiltration flux measurements using DI water, by soil and pre-treatment water quality. Values were calculated as (pre-treatment water flux - DI water flux)/pre-treatment water flux. No significant differences were observed among soil types. Error bars are standard error of mean differences (n=5).

Discussion

For the three soils evaluated, exposure to the high-SAR CBM water could be expected to result in a greater dispersal of fines, and possibly of organic matter, than would exposure to the lower-SAR PR water (Levy et al. 1998, Sumner 1995). This dispersion could result in a decrease in mean pore diameter, and resultant slowing of water movement through the soil column, as Na⁺ replaced smaller, bivalent cations on the exchange complex, and as clay particles moved apart. The sandy loam and clay loam soils exhibited lower water fluxes when pre-treated (and measured) with CBM water compared with PR water.

The silt loam soil, which did not show a significant difference in water flux between the two pre-treatment water qualities, had a very high mean baseline soluble calcium content in the A horizon (16.6 meq/L, with 7.1 meq/L in the B horizon; Appendix C, Table C2). This compares with averages of 7.8 and 5.9 meq/L for the A and B horizons in the sandy loam soil, and 3.1 and 7.9 meq/L in the clay loam soil. Mean baseline EC values for the silt loam soil were 2.91 and 1.08 dS/m for the A and B horizons, respectively; higher than baseline EC values for the other soils (Appendix C, Table C2). The calcium and the relatively high baseline salinity in the untreated silt loam soil may have effectively buffered the effects of the sodium applied in CBM water, thus maintaining clay and organic matter floccules, and preventing a significant decrease in water flow rate relative to PR water application (Hillel 1998, Shainberg and Letey 1984).

Exposure to low-salinity waters may cause reduction of soil permeability via dispersion of fine soil particles in soils equilibrated with sodic application waters, as water molecules enter spaces between clay platelets, hydrate Na⁺ ions, and separate the platelets (Quirk and

Schofield 1955, Sumner 1995). The relative decrease in measured infiltration flux using DI water on the two finer-textured, larger clay-fraction soils was not different between pretreatment water qualities (CBM vs. PR). Relative flux decreases in the coarser, low-clay sandy loam soil were affected more strongly by CBM water than by PR water pre-treatment. While this result runs counter to expectations for the soil textures (Levy 1999, McNeal and Coleman 1966, Frenkel et al. 1978), it is possible that dispersion of soil fines with DI treatment in the CBM pre-treated sandy loam soil caused a significant change in pore size and connectivity compared to PR pre-treatment. In the two finer soils we would expect any changes in water flow to result from aggregate swelling and slaking as well as soil particle dispersion (Sumner 1995, Chaudhari 2001). Comparison of baseline and treated soil chemistries indicates that the SAR of the sandy loam soil was increased more with CBM pretreatment than for the other two soils (Table 8). Mean SAR values in the A and B horizons of CBM-pre-treated sandy loam soil were 80.8 and 78.1 times the baseline values, while SARs in the A and B horizons of the clay loam and silt loam soils increased to only 3.8 and 1.4, and 16.5 and 11.4 times baseline values, respectively (Fig. 5).

An alternative explanation for the greater change in relative mean water flux difference between pre-treatment water qualities for the sandy loam is the smaller standard error in the sandy loam data set than for the other two soils (Appendix D, Table D7; standard error of 0.018 for the untransformed sandy loam measurements, compared with 0.050 for the silt loam and 0.052 for the clay loam). Infiltration water flux measurements were more variable among replicate soil columns for the heavier silty loam and clay loam soils at all supply pressures (Appendix D, Table D8).

Differences in susceptibility to a sodium-induced decrease in soil water flow rates is largely a function of clay content (assuming the same clay mineralogy), as clay is the primary soil component on which sodium is known to act (Shainberg and Letey 1984, Quirk and Schofield 1955). Soil B horizons are generally higher in clay than A horizons, which may increase B horizon soil vulnerability to effects of sodic waters (Shaw et al. 1998). The lack of full validation for the first portion of Hypothesis 3, with no difference observed between horizons for the silt loam or clay loam soils in relative water flux difference, is likely due to the fact that the A and B horizons did not differ greatly in clay content for any of the three soils used in this study (Table 6). Silt and sand percentages, as well as baseline soil chemistry (Appendix C) were also very similar between the two horizons for all three soils.

The sandy loam soil again had a smaller standard error of measurements than did the other two soils (Table D7 in Appendix D). Inherent variation in soil hydraulic properties is recognized as greater for finer soils (Carsel and Parish 1988), and it is more difficult to consistently repack finer-textured soils, potentially decreasing the repeatability among columns.

The second portion of Hypothesis 3 was also only partially validated. No horizon by pre-treatment water quality interaction was observed for the silt loam and sandy loam soils. The clay loam soil did show a difference in A and B horizon response to the two pre-treatments (Fig. 6), but there is no ready explanation for the apparently greater impact of CBM water on the A horizon and of PR water on the B horizon. Subsequent multiple comparisons tests for this soil did not identify significant differences between any horizon by pre-treatment water quality pairs.

The presence of the shrink-swell smectite clay minerals and the larger specific surface area for this clay type indicate an increase in the potential for sodium to act to swell and slake aggregates, to disperse clay particles, and thereby to reduce mean pore size and connectivity, resulting in decreased flow rates (Quirk and Schofield 1955, Regea et al. 1996). Because the soils were sieved then repacked into soil columns, a substantial lack of larger soil aggregates may have altered the potential for reduced flow rates in the clay loam soil, assuming partial aggregate destruction with CBM water exposure. This might not be the case for field soils, however. No two- or three-way interactions involving soil type were observed in the statistical evaluations. Contributions to variation in the ANOVA model were distributed relatively evenly among several factors, and only the horizon by pre-treatment water quality interaction was significant (Horizon*PreTreatmentWQ, P=0.093).

The conventional methods used for this column study may have limited its ability to represent conditions that might occur in the field. These methods included most importantly the sieving and repacking of soils, which likely reduced inter-soil variation in macro-scale aggregation, an important contributor to hydraulic behavior. The study also did not include seasonal soil mixing by freeze-thaw, or other phenomena known to influence infiltration and hydraulic conductivity in the field.

The results of this soil columns study provide mixed implications for the potential use of CBM water for irrigation in the PRB. The clay loam and sandy loam soils, which had very different particle size distributions and clay contents but which both had modest calcium concentrations (in comparison to the silt loam soil) appeared to transmit CBM water more slowly than PR water, after equilibration with those water qualities. The silt loam soil A

horizon, which was higher in calcium, appeared to resist the infiltration-inhibiting effects of the CBM water's high SAR. This suggests that consideration of soil salt chemistry may be at least as important as identification of soil texture, clay content and clay mineralogy when agricultural use of CBM water is considered.

If high-SAR CBM water is used for irrigation, it is critical that exposed soils maintain their capacity to absorb and conduct low-salinity rainwater during summer storms and snowmelt in late winter and spring, as well as any lower-salinity surface or groundwaters that may also be used for irrigation or leaching (Bethune and Batey 2002). Results presented here comparing infiltration flux measurements using DI water compared to those for the same columns using pre-treatment quality (CBM or PR) waters also suggest that soil texture or clay fractions should not be the sole or even primary considerations. It is possible that a more coarsely-textured, lower-clay soil such as the sandy loam used in this study, may exhibit significant decreases in water flow after CBM water exposure, and, that the salt chemistry of the untreated soil compared to that of the application water may be an important component in decisions about using CBM water for irrigation.

Irrigation with CBM water over several seasons is a possibility presented to some land managers in the PRB. In this experiment, soils were exposed to 2-3 pore volumes of CBM or PR water in 10-15 treatments over a few days or weeks. This pre-treatment regime was not intended to fully replicate exposure of field soils to irrigation with the same waters over multiple seasons. It is possible that, with a more prolonged exposure to CBM water, results may have been different. For example, sandy soils may show a decrease in infiltration or hydraulic conductivity after initial exposure to high-SAR application waters, but then exhibit

a "recovery" to higher infiltration flux or conductivity with time, as fines are dispersed and leached from the profile completely (Sumner 1995). Conversely, more aggregated soils, with higher clay and silt contents, may be resistant to sodicity effects over an initial exposure period, maintaining hydraulic conductivity through macropore flow, but may show a decline in water flow as aggregates are broken down and larger pores are narrowed or clogged with dispersed fines (Sumner 1995).

These experimental results tend to verify the contention expressed by other researchers that hydraulic effects of a sodic applied water on a soil cannot be adequately predicted according to any simple formula incorporating EC, SAR, soil texture or soil clay content as the only factors, but that there appear to be fairly complex interactions of several soil and water quality characteristics determining the outcome (Malik 1992, McNeal and Coleman 1968).

REFERENCES

ALL Consulting and CH2M HILL. 2001. Water resources technical report. Montana statewide oil and gas environmental impact statement and amendment of the Powder River and Billings resource management plans. Prepared for the U.S. Dept. of Interior, Bureau of Land Management, Miles City Field Office. Miles City, MT.

Ankeny, M.D., M. Ahmed, T.C. Kaspar, and R. Horton. 1991. Simple field method for determining unsaturated hydraulic conductivity. Soil Sci. Soc. Am. J. 55-467-470.

Bauder, J.W. 2001. Recommended in-stream standards, thresholds, and criteria for irrigation or water spreading to soils of alluvial channels, ephemeral streams, floodplains, and potentially irrigable parcels of land within the boundaries of the Northern Cheyenne Reservation: Final report (Unpublished). Montana State University, Bozeman.

Bethune, M.G., and T.J. Batey. 2002. Impact on soil hydraulic properties resulting from irrigating saline-sodic soils with low salinity water. Aust. J. Exp Agric. 42:273-279.

Bozeman, Montana Water Quality Report. [2003] [Online]. Available at: http://www.bozeman.net/wtp/wtp.htm. (Verified 20 Aug. 2004).

Brooker, J.W. 2002. Soil survey of Gallatin County area, Montana. [Washington, D.C]: Natural Resources Conservation Service. 1 case (2 pts., 45 folded p. of plates).

Carsel, R.F., and R.S. Parish. 1988. Developing joint probability distributions of soil water retention characteristics. Water Resour. Res. 24:755-769.

Chaudhari, S.K. 2001. Saturated hydraulic conductivity, dispersion, swelling, and exchangeable sodium percentage of different textured soils as influenced by water quality. Commun. Soil Sci. Plant Anal. 32:2439-2455.

Coalbed methane development in Montana: Hearing, U.S. Senate, Committee on Appropriations, March 10, 2001. Hearing before a Subcommittee of the Committee on Appropriations. S.Hrg. 107-104 (Available online at http://www.access.gpo.gov/congress/senate) (Verified 6 Sept. 2004).

Essington, M.E. 2004. Soil and water chemistry: An integrative approach. CRC Press, Boca Raton.

Flores, R.M., G.D. Stricker, J.F. Meyer, T. Doll, P.H. Norton, Jr., R.J. Livingston, and M.C. Jennings. 2001. A field conference on impacts of coalbed methane development in the Powder River Basin, Wyoming. U.S. Geol. Surv. Open File Report 01-126. (Available online at http://geology.cr.usgs.gov/energy/OF01-126/text_OF01-126.pdf) (Verified 5 Aug. 2004).

Frenkel, H., J.O. Goertzen, and J.D. Rhoades. 1978. Effects of clay type and content, exchangeable sodium percentage, and electolyte concentration on clay dispersion and soil hydraulic conductivity. Soil Sci. Soc. Am. J. 42: 32-39.

Gable, E. 2003. Powder River Basin development proceeds despite lawsuits. Land Letter 10, May 8. (Available online at: http://web.lexis-nexis.com/universe). (Verified 21 Oct. 2004).

Gardner, W.R. 1958. Some steady-state solutions of the unsaturated moisture flow equation with application to evaporation from a water table. Soil Sci. 85:244-249.

Hillel, D. 1998. Environmental soil physics. Academic Press, San Diego, CA.

Hopmans, J.W., J. Simunek, N. Romano, and W. Durner. 2002. The soil solution phase: inverse methods. p. 963-1074. *In* Dane J.H., and G. C. Topp (ed.) Methods of soil analysis, Part 4, Physical methods. SSSA, Madison, WI.

Jarvis, N.J., and I. Messing. 1995. Near-saturated hydraulic conductivity in soils of contrasting texture measured by tension infiltrometers. Soil Sci. Soc. Am. J. 59:27-34.

Leij, F.J., W.J. Alves, M. Th. van Genuchten, and J.R. Williams. 1996. The UNSODA unsaturated hydraulic conductivity database. EPA/600/R-96/095. U.S. Environmental Protection Agency, Cincinnatti, OH.

Levy, G.J., I. Shainberg, and W.P. Miller. 1998. Physical properties of sodic soils. p. 77-94. *In* Sumner, M.E., and R. Naidu (ed.). Sodic soils: Distribution, properties, management, and environmental consequences. Oxford University Press, New York.

Logsdon, S.D. and D.B. Jaynes. 1993. Methodology for determining hydraulic conductivity with tension infiltrometers. Soil Sci. Am J. 57:142-1431.

Meshnick, J.C. 1977. Soil survey of Big Horn County, Montana. U.S. Soil Conservation Service, n.l.

Mualem, Y. 1976. A new model for predicting the hydraulic conductivity of unsaturated porous media. Water Resour. Res. 12:513-522.

Orderly Development of Coalbed Methane Resources from Public Lands, September 6, 2001. Oversight hearing before the Subcommittee on Mineral and Energy Resources, Committee on Resources, U.S. House of Representatives. Serial No. 107-58. (Available online at http://www.access.gpo.gov/congress/house) (Verified 6 Sept. 2004).

Pennell, K.D. 2002. Specific surface area. P. 295-315. *In* Dane J.H., and G. C. Topp (ed.) Methods of soil analysis, Part 4, Physical methods. SSSA, Madison, WI.

Perroux, K.M., and I. White. 1988. Designs for disc permeameters. Soil Sci. Soc. Am. J. 52: 1205-1215.

Quirk, J.P., and R.K. Schofield. 1955. The effect of electrolyte concentration on soil permeability. J. Soil Sci. 6:163-178.

Radcliffe, D.E., and T.C. Rasmussen. 2001. Soil water movement. p. 85-126. *In* Warrick, A.W. (ed.) Soil physics companion. CRC Press, Boca Raton.

Regeo, M, T. Yano, and I. Shainberg. The response of low and high swelling smectites to sodic conditions. Soil Sci. 162:299-307.

Rengasamy, P., and K.A. Olsson. 1991. Irrigation and sodicity: an overview. p. 195-203. *In* Naidu, R., M.E. Sumner, and P. Rengasamy, eds. Australian sodic soils: Distribution, properties and management. CSIRO, East Melbourne, Victoria.

Reynolds, W.D., and D.E. Elrick. 1991. Determination of hydraulic conductivity using a tension infiltrometer. Soil Sci. Soc. Am. J. 55:633-639.

Robinson, K.M. 2003. Effects of saline-sodic water on EC, SAR, and water retention. M.S. Thesis. Montana State Univ., Bozeman.

Shainberg, I., and J. Letey. 1984. Response of soils to sodic and saline conditions. Hilgardia 52:1-57.

Sumner, M.E. 1995. Sodic soils: New perspectives. p. 1-33. In Naidu, R., M.E. Sumner, and P. Rengasamy, eds. Australian sodic soils: Distribution, properties and management. CSIRO, East Melbourne, Victoria.

U.S. Bureau of Land Management, Buffalo Field Office. 2003. Final environmental impact statement and proposed plan amendment for the Powder River Basin Oil and Gas Project. WY-070.02-065. (Available online at http://www.wy.blm.gov/nepa/prb-feis/index.htm) (Verified 7 Sept. 2004).

U.S. Dept. of Energy. 2002. DOE Study raises estimates of coalbed methane potential in Powder River Basin: Actual production will hinge on water disposal method. Available online at:

http://www.netl.doe.gov/publications/press/2002/tl_cbm_powderriver.html (Verified 15 Nov. 2004).

U.S. Geological Survey. n.d. Water quality data for Montana [Online]. Available at: http://waterdata.usgs.gov/mt/nwis/nwis (Verified 24 Aug. 2004).

U.S. Natural Resources Conservation Service Montana. 2004. Montana soils data [Online]. Available at: http://www.nris.state.mt.us/nrcs/soils/ (Verified 23 Aug. 2004).

van Genuchten, M.Th.. 1980. A closed-form equation for predicting the hydraulic conductivity of unsaturated soils. Sci. Soc. Am. J. 44:892-898.

Wraith, J.M., and D. Or. 1998. Nonlinear parameter estimation using spreadsheet software. J. Nat. Resour. Life Sci. Educ. 27:13-19.

CHAPTER 3

SIMULATION OF SOIL PROFILE WATER BALANCE IN RESPONSE TO IRRIGATION WITH COALBED METHANE AND POWDER RIVER WATERS

Introduction

Water co-produced with coalbed methane (CBM) extraction represents a significant potential source of irrigation water in southeastern Montana's semiarid Powder River Basin (PRB), where methane development is expected to increase to an estimated 26,000 wells over the next decade (U.S. BLM et al. 2003). Each well generates an average 108,000-136,000 L (28,000-36,000 gallons) per day during the first 2 years of gas production, with an average of 13,000 L (3,600 gallons) per day over a 20-year production life (ALL Consulting and CH2M HILL 2001). Possible CBM water disposition methods include release of CBM water into surface channels currently used as sources for agricultural flood irrigation, and direct application of CBM water onto crop or pasture lands via sprinkler irrigation (Coalbed methane in Montana 2001, The orderly development of coalbed methane 2001). Flood irrigation (water spreading) of lowland fields with access to surface water channels two or three times during the growing season is now commonly practiced in the PRB (J.W. Bauder, personal communication, 2004). Sprinkler irrigation with CBM water onto upland or other acres without access to surface water, with continuous sprinkler operation throughout the growing season, is a current and potentially expanding use for CBM product water (J.W. Bauder, personal communication, 2004).

One concern related to agricultural use of CBM product water is that it often has a high salinity and sodicity, and that the presence of high salts and sodium poses a potential risk to the soil's structure and porosity, which determine its water-conducting capacity. PRB soils are often high in dissolved salts and sodium, due to the region's marine shale geology and dry climate (Bauder and Brock 2001, Lowry and Wilson 1986). CBM water from the Montana portion of the basin is similar to Powder River water in salinity, as measured by electrical conductivity (EC), and higher than the Tongue River, the other main channel in the basin (U.S. Geological Survey n.d.). Montana PRB CBM water is significantly higher in sodium, as measured by sodium adsorption ratio (SAR) than are waters from the Powder or Tongue River (U.S. Geological Survey n.d.).

The Montana Board of Environmental Review (2003) set monthly mean and maximum EC and SAR standards for the four main river channels in the PRB. These standards are based on measured EC and SAR values from those channels during the 1990s. During the March-October irrigation season, EC must average between 1.0 and 2.0 dS/m (1.5-2.5 maximum), and SAR between 3.0 and 5.0 (4.5-7.5 maximum). CBM wellhead water values reported by the Montana Department of Environmental Quality in 2000 from the CX Ranch near Decker, just north of the Montana-Wyoming border, have an average EC of 2.2 dS/m, and an average SAR of 47 (ALL Consulting and CH2M HILL 2001). Researchers with the U.S. Geological Survey (Rice et al. 2002) reported similar EC and SAR values from CBM wells just south of the Montana-Wyoming border.

Application of high-Na waters can decrease soil infiltration capacity and hydraulic conductivity, particularly when the soil contains significant percentages of smectite clay

minerals, such as the montmorillonite clays present in some areas of the PRB (Meshnick 1977). The large clay surface areas associated with these minerals, combined with the lower electrochemical affinity for soil surfaces and large hydrated radius of monovalent Na⁺ compared to calcium (Ca²⁺), magnesium (Mg²⁺) and other soil cations, can cause clay platelets to separate in the presence of sodic waters. This separation may cause swelling and slaking of soil aggregates and dispersion of clay particles, reducing water flow between soil aggregates and clogging smaller soil pores (Ayers and Wescott 1985, Levy 1999).

High sodicity of irrigation waters is a particular issue where total salinity is low relative to Na concentration, as when snowmelt or rainwater is absorbed into a sodic soil. In such cases, there is insufficient concentration of small-radius, high surface-attracted cations (e.g. Ca²⁺, Mg²⁺) to counter the tendency of Na⁺ to separate clays, and cations are pulled away from mineral surfaces by the concentration diffusion gradient between the soil solution and soil surface exchange (Quirk and Schofield 1955, Shainberg and Letey 1984). In the process, silts and other fines may also be dispersed, contributing to decreases in soil permeability through clogging of pores (Sumner 1995, Minhas and Sharma 1986).

An additional concern is that wellhead-measured EC and SAR values may not reflect salinity and sodicity of CBM waters that have been allowed to equilibrate with atmospheric conditions. Bicarbonates characterizing the chemical signature of PRB CBM waters (van Voast 2003) may precipitate with calcium in soil or surface water to form calcium carbonate. This process lowers the EC and increases the SAR.

Various computer simulation models have been used to examine water movement in soil profiles affected by salts and Na. Although models are often limited by the availability

of requisite data over time and space, and represent a simplification of the extremely complex conditions affecting soils on the landscape, they may present a reasonably reliable picture of specific soil-water-plant interactions (Mulligan and Wainwright 2004). As such, they may offer a cost effective source of guidance for some land and irrigation management decisions.

Cai et al. (1994) used the U.S. Salinity Laboratory's Hydrus-1D model (Simunek et al. 1998b) with data from a related field study to illustrate retention and flow of water and solutes in a high-clay soil in Australia's Murray-Darling basin, when that soil was exposed to summer precipitation and was ponded during winter with low-salinity groundwater. Feng et al. (2003a, 2003b) developed a model to simulate effects of variations in irrigation frequency, applied water volume, and salinity on crop yield, soil matric and osmotic pressure changes, and salt distribution over 5 years. They compared model results with field-measured relative crop yield and salt distribution. Tedeschi and Menenti (2002) used the SWAP (Soil-Water-Atmosphere-Plant) model, calibrated with data from a crop study, to test effects of irrigation with saline and fresh water at different frequencies on soil structure, soil salinity, and soil water balance.

Objectives

The objective of the model simulations was to explore the effects of application of water in a range of sodicities on variably textured PRB soils under flood and sprinkler irrigation. The model simulations were intended partly as a heuristic exercise, to indicate potential outcomes of specific sets of circumstances, and more importantly to provide "food

for thought" and perhaps to stimulate additional investigation. Expectations were, in general, that model predictions for soils with a higher clay percentage would show larger increases in soil water storage and runoff, and larger decreases in drainage, with increasing simulated sodicity of irrigation waters, than would soils with a lower clay percentage, and that soils under simulated flood irrigation would show larger reductions in infiltration, with increasing sodicity of irrigation waters, than would soils under simulated sprinkler irrigation.

Methods

The Hydrus-1D Model

Hydrus-1D (ver. 2.02, 2003) was developed by scientists at the U.S. Department of Agriculture's George E. Brown Jr. Salinity Laboratory for modeling one-dimensional water and solute movement in variably saturated media (Simunek et al. 1998b). It allows for user specification of time-variable surface conditions (precipitation, potential evaporation, potential transpiration), soil material layering, initial soil water content or pressure head depth distribution, vegetative groundcover type, root density depth distribution, and upper and lower boundary flow conditions. Outputs include graphical and tabular time series, including pressure head and water content for user-selected depths within the soil profile, and surface, root zone and lower boundary potential and actual water fluxes, pressure heads, and hydraulic properties for user-specified time increments.

The Hydrus-1D software uses the Richards (1954) equation to describe water flow in saturated and unsaturated soils, incorporating a sink term for root water uptake.

$$\delta\theta/\delta t = \delta/\delta x \left[K \delta h / x + \cos \alpha \right] - S$$
 [9]

where θ is volumetric water content $[L^3/L^3)]$, t is time, x is a vertical spatial coordinate with positive values upward [L], h is water pressure head [L], α is the angle between the flow direction and the vertical axis, and S is a root water uptake sink term $[L^3/(L^2t)]$. K(L/t) is the soil hydraulic conductivity function (Simunek et al. 1998a).

The root water uptake term, S, is defined by Feddes et al. (1978) as a function of soil matric potential

$$S(h) = \alpha(h)S_p \tag{10}$$

where $\alpha(h)$ is a function of the soil matric potential ($0 \le \alpha \ge 1$) and is unitless, and S_p is the potential water uptake rate $\lceil 1/t \rceil$ (Simunek et al. 1998a).

One option offered by Hydrus-1D for characterizing soil hydraulic functions is use of the van Genuchten (1980) equations describing water retention [11] and hydraulic conductivity [12] as functions of matric potential:

$$\theta [h] = \theta_r + \{ (\theta_s - \theta_r) / [1 + |\alpha h|^{-n}]^m \}$$
[11]

where θ_r is residual water content, θ_s is saturation water content, α is a fitting parameter (1/L) inversely related to the bubbling pressure (the matric potential required to empty the largest soil pore of water), n is a unitless parameter related to pore connectivity and tortuosity, and m=1-1/n and is unitless (Simunek et al. 1998).

The corresponding soil hydraulic conductivity function is expressed as:

$$K[h] = Ks\{1-(\alpha h)^{n-1} [1+(\alpha h)^{n}]^{-m}\}^{1/l}/[1+(\alpha h)^{n}]^{m/2}$$
[12]

where K is hydraulic conductivity, Ks is saturated hydraulic conductivity, and l is a unitless value related to pore tortuosity and connectivity and is assumed equal to 0.5.

Soil Water Balance Simulations

Forty-eight soil water flow simulation scenarios were defined, using Hydrus-1D software (Simunek et. 1998b), to explore potential soil hydraulic impacts of sprinkler and flood irrigation with water having a range of sodicities on four variably-textured soils cropped to alfalfa.

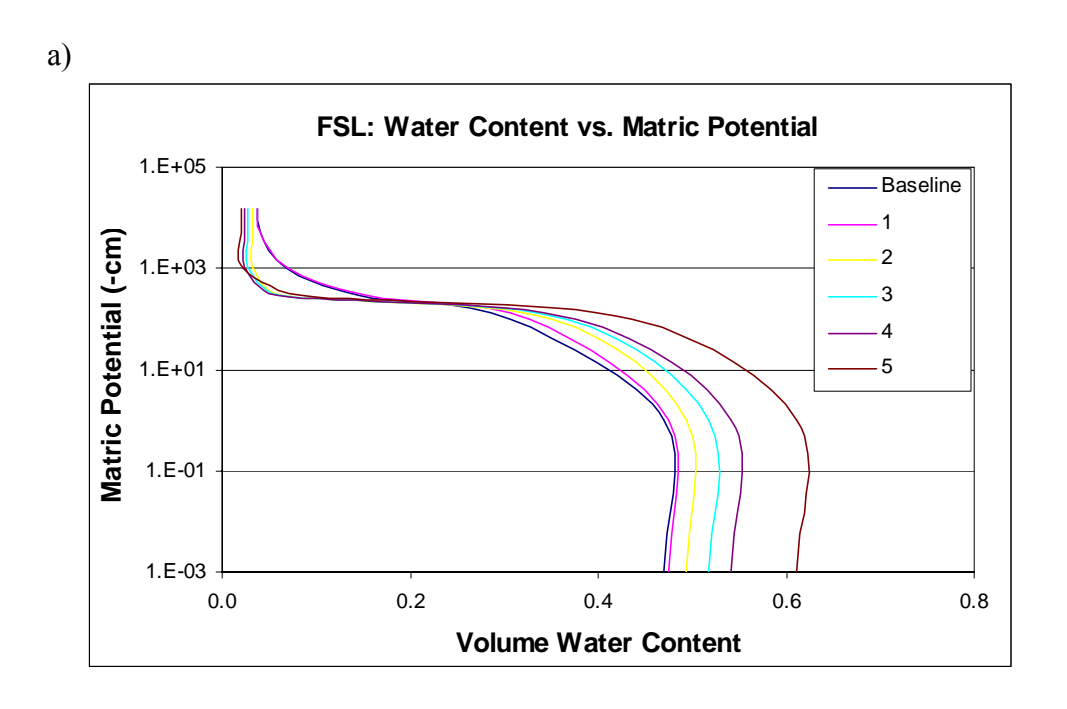
Model outputs analyzed include seasonal cumulative values for root water uptake (transpiration), drainage across the bottom of the soil profile, change in soil water storage, evaporation, evapotranspiration (ET), root water uptake relative to evapotranspiration (RWU/ET), and infiltration.

Simulations were conducted for fine sandy loam, silt loam, silty clay loam, and silty clay soils. Sprinkler and flood irrigation simulations were completed for six hypothesized water qualities, representing PR water and five increasingly sodic waters. Because the Hydrus-1D model cannot vary soil hydraulic properties according to soil water quality, each soil-water quality scenario was defined solely by a corresponding set of six hydraulic parameters input to the model. The van Genuchten single porosity hydraulic model was used to define the soil water retention $\theta[h]$ and hydraulic conductivity K[h] functions.

Measured soil water retention data (water content at four pressure heads) for southeastern Montana irrigable soils from a study by Robinson (2003) were used to optimize the van Genuchten water retention parameters, θ_r , θ_s , α , and n for four soils having significant acreage under irrigation in the Buffalo Rapids irrigation district along the Yellowstone River. These parameter sets were considered to represent baseline (exposed to PR water) conditions. Best-fit water retention parameters were obtained in MS Excel[®] using a modified version of

the nonlinear optimization procedure presented by Wraith and Or (1998). "Baseline" Ks values for each soil were taken from the catalog of soil textural hydraulic parameter values included in the Hydrus-1D software as measured values were not available. No hysteresis was assumed.

Based on a review of the literature, the hydraulic parameters used for simulation of increasingly sodic water quality conditions in all soils were estimated by increasing θ_s values by 1, 5, 10, 15, and 30% over baseline values. Other retention parameters (θ_r α , and n) were adjusted by eye to create $\theta[h]$ functions approximating the shape of retention curves reported and illustrated by Crescimanno et al. (1995) for clay soils, which were used to model the silty clay and silty clay loam functions, and by Lima et al. (1990) for a loam soil, which was used to model the silt and fine sandy loam functions. Proportional decreases in the value of Ks under increasingly sodic water quality conditions were estimated based on values reported by Levy et al. (2002) and McNeal and Coleman (1966). For brevity, the modified hydraulic functions based on 1, 5, 10, 15, and 30% changes in θ_s are hereafter referred to as Scenarios 1-5, respectively. The parameters for baseline and increasingly sodic scenarios are listed for each soil in Table E1, Appendix E. Corresponding water retention and hydraulic conductivity functions for each soil are illustrated in Figs. (10) and (11). The studies upon which parameter adjustments were based included treatments with a variety of EC-SAR water combinations on soils different than those modeled here, and data were not identified in published literature or elsewhere that would allow for a direct correlation of soil type or application water quality to specific increases in θs or corresponding adjustments to the other Van Genuchten parameters in a specific soil.



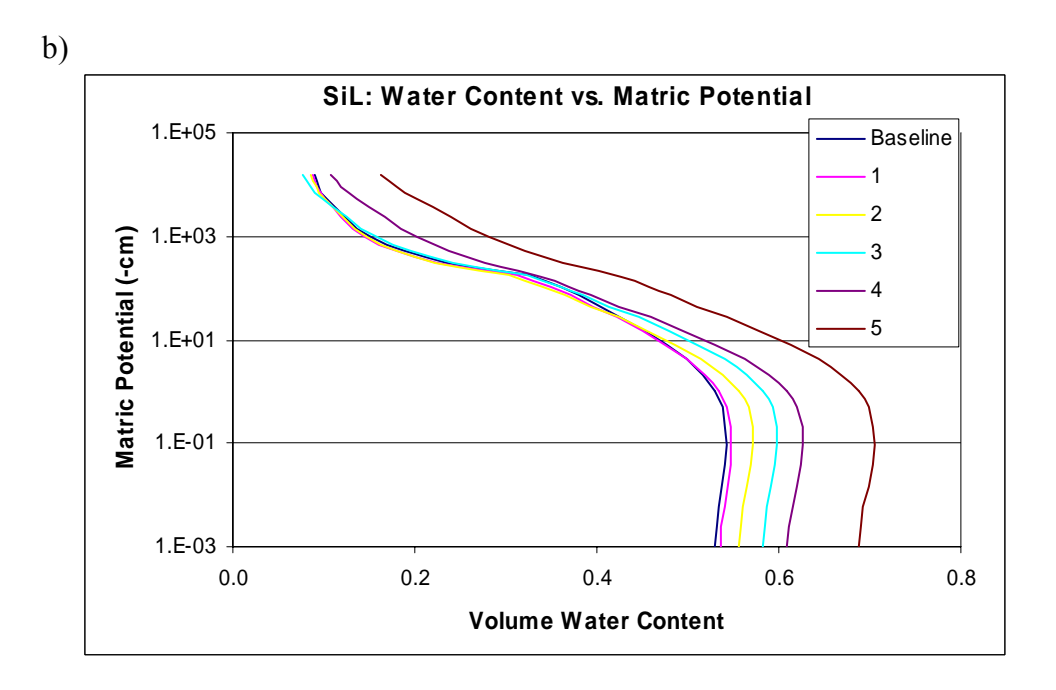
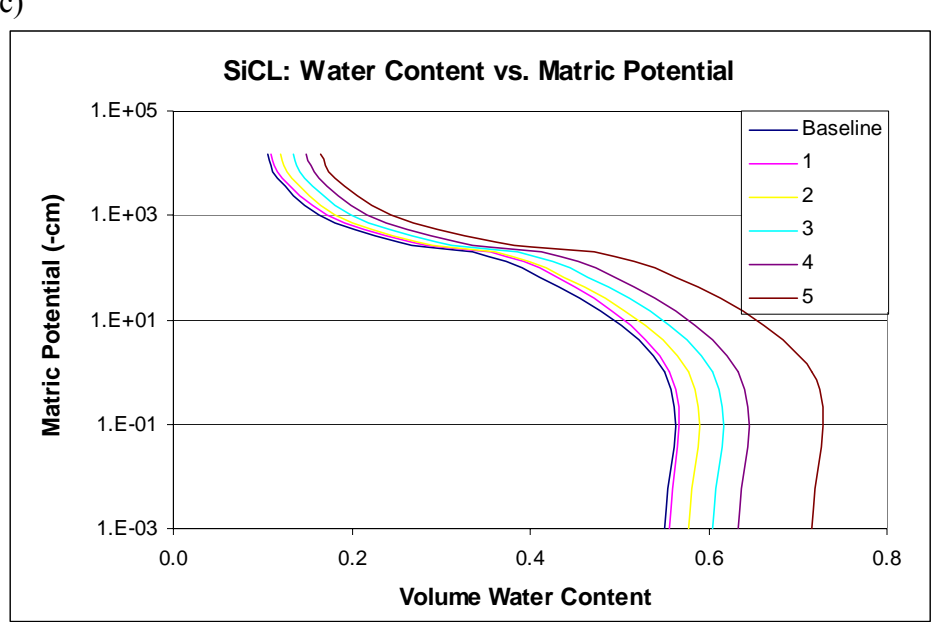


Fig. 10. Water retention functions $\theta[h]$ used as input for baseline and progressively sodic water quality simulations 1-5. Functions are for a) fine sandy loam, b) silt loam, c) silty clay loam, d) silty clay soils.

c)



d)

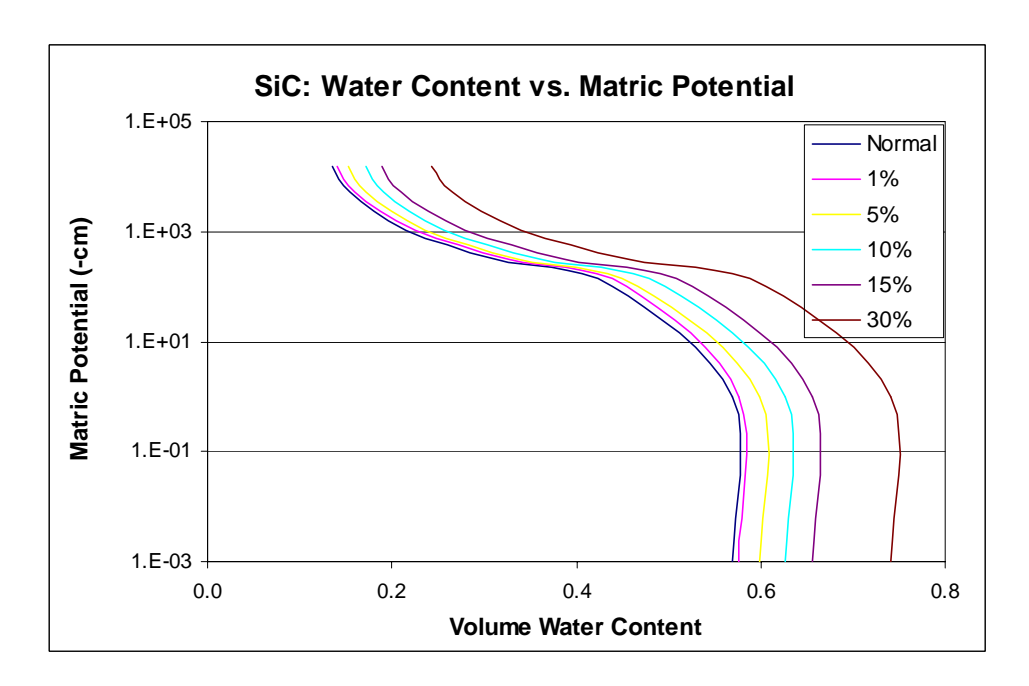
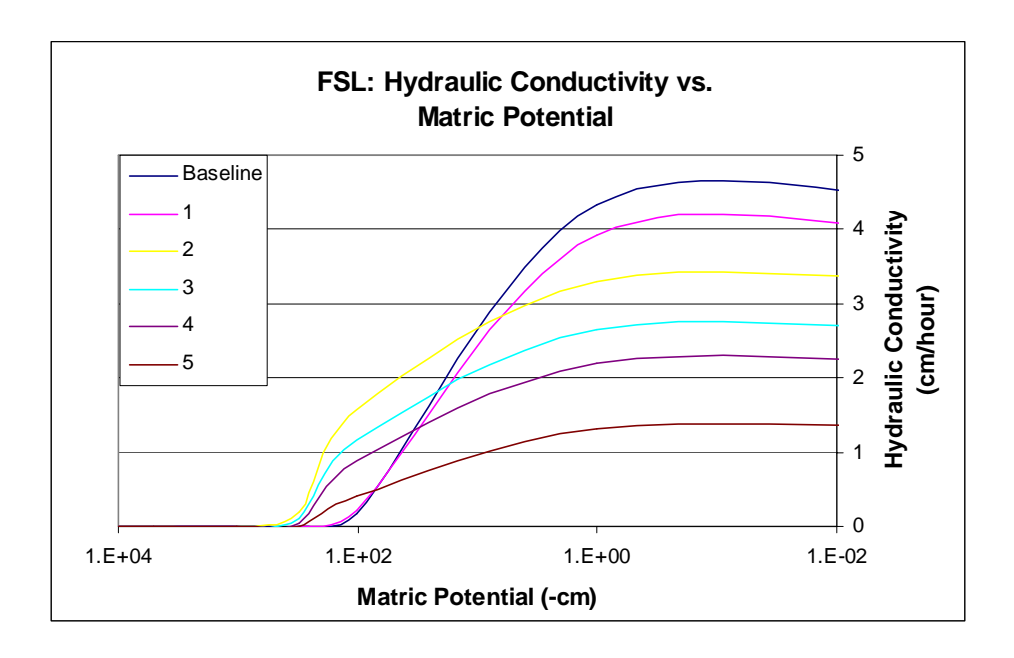


Fig. 10 (cont.)

a)



b)

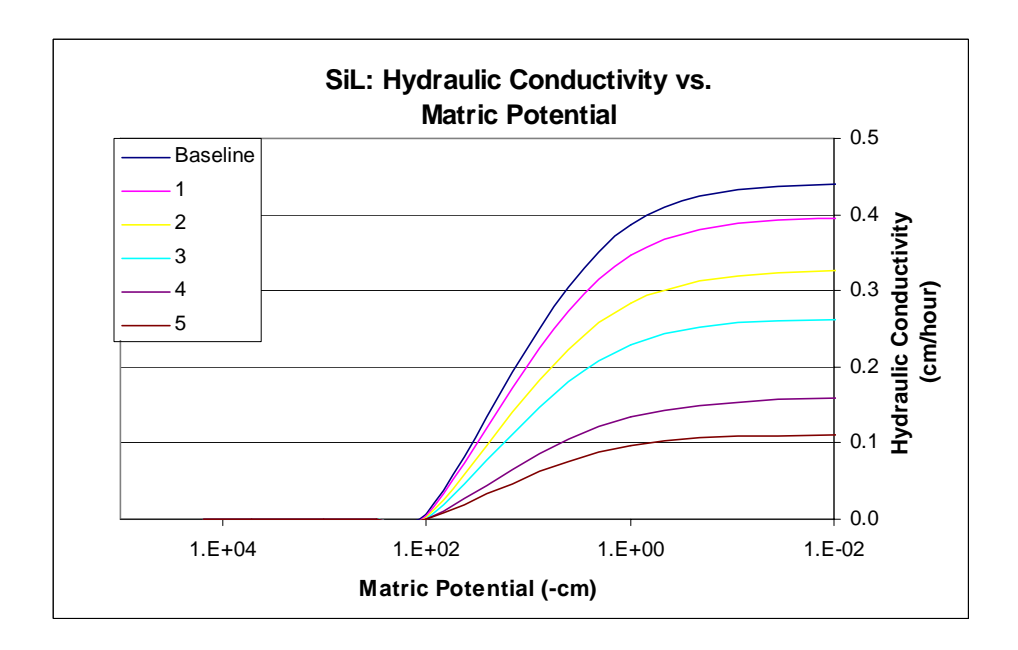
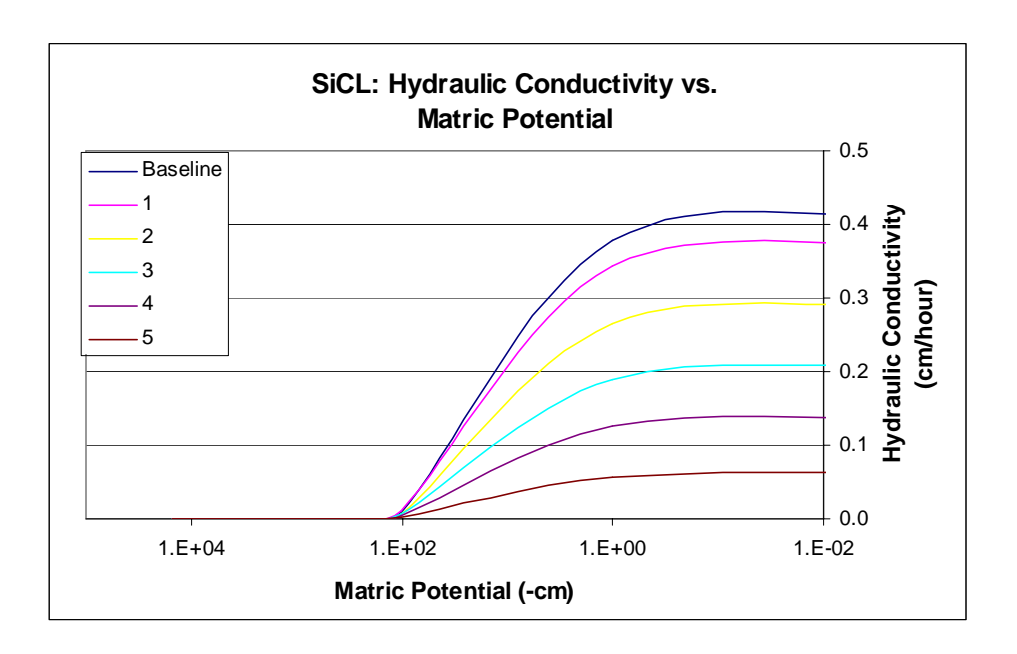


Fig. 11. Hydraulic conductivity functions K[h] used as input for baseline and progressively sodic simulations 1-5. Functions are for a) fine sandy loam, b) silt loam, c) silty clay loam, d) silty clay soils.

c)



d)

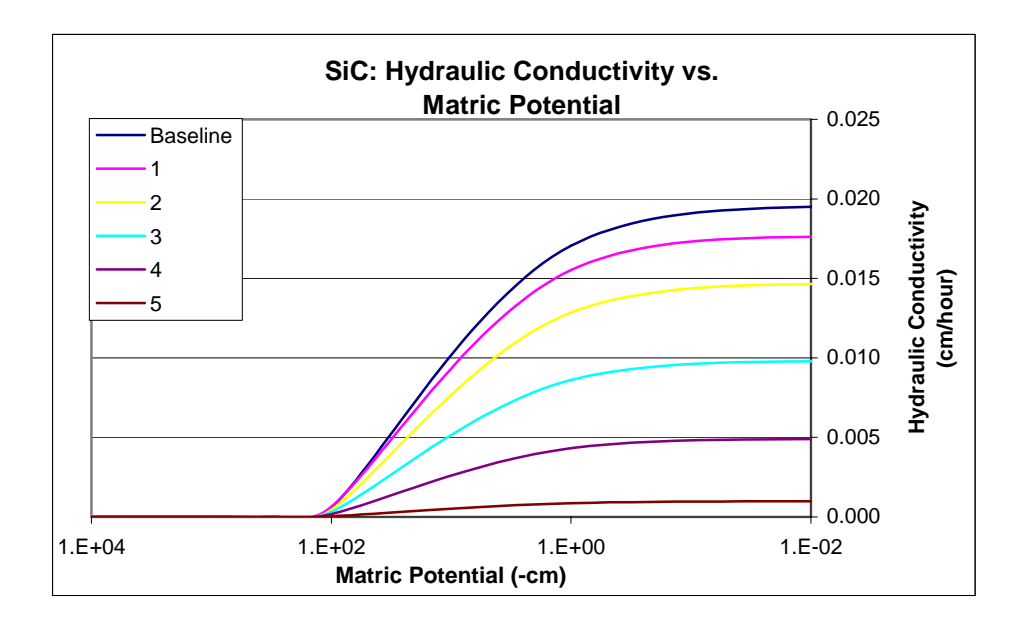


Fig. 11 (cont.)

All soil profile simulations were based on a uniform soil material to 1 m depth. Steve Van Fossen, USDA Natural Resources Conservation Service soil scientist in Miles City, Montana, (personal communication, 2004), provided information to support estimates that early spring soil water extends, on average, to depths of approximately 61 cm in fine sandy loams, 46 cm in silt loams, 32 cm in silty clay loams, and 26 cm in silty clay soils. Initial (April 15) soil pressure head was therefore set to 336 cm (0.33 bar, or approximately field capacity) from the soil surface through the specified wetted depth, and to 10,197 cm (10 bar) from the lower end of the wetted zone to the 1 meter lower boundary, with a 5 cm transition zone in between. Fig. 12 illustrates the Hydrus graphical profile definition screen in which initial pressure head distribution with depth was specified.

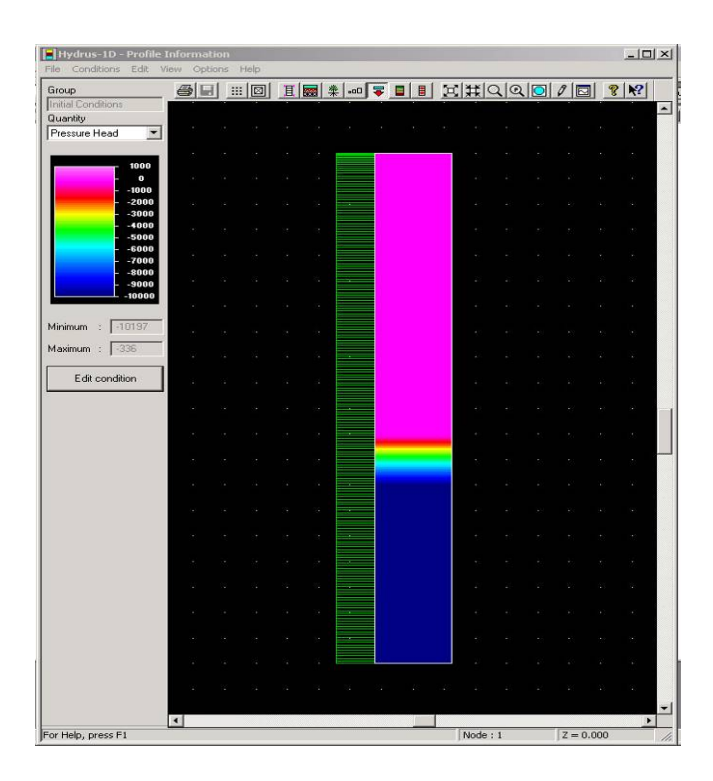


Fig. 12. Hydrus 1-D graphical input screen for initial pressure head distribution by depth in the soil profile.

All simulations were set to run with an alfalfa crop over a single 168-day growing season, from April 15 to September 29, and included two harvests, on July 1 and August 10 (J.W. Bauder, personal communication, 2004). Climatic data used for time-variable surface boundary condition input to the model included daily precipitation, potential evaporation, and potential transpiration estimates based on 6 years (1999-2004) of weather station data from the U.S. Bureau of Reclamation's Agrimet Great Plains station at Terry, Montana (U.S. Bureau of Reclamation, n.d.). Representative daily values were estimated based on the 6-year data, and entered as flux values in cm/h. Seasonal precipitation totaled 21.8 cm.

Irrigation water volumes were estimated based on information from Jim Bauder, Montana State University Extension Soil and Water Quality Specialist (J.W. Bauder, personal communication, 2004) and added to the rainfall values on the dates of simulated irrigation. For the flood irrigation scenarios, irrigation water fluxes of 0.8483 cm/h (20.32 cm/day) were added over a single 24-h period for each of the two flood irrigations on June 1 and July 10. Seasonal precipitation plus flood irrigation water totaled 63.6 cm. Sprinkler irrigation fluxes were input as 0.0833 cm/h (2 cm/day) over a 24-h period every third day, based on an estimated water delivery volume from the pivot-arm midpoint of a center pivot sprinkler. Seasonal precipitation plus sprinkler irrigation totaled 135.8 cm, more than double the amount for flood irrigation.

Simulations for all sprinkler irrigation scenarios, and for flood irrigation in the lowerclay (fine sandy loam and silt loam) soils, were constructed as single 168-day (4032 h) runs. In order to simulate flood irrigation water entry via expected large surface cracks in the silty clay loam and silty clay soils, these models were constructed in five consecutive component runs. The first, third, and fifth component intervals represented the portions of the growing season (April 15–May 31, June 2-July 9, July 11-September 29), when precipitation in the form of rainwater was the only water infiltrating the soil surface. The second and fourth intervals represented the daylong flood irrigation events on June 1 and July 10. In these two 24-h runs, 15% soil water content was added to the profile's initial condition (i.e. the final simulated depth-wise water content output for the previous model run) and the initial pressure head profile was adjusted to reflect the added soil water, based on the $\theta[h]$ relationship for that soil. This was intended to represent water that bypasses infiltration through the soil's upper surface by entering surface-connected cracks and infiltrating at depth in the profile. Assuming that cracks would extend to an average depth of 61 cm (2 ft.), this 15% water content represented 9.15 cm of the 20.32 cm total flood irrigation water. The remaining irrigation water (11.17 cm) was added to the day's precipitation as a standard time-variable upper boundary condition input.

Daily crop-specific potential evapotranspiration (ETp) values for alfalfa, from the Agrimet database, were separated into potential evaporation and potential transpiration by assuming a sigmoidal increase in potential transpiration (crop growth) as a fraction of evapotranspiration (Tp/ETp) from an initial (April 15) value of 0% to a maximum of 85% preceding the first harvest on July 1, and from 5% ETp on July 1 to a 70% maximum preceding the second harvest on August 10. Another 5% to 40% increase was assumed from August 10 to mid-September, when crop scenescence and a corresponding decline in potential transpiration were assumed. Seasonal potential evaporation and potential transpiration totaled 42.8 and 43.0 cm, respectively.

The Feddes (1978) root water uptake model [10] was selected, with no plant solute stress factor included in the model. Critical Feddes pressure head and potential transpiration rate parameters for alfalfa (based on Taylor and Ashcroft 1972) were taken from the Hydrus-1D root water uptake database. The majority of alfalfa roots (85-90%) were assumed to be included in the 1 m depth of soil modeled (Abdul-Jabbar et al. 1982), and roots were assumed to be fully-developed at the start of the growing season; no root growth factor was included in the uptake model. Relative root density distribution with depth, R(d), was modeled after Jackson et al. (1996):

$$R(d) = -\beta^{d} * ln(\beta)$$
 [14]

where β is a coefficient for diminishing root density with depth, equal to 0.943 for temperate grasslands (Jackson et al. 1996), and d is depth. Fig. (13) shows the relative root density distribution with depth in the soil profile.

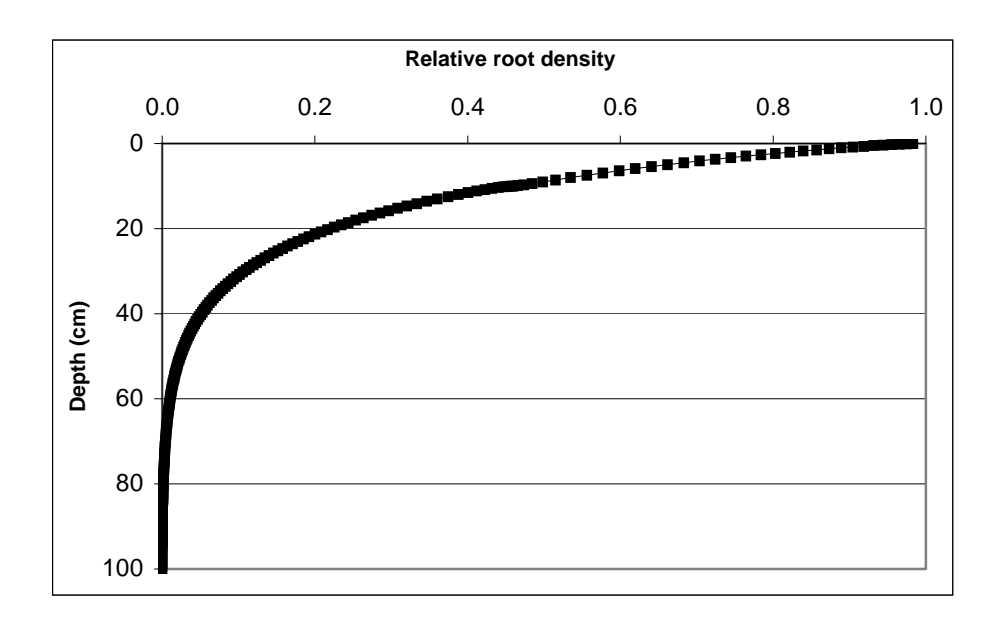


Fig. 13. Relative depth density of simulated alfalfa roots in the soil profile.

Soil surface pressure head at the point of transition to stage 2 evaporation was set as 12,000 cm for the fine sandy loam and 10,000 cm for the three finer-textured soils. The maximum allowed pressure head (ponding depth) at the soil surface was set at 0.5 cm, except during the 24-h intervals corresponding to the flood irrigation events, where it was set at 21 cm to accommodate any ponding that might result from the 20.32 cm irrigation. The water table was assumed to be several meters below the bottom of the 1 m profile, and the lower boundary condition was defined as free drainage.

Simulated soil profile information was output for the initial (0.001) and final (4032) hours of each model run in order to retrieve values of interest. In the five-part flood irrigation simulations for the SiCL and SiC soils, initial and final values were obtained for each of the five component runs. Values for cumulative seasonal root water uptake, drainage, evaporation, and infiltration were obtained from the time series output files (t-level.out) at the end of each simulation run. The soil profile output file (nod_inf.dat) was used to retrieve initial and final soil water and pressure head values. Change in soil water storage was calculated as the mean difference between final and initial soil water content for each of the 201 nodes discretizing the soil profile, multipled by the corresponding depth between nodes. ET was calculated as the sum of evaporation and root water uptake (transpiration). Runoff was calculated by mass (water) balance, and was assumed to be the difference between total water applied over the season and the sum of root water uptake, drainage, evaporation, and change in soil profile water storage.

Results

Fine Sandy Loam Soil under Sprinkler Irrigation.

The growing season water balance of this coarsest-textured soil appeared not to be adversely affected by any of the sodic water application scenarios (Fig. 14a). Selected numerical results for all simulations are provided in Table E2, Appendix E. Cumulative root water uptake and evaporation remained constant under all simulations, at 43.1 and 42.8 cm, respectively. The proportion of total ET that was in the form of transpiration (RWU/ET), hence contributing to alfalfa yield, was therefore 0.5 in all cases (Fig. 15a). Runoff did not occur for this soil. Under Scenario 5, soil water storage increased by 25% from the baseline condition, from 9.9 cm to 12.4 cm, although soil water storage decreased by between 1 and 96% relative to baseline under intermediate Scenarios 1-4. Deep drainage exhibited a corresponding trend, decreasing by 6.5% from 40.2 to 37.6 cm between baseline and Scenario 5, but increasing between 0.2 and 31% under the intermediate scenarios. Scenario 2 resulted in the most changed soil water storage and deep drainage values, compared to baseline.

Fine Sandy Loam Soil under Flood Irrigation.

Greater differences among sodicity scenarios in simulated soil water balance components were observed under flood than under sprinkler irrigation for the fine sandy loam (Fig. 14a). Root water uptake increased incrementally across scenarios from 28.4 to 34 cm or 20%, between baseline and Scenario 5. Evaporation was 12% (18 vs. 20.2 cm) and ET 17% (46.4 vs. 54.3 cm) greater than baseline for water quality Scenario 5, although both

values rapidly increased from baseline to a maximum with Scenario 2. The RWU/ET ratio remained fairly constant at around 0.6 (Fig. 15a). There was no runoff predicted for any scenarios. Soil water storage decreased under all simulated water qualities, and the soil lost 568% more water than for baseline conditions with Scenario 2 (1.9 vs. 12.7 cm), and 47% more with Scenario 5 (4.7 cm, Fig. 14a). Deep drainage under Scenario 5 decreased by 24% relative to baseline conditions, from 18.4 to 13.9 cm, although drainage increased from baseline slightly under Scenarios 2 and 3 to 20.8 and 19.1 cm. All applied water infiltrated, as for sprinkler irrigation, where more than twice as much total water was applied during the season.

Silt Loam Soil under Sprinkler Irrigation

This soil appeared not to be greatly affected by simulated sodic water quality Scenarios 1-3 under sprinkler irrigation, but substantial changes in soil water balance components were observed for Scenarios 4 and 5 (Fig. 14b). Root water uptake decreased across simulated sodic water qualities, and Scenario 5 caused a 90% decrease from baseline, from 43.1 to 4.3 cm. Root zone pressure head changes indicated that the mean soil matric potential remained above the critical -25 cm level for maximum alfalfa root water extraction during much of the season for Scenarios 4 and 5 (Fig. 17). Cumulative seasonal evaporation remained nearly constant, but ET (evaporation plus transpiration) declined 46% from 85.9 to 46.7 cm, and the RWU/ET ratio dropped from a baseline value of 0.50 to 0.09 for Scenario 5. Runoff was zero under all conditions. Deep drainage increased by 38% (from 28.3 to 33.6 cm), although it decreased from baseline under intermediate scenarios, with a minimum value of 14.9 cm

for Scenario 3, and soil water storage increased incrementally by 105%, between baseline and Scenario 5 from 25.7 to 52.8 cm.

Silt Loam Soil under Flood Irrigation

Scenario 4 under flood irrigation appeared, as for sprinkler irrigation, to represent a threshold for the soil water balance in this soil, although with flood irrigation the impact appeared not to have been as severe as under sprinkler irrigation (Fig. 14b). Scenario 4 resulted in a 35% decrease from baseline in root water uptake from 31.5 to 20.6 cm, with incremental changes across intermediately sodic scenarios. Seasonal evaporation also declined for Scenario 5 by 5%, to 17.1 from 18 cm, as did ET, by 12% from 49.5 to 37.7 cm (Fig. 14b). The RWU/ET ratio was near constant (0.64-0.65) between baseline and Scenario 3, but declined to 0.61 and 0.55 in Scenarios 4 and 5 (Fig. 15b). Simulated runoff was observed for flood irrigation, and increased in approximate proportion to increasing simulated sodicity between baseline and Scenario 5, by 236% from 8.1 to 27.2 cm. The latter amount represents 43% of the total 63.6 cm of water added over the season. The soil lost 1.4 cm of water under Scenario 5 in contrast to storing 5.2 cm under baseline conditions, and decreases in soil water storage were progressively greater under Scenarios 1-4. Deep drainage went from a minimal 0.8 cm under baseline hydraulic conditions, to 0.1 cm under Scenario 1 and to zero under each of the more sodic water quality scenarios. Infiltration was less than the total applied water for all scenarios, including baseline, and declined, in proportion to simulated sodic water quality by 35% (from 55.1 to 35.9 cm) between baseline and Scenario 5 (Fig 16a).

Silty Clay Loam Soil under Sprinkler Irrigation

This soil did not exhibit large changes in most water balance components under any of the simulated sodic irrigation water Scenarios (Fig. 14c). Root water uptake declined by only 4% under Scenario 5 as compared to baseline, from 42.8 to 41 cm, and increased by less than 1 cm under Scenarios 1-4. Seasonal evaporation remained constant among scenarios at 42.8 cm. ET declined by 2% (from 85.6 to 83.8 cm) between baseline and Scenario 5, but increased very slightly across Scenarios 1-2 (to 85.9 cm) and 3-4 (to 85.8 cm). The RWU/ET ratio remained at about 0.5 under all conditions (Fig. 15c). Runoff was zero under all scenarios. Deep drainage declined notably, and in proportion to simulated sodicity, by 65% (from 23.6 to 8.2 cm) between baseline and Scenario 5. Soil water storage increased correspondingly, by 67% (from 26.3 to 44 cm).

Silty Clay Loam Soil under Flood Irrigation

Under flood irrigation, as under sprinkler irrigation, most water balance components remained near baseline values for all simulated water quality scenarios (Fig. 14c).

Cumulative root water uptake increased across scenarios by 8%, from 31.1 to 34.3 cm.

Seasonal evaporation increased from baseline to Scenario 5 by 4% (from 18.3 to 19.0 cm), with intermediate scenarios having intermediate values of 18.5 or 18.6 cm. ET increased 8% from 49.4 cm to 53.3 cm between baseline and Scenario 5, also showing incremental increases under intermediate scenarios. The RWU/ET ratio remained near-constant, at 0.63 for baseline and for Scenarios 1-3, and at 0.64 for Scenarios 4 and 5 (Fig. 15c). Runoff was zero for all scenarios. Deep drainage first increased from a baseline of 3.9 cm to 5.0 under

Scenario 1, then decreased from 3.8 cm to zero across Scenarios 2-5. Soil water storage increased incrementally from baseline with increasingly sodic simulated water qualities, by 34% from 8.5 cm to 11.4 cm. Infiltration declined in proportion to increases in simulated sodicity by 11% from 45.5 cm to 40.3 cm between baseline and Scenario 5 (Fig. 16b).

Silty Clay Soil under Sprinkler Irrigation

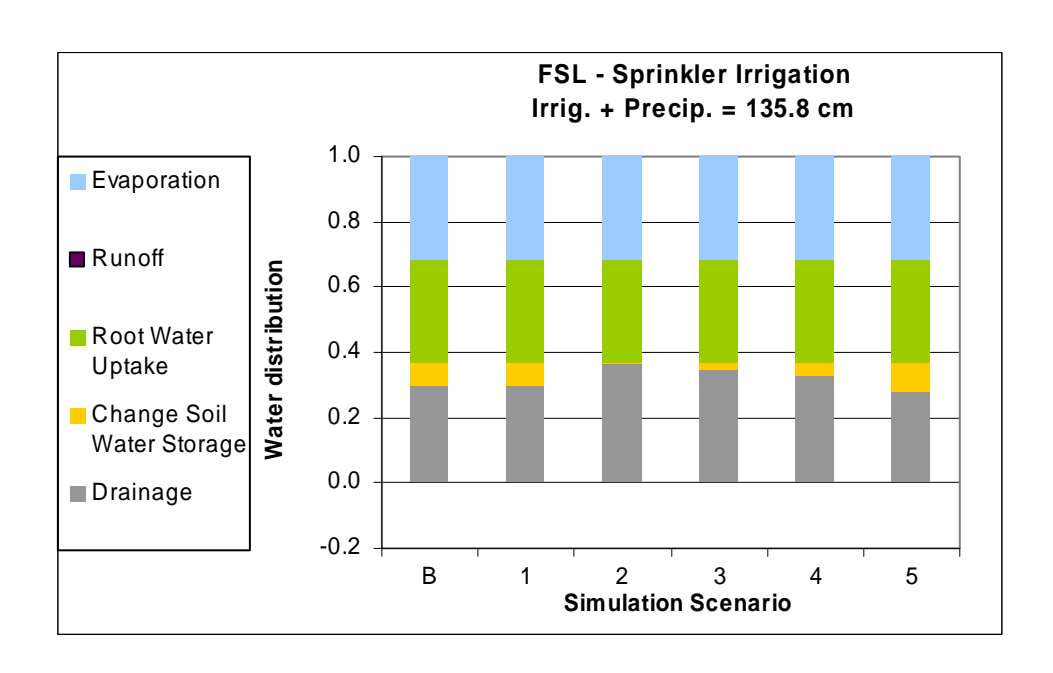
This soil exhibited large increases in surface runoff with increased simulated sodicity of applied water, with corresponding decreases shown in most other water balance components (Fig 14d). Root water uptake was the exception to this trend. It increased incrementally from 16.3 to 24.5 cm (50%) between baseline and Scenario 4, then declined to 17.6 cm (8% above baseline) under Scenario 5. Model predictions showed root zone pressure head for Scenario 1 and 2 above the critical upper bound pressure head of -10 cm for any alfalfa root water extraction, and Scenario 5 pressure head was below the critical lower bound value of -8000 cm for the latter part of the growing season (Fig. 18). Evaporation decreased in proportion to increasing simulated water sodicity by 19% from a baseline value of 39.2 to 31.8 cm for Scenario 5. Because of the trend in root water uptake, ET increased from baseline to Scenario 4 by 8% (from 55.5 cm to 60.2 cm), then declined to 49.4 cm under Scenario 5, an 11% decrease from baseline. RWU/ET increased from 0.29 to 0.41 between baseline and Scenario 5, with increases for intermediate scenarios proportional to simulated sodicity, except for a slight decrease under Scenario 2 (Fig. 15d). Runoff was significant under all scenarios, increasing from 30.8 cm under baseline conditions, to 79.5 cm under Scenario 5, a 158% increase. Deep drainage decreased from an 8.7 cm baseline, to 4.6

cm under Scenario 1, to zero under Scenarios 2-5. Soil water storage declined in proportion to simulated sodicity between baseline and Scenario 5 by 83% (from 40.8 cm to 6.9 cm). Infiltration also decreased incrementally by 53% from a baseline of 93.9 cm to 44.7 cm under Scenario 5 (Fig. 16c).

Silty Clay under Flood Irrigation

Under flood irrigation as well as for sprinkler irrigation, the silty clay soil showed increasing runoff and decreases in other water balance components, except for root water uptake (Fig. 14d). Under Scenario 5, root water uptake decreased from baseline by 23% (from 31.5 to 24.3 cm), but was similar to baseline under intermediate scenarios. Between baseline and Scenario 5, evaporation decreased by 12% (from 18.0 to 15.9 cm). ET also decreased between baseline and Scenario 5 by 19% (from 49.5 to 40.2 cm), with a slight increase under Scenario 1. The RWU/ET ratio declined from 0.64 to 0.6 across the simulated sodic water qualities, with a slight increase under Scenario 3 (Fig. 15d). Runoff increased incrementally across scenarios, by 266% between baseline and Scenario 5, from 5.6 to 20.5 cm, almost a third of the season's 63.6 cm of water. There was no deep drainage under any of the simulation scenarios, and soil water storage declined in proportion to simulated water sodicity, 67% between baseline and Scenario 5 (from 8.5 to 2.8 cm). Infiltration also decreased incrementally by 37% from a 36.2 baseline to 22.8 cm with Scenario 5, which represented only 36% of the season's applied water (Fig 16c).

a)



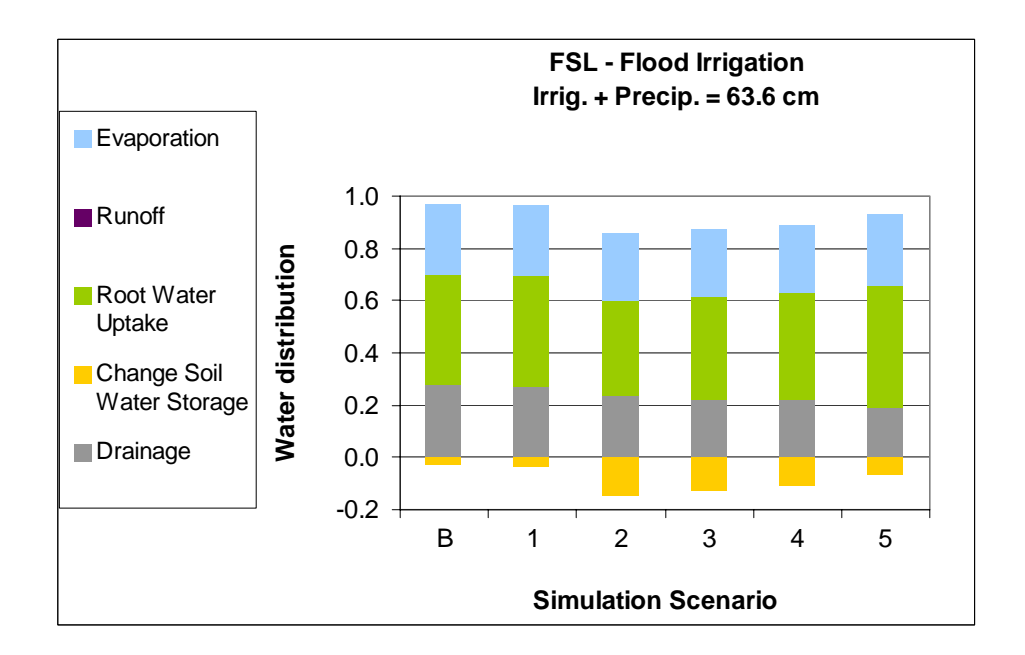
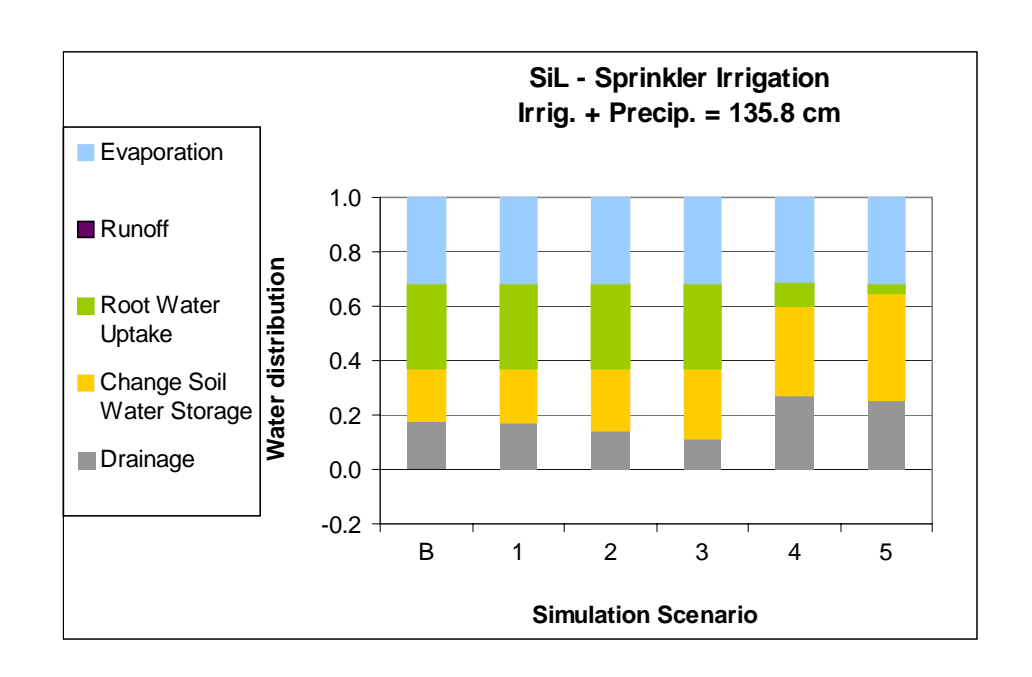


Fig. 14. Hydrus-1D simulation results: Cumulative water distribution by soil and irrigation method for baseline and progressively sodic irrigation water qualities. Results are for a) fine sandy loam, b) silt loam, c) silty clay loam, d) silty clay soils.

b)



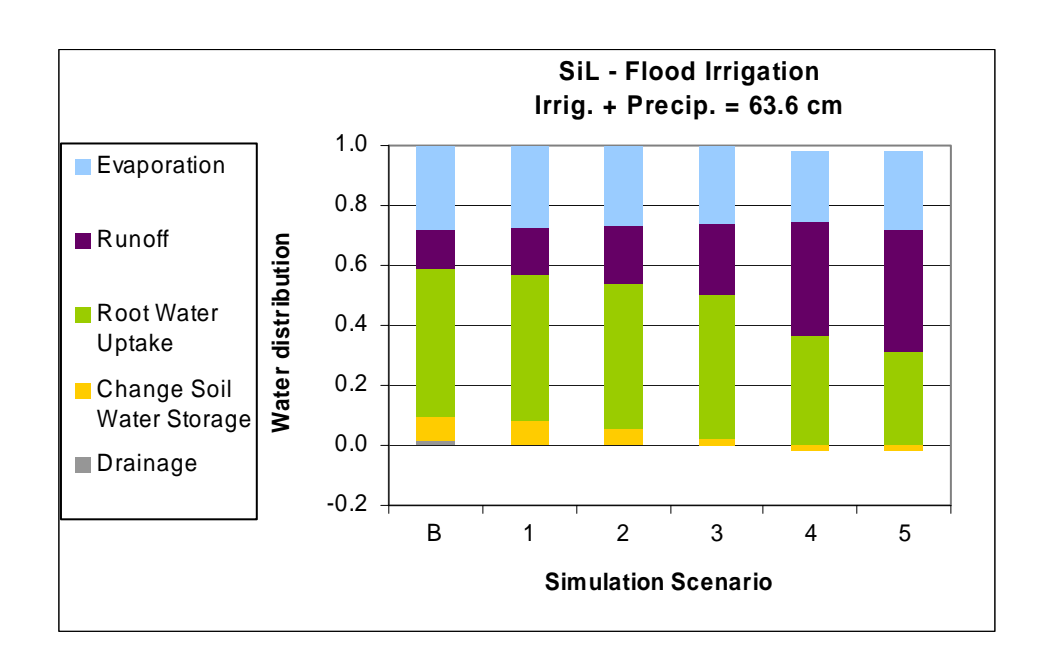
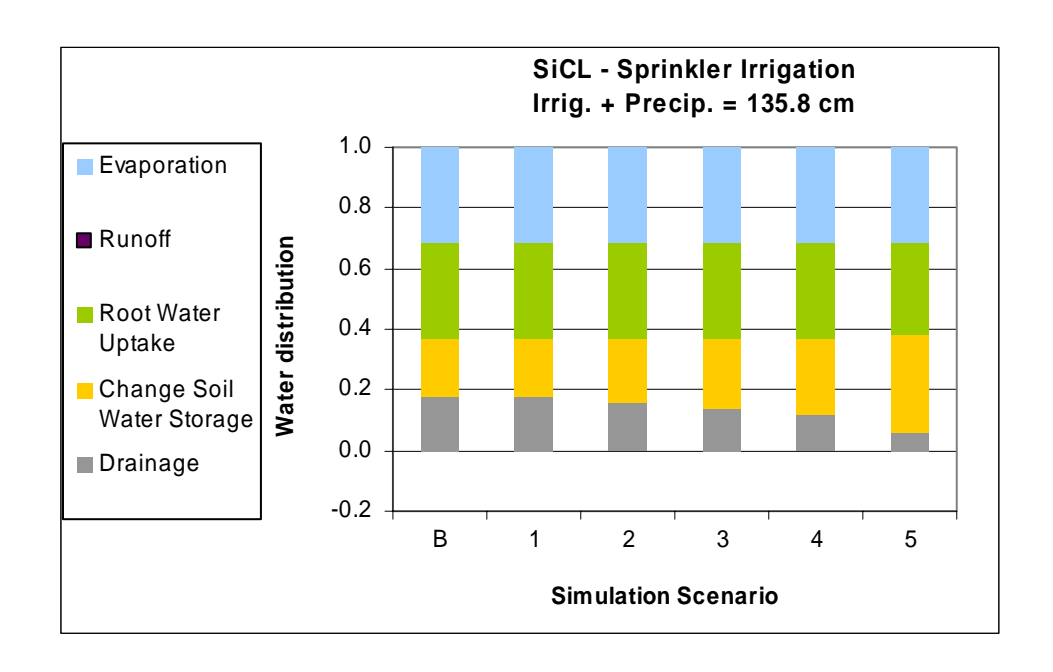


Fig. 14 (cont.)

c)



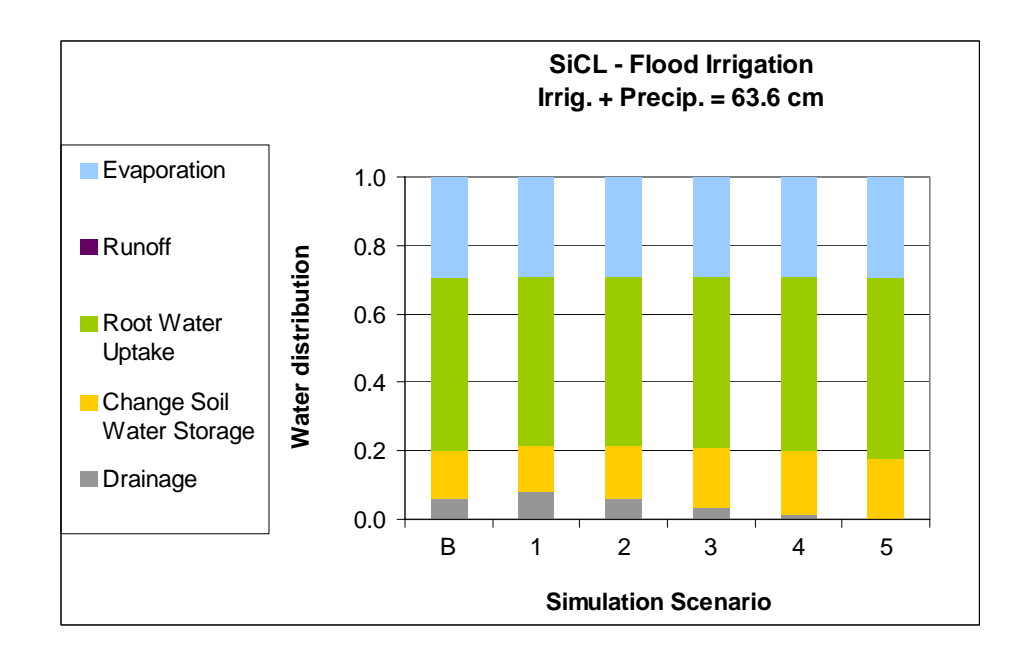
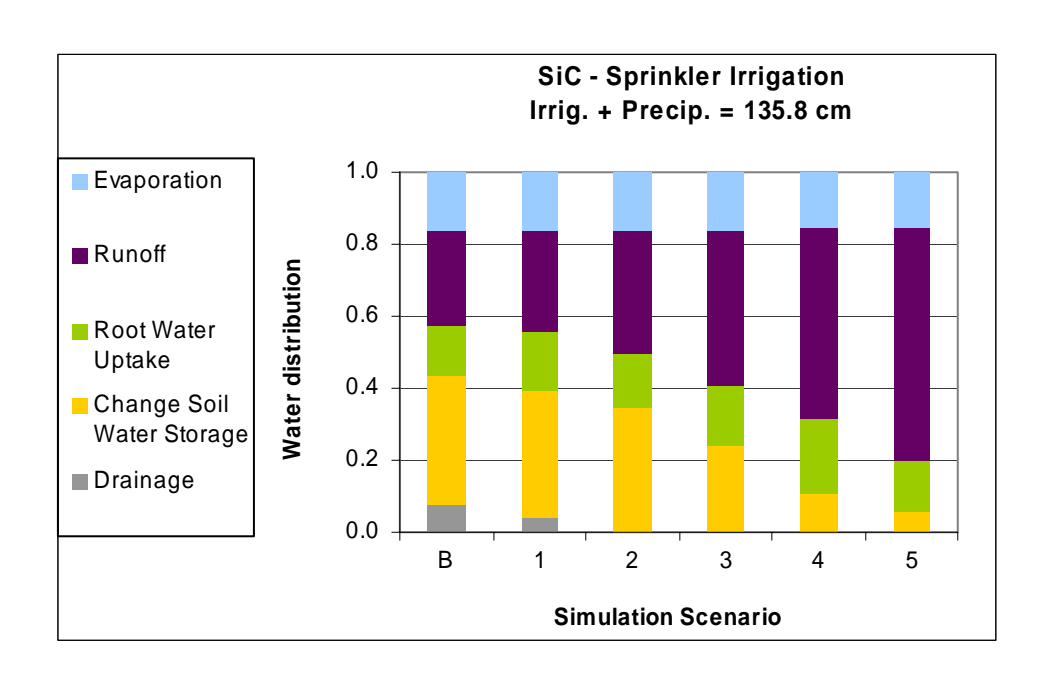


Fig. 14 (cont.)

d)



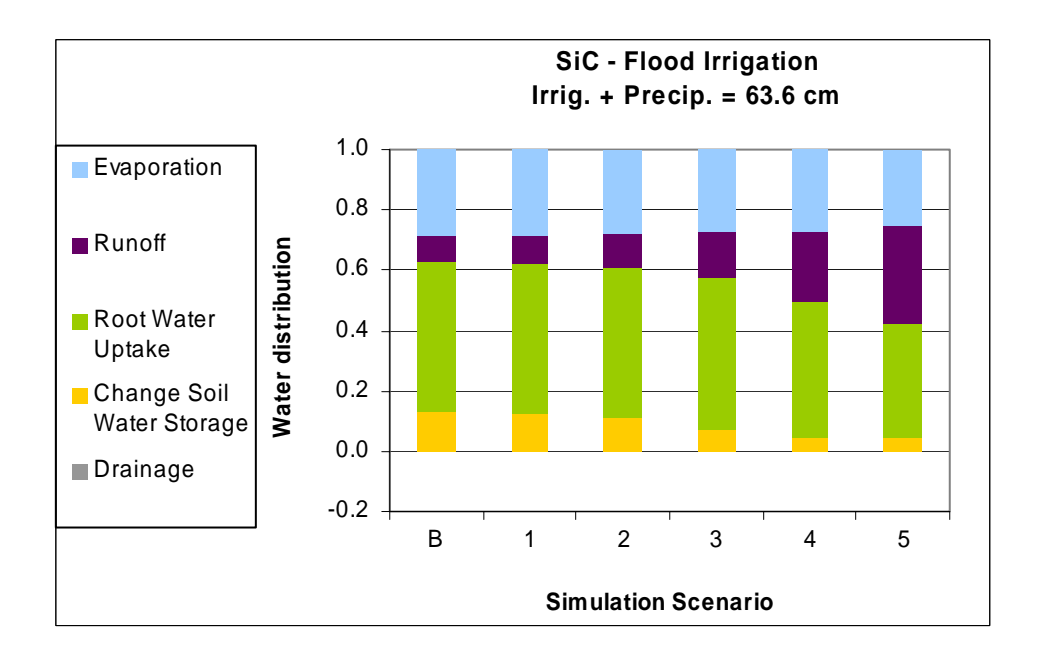
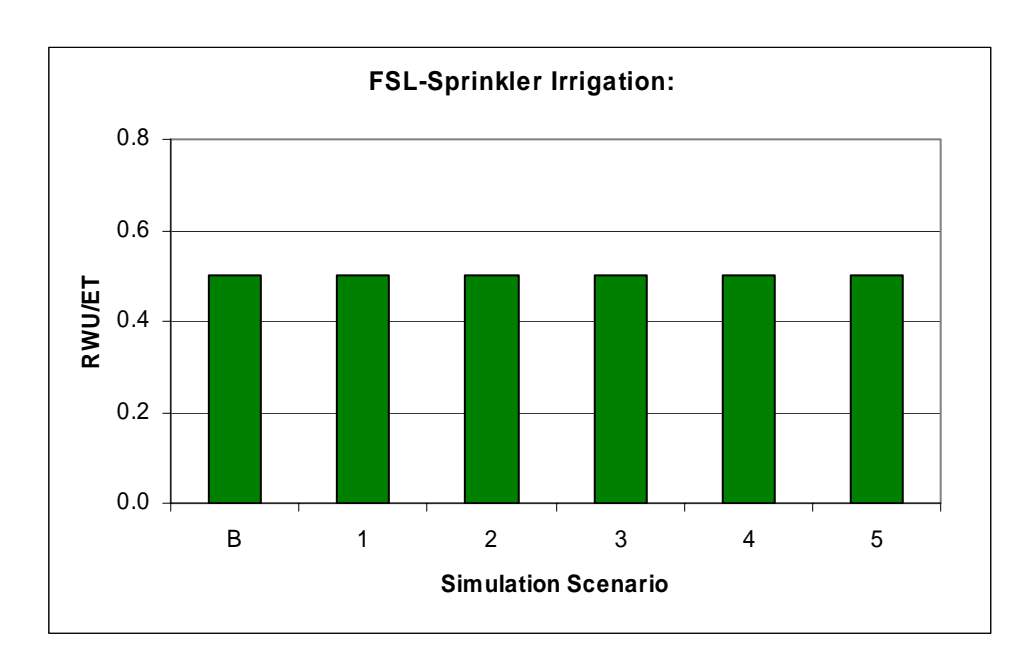


Fig. 14 (cont.)

a)



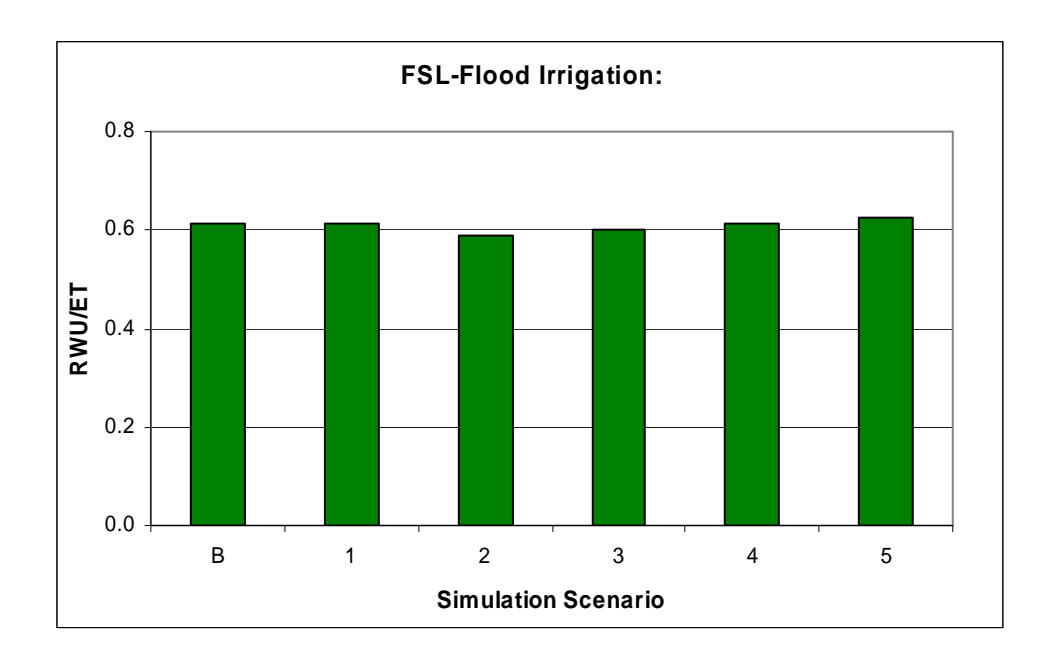
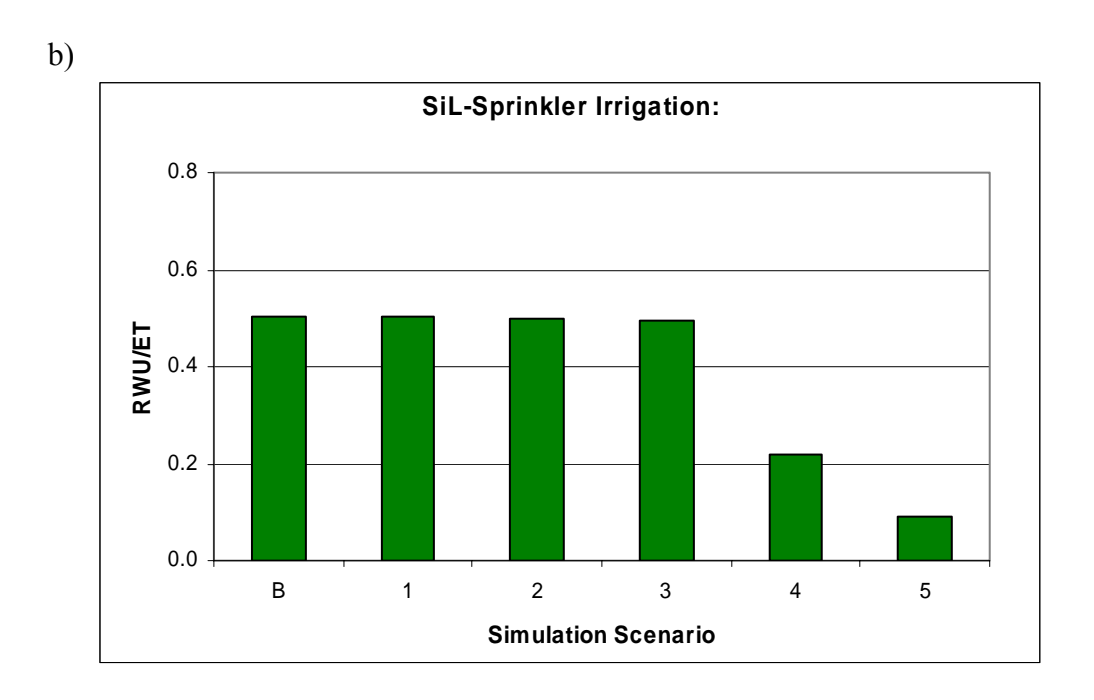


Fig. 15. Ratio of root water uptake (transpiration) to total evapotranspiration (RWU/ET) by soil and irrigation method for baseline and progressively sodic irrigation water qualities. Results are for a) fine sandy loam, b) silty loam, c) silty clay loam, d) silty clay soils.



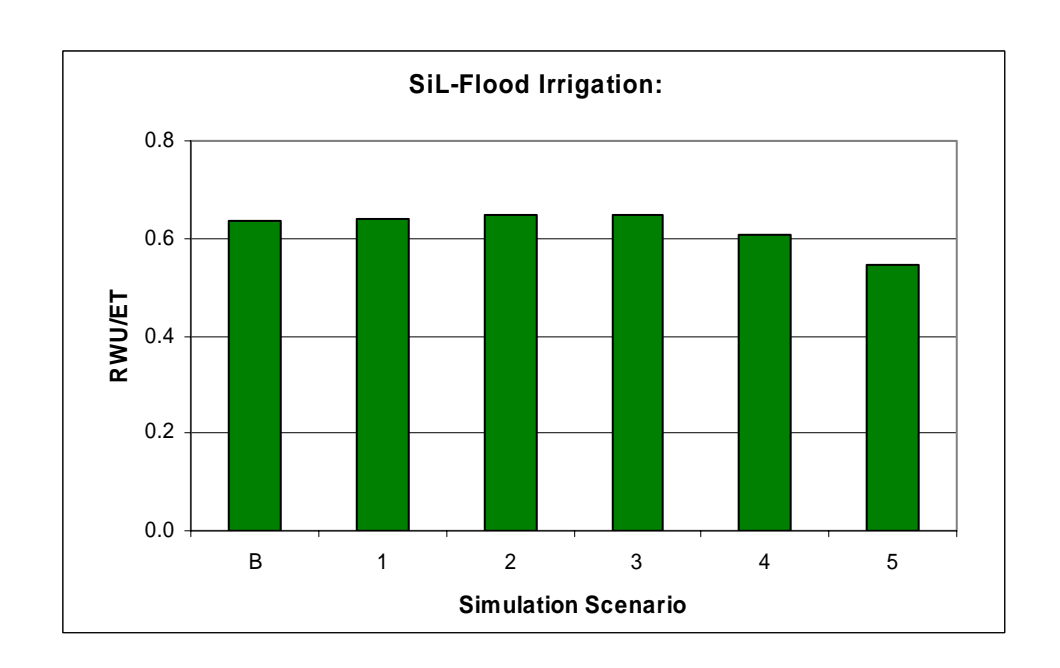
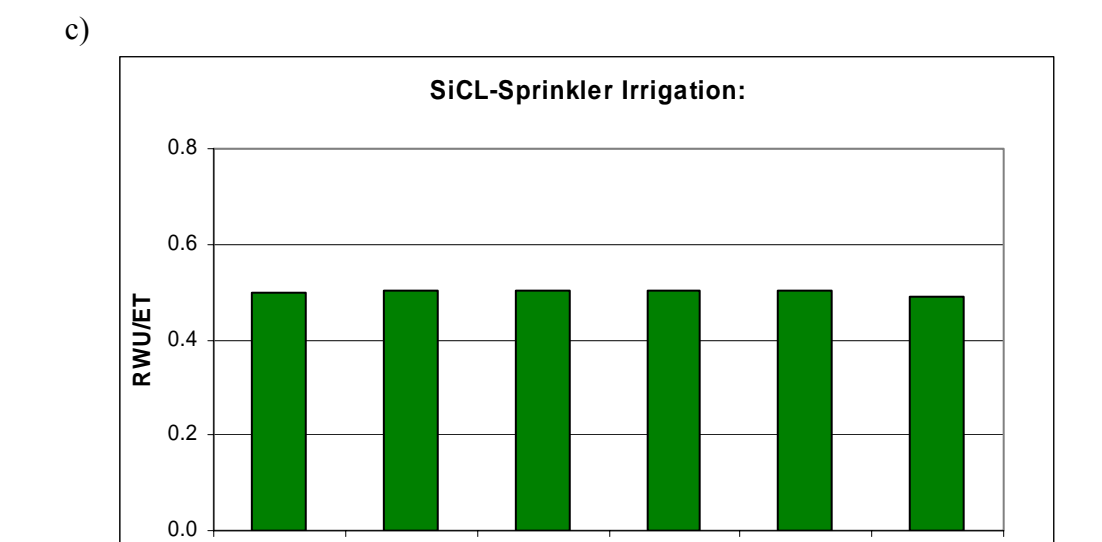


Fig. 15 (cont.)



Simulation Scenario

В

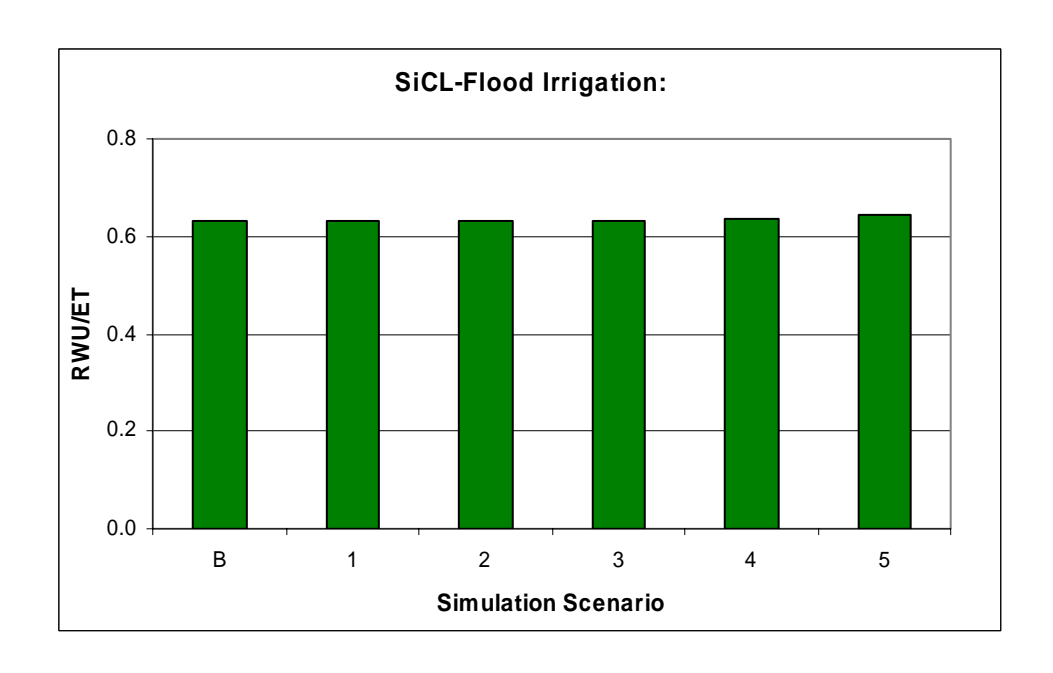
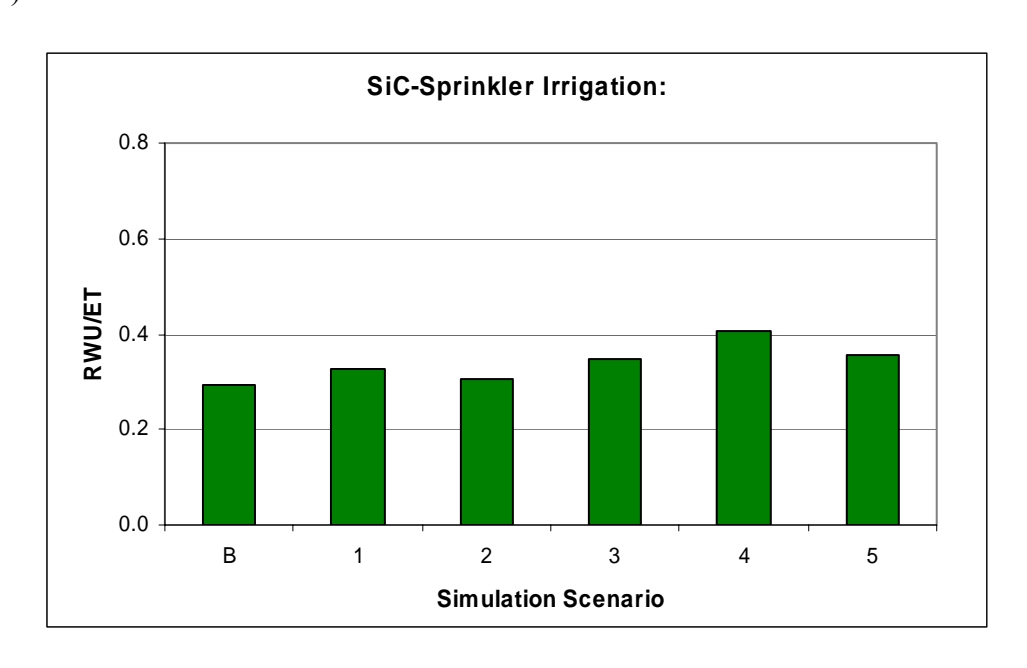


Fig. 15 (cont.)

d)



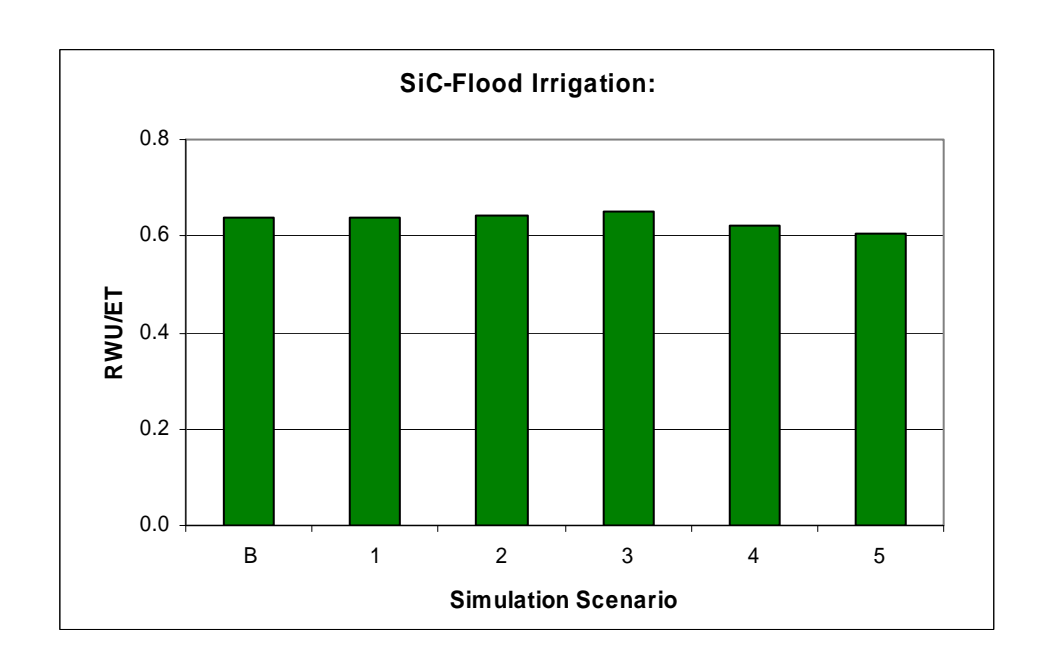
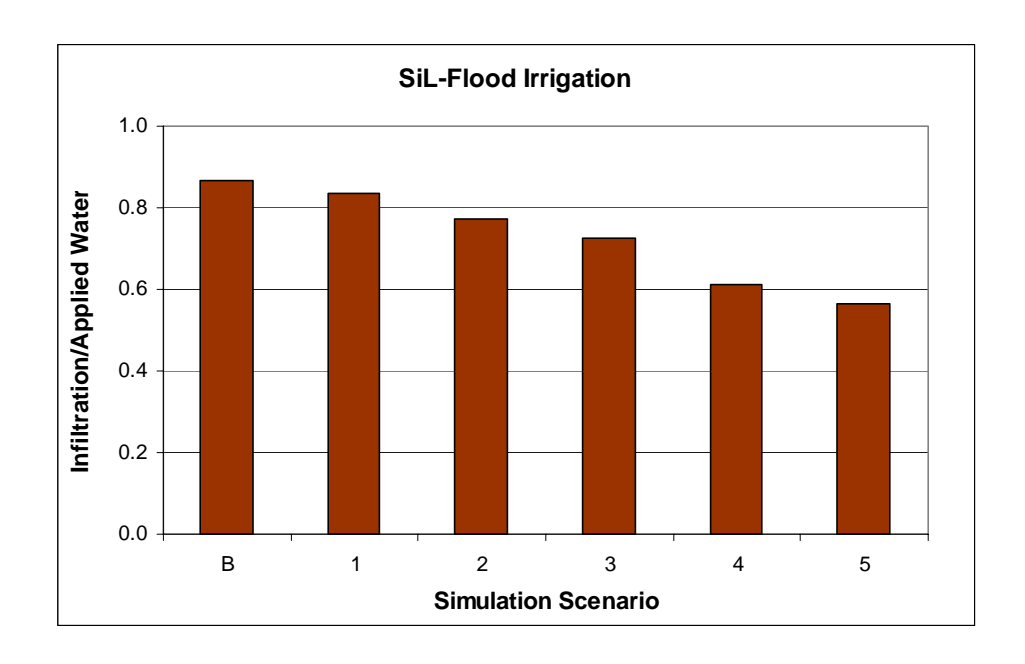


Fig. 15 (cont.)

a)



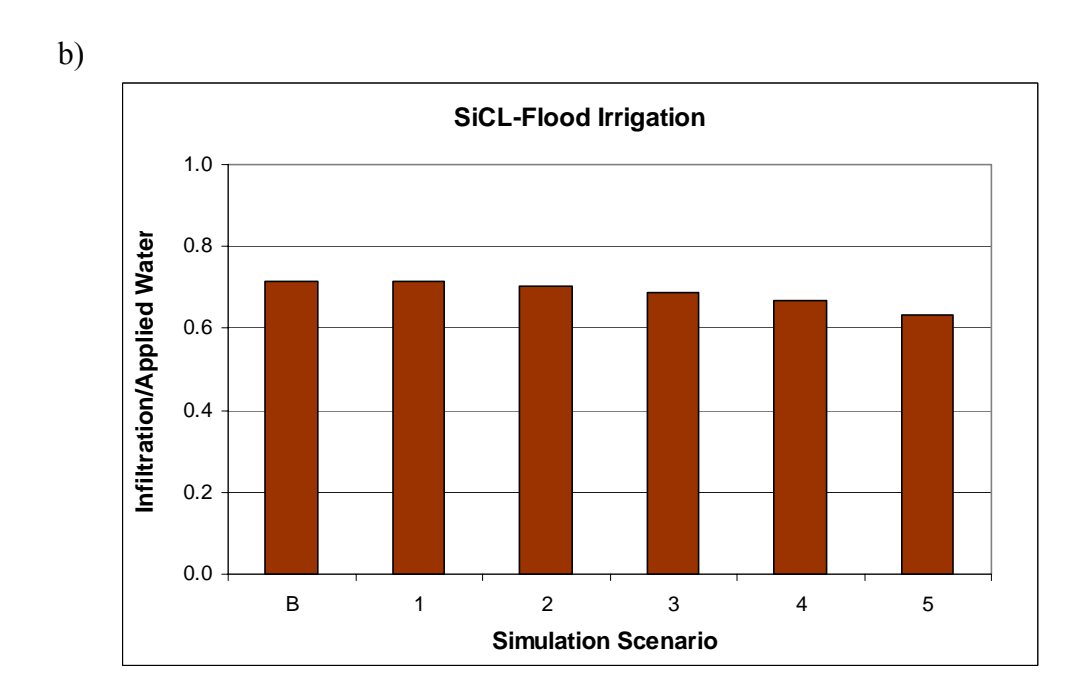
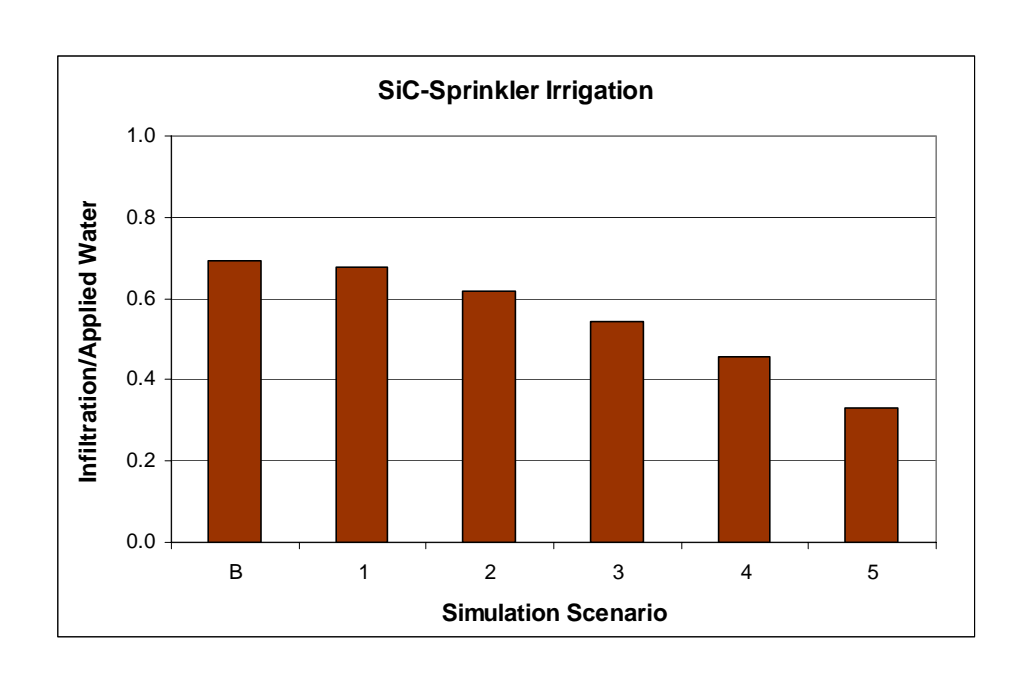


Fig. 16. Cumulative infiltration by soil and irrigation method for baseline and progressively sodic irrigation water qualities. Results are for a) silt loam, b) silty clay loam, c) silty clay soils.

c)



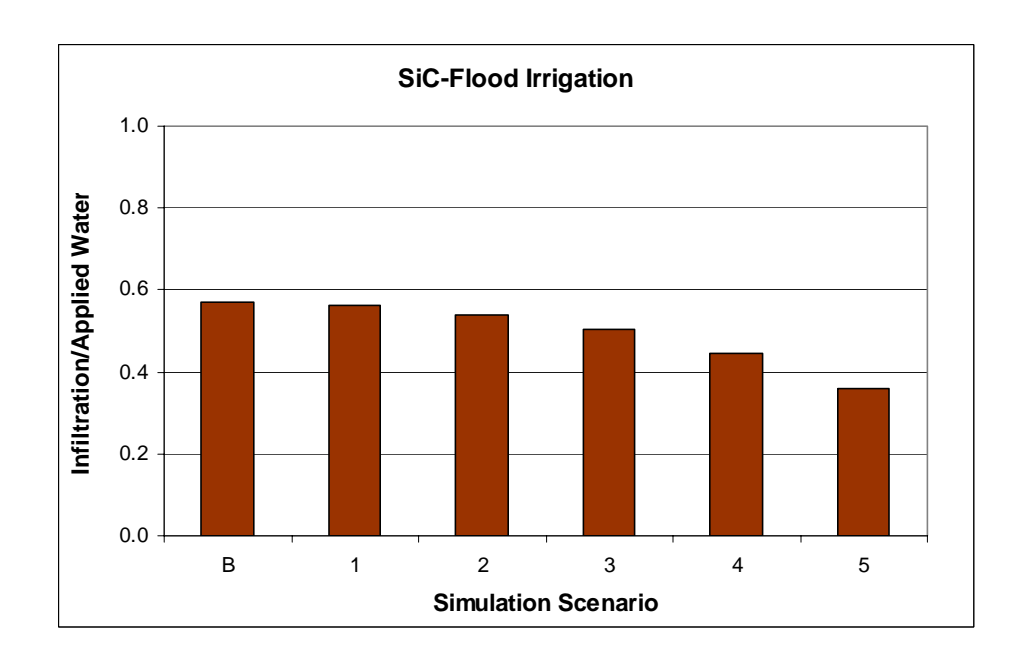


Fig. 16 (cont.)

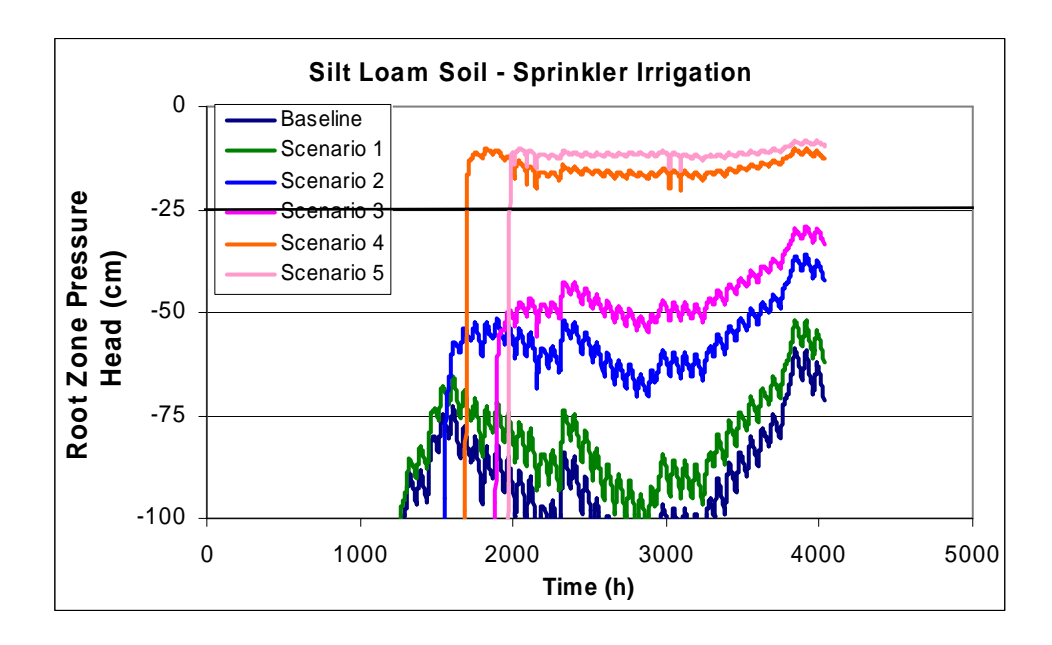


Fig. 17. Root zone pressure head for silt loam soil under sprinkler irrigation, for baseline and progressively sodic irrigation water qualities. Critical upper bound pressure head for maximum alfalfa root extraction of soil water is -25 cm.

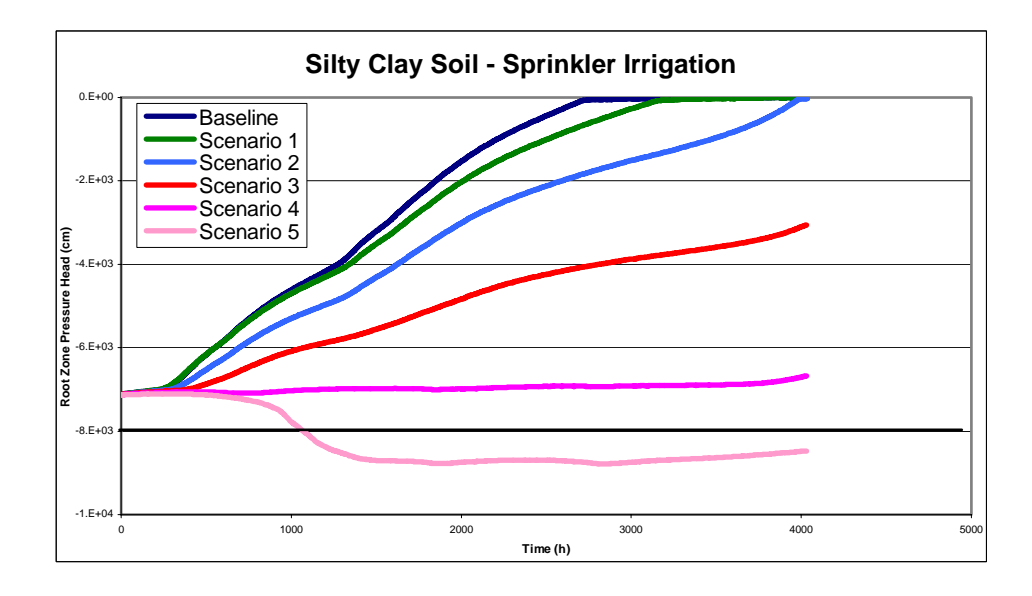


Fig. 18. Root zone pressure head for silty clay soil under sprinkler irrigation, for baseline and increasingly sodic irrigation water qualities. Critical upper and lower bound pressure heads for alfalfa root extraction of (any) soil water are -10 cm and -8000 cm.

Discussion

Laboratory studies attempting to correlate degree of hydraulic impact of sodic application waters with clay content or clay mineralogy of soils have shown mixed results. Some researchers have found no direct relationship between soil clays and measurements of hydraulic conductivity or other hydraulic properties with exposure to waters in a range of salinities and sodicities (McIntyre 1979, Chaudhari and Somawnashi 2003), while others (McNeal and Coleman 1968) have correlated smectite clay mineral content with reductions in soil permeability.

The expectation that the model would predict larger increases in soil water storage, decreases in drainage, and increases in runoff for soils with a higher than lower clay percentage under increasingly sodic simulated conditions was partially met with respect to soil water storage (Fig.14). Soil water storage decreased, commensurate with increases in surface runoff and decreased infiltration, for both simulated irrigation methods in the silty clay, the highest clay soil type modeled (Fig. 14c). In this soil, a larger percentage of applied water (31% at baseline and 67% under Scenario 5) did not infiltrate into the soil matrix to be stored. The next-highest clay-fraction soil, the silty clay loam, did show soil water storage increases for both irrigation types across increasingly sodic simulations, as did the silt loam under sprinkler irrigation (Fig. 14b and c). For these scenarios, cumulative infiltration remained identical or nearly identical for all simulated sodicity levels, and the imposed increases in saturated soil water content (θ s) allowed the soils to store more water under wetter conditions. The silt loam under flood irrigation showed decreases in storage corresponding to increases in simulated sodicity, as more water ran off the soil surface (Fig

14b). The simulated soil with the lowest clay content, the fine sandy loam, demonstrated a bowed response across the sodicity scenarios under both irrigation types, first decreasing in storage (or increasing in seasonal soil water loss) between baseline and Scenario 2, but then increasing between Scenarios 3 and 5 (Fig. 14a). The soil water storage trend for this soil was balanced by increases in deep drainage between baseline and Scenario 2, and decreases in drainage between Scenarios 3 and 5.

The expectation relating to relative soil clay percentages was generally validated for drainage, as the silty clay and silty clay loam soils showed the largest decreases in drainage relative to baseline values. There was no predicted drainage for any of the silty clay soil flood irrigation simulations. The silt loam, in contrast to expectation, exhibited increased deep drainage with increased simulated sodicity under sprinkler irrigation, but showed decreases from a baseline value of 0.8 cm to zero under Scenarios 2-5 under flood irrigation. The fine sandy loam showed a bowed relationship in water distribution between deep drainage and soil water storage, as noted above.

This expectation was also generally met for runoff, which showed larger absolute and relative increases with increases in simulated sodicity for the silty clay soil under both irrigation methods compared to the lower-clay soils. The silt loam also exhibited increasingly high runoff values with increasing simulated sodicity under the high-intensity flood irrigation. In the silt loam under sprinkler irrigation, where water was applied at a slower rate than for flood irrigation and was therefore stored by soil rather than running off the surface, values increased only slightly from a baseline of zero to a few cm in Scenarios 3

and 5. There was no predicted runoff over the season for the fine sandy loam or silty clay loam under either irrigation method.

The modeling study by Cai et al. (1994) found that *Ks* was the model input parameter most strongly correlated with infiltration rate in a high-clay soil under saline water ponding. Tedschi and Menenti (2002) and Feng et al (2003a) observed a relationship in their models between reduced infiltration rate and decreased frequency of irrigation.

The expectation of greater reductions in surface infiltration under increasingly sodic simulated irrigation waters for the high-intensity flood irrigation than for sprinkler irrigation was only partially met in the current study. The fine sandy loam did not show decreases in cumulative infiltration with increasing simulated sodicity under either irrigation method. The soil apparently had a sufficiently large Ks, even under the more sodic irrigation water scenarios, that it was able to conduct water in the relatively large quantities it was applied, from the saturated soil surface through the soil matrix. The fine sandy loam Ks values were reduced by 70% between the baseline and Scenario 5 simulations. In line with the expectation, the silt loam and silty clay loam soils did not show any infiltration decrease over the range of sodic conditions with sprinkler irrigation, but did show a decrease with flood irrigation which had a ten-fold greater water application rate. For Scenario 5, the silt loam and silty clay loam Ks values were decreased from baseline values by 75 and 85%, respectively. The silty clay soil showed greater absolute and relative infiltration decreases across simulated sodicities under sprinkler irrigation than for flood irrigation. Ks values for the silty clay were very small for all hydraulic conditions, and Ks was decreased by 95% from baseline for Scenario 5. With this soil, a substantial percentage of applied water (23%)

at baseline and 79% under Scenario 5) was removed from the soil surface as runoff before it could be infiltrated.

Some studies that combined field-measured data and modeling results have found correlations between increases in irrigation water sodicity and decreases in actual or relative crop yield (Tedeschi and Menenti 2002, Feng et al. 2003a), however, these decreases are correlated with increases in soil salinity, and the corresponding increase in osmotic stress on root water extraction. The simulations in this study did not include crop solute stress or salt transport components.

Based on simulation of water balance only, the fine sandy loam and silty clay loam soils exhibited nearly identical RWU/ET ratios across the simulated conditions, and the silty clay soil showed no clear trend, with small increases and decreases across Scenarios 1-5 under both irrigation simulations. With the fine sandy loam and silty clay loam soils, the decreases in mean pore size that might occur as a result of soil particle dispersion with increasingly sodic application waters, described in the simulations by changes in the water retention and hydraulic conductivity relationships, did not significantly affect the soils' abilities to maintain suitable water status for alfalfa root water uptake. Aeration and wetness remained adequate for alfalfa roots to extract similar amounts of soil water for all the simulation conditions. Compared to the silt loam soil, for which baseline parameter values were close in value to the silty clay loam soil, residual water content (θr) values were increased in the silty clay loam, rather than decreased (after Cresciamanno et al. 1995, Fig. 11b and 11c), to model increasingly sodic water retention functions. This characteristic of the imposed water retention function allowed the soil to hold more plant-available water with

the higher sodicity treatments, at the matric potentials maintained in the root zone during most of the season (-100 to -1000 cm) under both irrigation methods.

The silt loam soil simulations showed large reductions in RWU/ET under Scenarios 4 and 5 with sprinkler irrigation and smaller reductions under those scenarios with flood irrigation, as evaporation remained relatively constant but transpiration declined sharply (Table E2, Appendix E). Under Scenarios 4 and 5 with sprinkler irrigation, this soil's root zone was close to saturation for the second half of the growing season, at a matric potential above the critical value of –25 cm at which alfalfa roots cease to extract soil water at the maximum rate (Taylor and Ashcroft 1972, Fig.17). Under flood irrigation, more water was lost as runoff for this soil than was transpired under increasingly sodic water treatments, resulting in reduced surface infiltration, drier soil between irrigation events, and less root zone water for the crop.

The silty clay soil under sprinkler irrigation showed a general trend of increase in RWU/ET (Fig 15d; and in absolute RWU, Table E2, Appendix E) between baseline and a maximum at Scenario 4, then a decline back toward baseline level under Scenario 5. Fig. 18 shows the seasonal difference in root zone pressure heads in the silty clay under sprinkler irrigation for the baseline and increasingly sodic scenarios. In this case, under Scenarios 2 through 4, matric potential was maintained for the season at pressure heads that enabled alfalfa roots to extract (any) soil water (-10 to -8000 cm). Other scenarios show partial-season saturation (baseline and Scenario 1) or drier soil (Scenario 5) conditions under which simulated RWU values were less than for Scenario 4.

Sprinkler irrigation involves water droplet impact on the soil surface, potentially causing a physical dispersal of fine soil particles in addition to potential infiltration rate reduction caused by the water's Na content (Oster 1994, Shainberg and Letey 1984).

Sprinklers also expose a larger water surface area to the atmosphere than does flood irrigation, increasing potential for evaporation before water contacts the soil surface. The Hydrus-1D model does not facilitate simulation of these physical distinctions between irrigation types and, hence, neither of these characteristics of sprinkler irrigation, potentially increasing evaporation and runoff in the field, were incorporated into the simulations in this study.

For sprinkler irrigation, where water supply to the soil surface was much more frequent than for flood irrigation, the Hydrus model predicted cumulative seasonal evaporation under all sodicity scenarios to be at or near potential evaporation (42.8 cm) for the fine sandy loam, silty loam, and silty clay loam soils. Evaporation decreased in the silty clay for both irrigation types as increased simulated sodicity increased runoff, leaving less water to evaporate from either the soil or the ponded water surfaces. Under flood irrigation simulations, soils dried out between flood events, and evaporation increased slightly with increasing simulated sodicity in the fine sandy loam and silty clay loam soils. Evaporation decreased slightly in the SiL and SiC soils, where, with increasingly sodic treatments, more flood irrigation water ran off the soil surface.

In the fine sandy loam and silty clay loam soils runoff was zero for all simulated sodicities under both sprinkler and flood irrigation. The infiltration and hydraulic conductivity of these soils remained sufficient to accommodate irrigation at the rates imposed

for both simulated irrigation types. In the silt loam soil, there was increasing runoff with increasing simulated sodicity for flood but not for sprinkler irrigation. For this soil under sprinkler irrigation, water that infiltrated at the lower sprinkler-applied rate was increasingly stored by the soil across sodicity treatments, and under flood irrigation, the soil was increasingly unable to keep up with the application water flux with increased sodicity, and more runoff occurred. In the silty clay soil, runoff increased less across the increasingly sodic scenarios with sprinkler than with flood irrigation. The silty clay soil showed greater absolute increases in runoff across sodicities for the sprinkler irrigation simulations, where runoff even under baseline conditions was considerable (30.8 cm), but greater increases relative to baseline for flood irrigation.

The model simulations presented here include some general limitations inherent to most models in replicating the complex conditions and interactions in play in the natural environment, as well as some specific limitations associated with the particular set of field conditions investigated in this study. In some cases, such as the simulated flood irrigation events, it was necessary to input precipitation/irrigation values at a lower flux than would occur in the field in order to avoid exceeding the numerical computation capacities of the software. As noted previously, it was not possible to include some potentially interesting mportant phenomena, including evaporation of sprinkler water before it reached the soil surface, and any physical effects resulting from water droplet impact on the soil surface. The simulations as constructed made no distinction between saline-sodic irrigation water application, and low salinity, low sodicity rainwater falling on the soil. The hydraulic parameters input as an initial condition remained the same over the entire season,

representing hypothetical cases where the soil properties were in equilibrium with irrigation water quality.

Reflection on the soil water balance simulation results suggests some considerations for PRB land managers examining the potential to use CBM product water for irrigation. One relates to the issue of multi-season use of sodic irrigation waters. Some coarser soils might exhibit an improvement in agronomic or hydraulic function as soil fines are redistributed, the mean pore diameter decreases, and the soil is able to retain more plant-available water. However, this situation may change over multiple irrigation seasons, as fine particles are leached from the profile and the soil can no longer retain the same level of water and nutrients (Sumner 1995).

Although soil clay content and clay mineralogy may be important factors when irrigation with CBM product water is being considered, this study, in common with some previous investigations (e.g. Minhas and Sharma 1986), did not observe a linear relationship between soil clay content or mineralogy and susceptibility to water balance changes induced by sodic application waters. A soil with more total clay or with a greater fraction of smectite clay minerals might function better than a lower-clay, lower smectite soil under some sodic irrigation water conditions, depending on specific changes to the soil hydraulic properties.

In this study, high-intensity, low frequency flood irrigation simulations created a higher cumulative seasonal runoff with increases in simulated irrigation water sodicity in the finer soils than did the lower-intensity, higher-frequency sprinkler irrigation. This may be a consideration for irrigation managers when they are presented with the option of using undiluted CBM water with existing water channels, gates, and spreader dikes. However,

prolonged use of sprinkler irrigation may cause salts to build up in the soil, increasing the osmotic gradient against which plants must extract water. Leaching on an annual basis with a sufficient volume of low-salinity water may prevent soil salinization and sodication, but this assumes that low-salinity water is available and accessible to the land in question. This may not be true in some parts of the PRB where irrigation with CBM water might be an option.

REFERENCES

Abdul-Jabbar, A.S., T.W. Sammis, and D.G. Lugg. 1982. Effect of moisture level on the root pattern of alfalfa. Irrig. Sci. 3:197-207.

ALL Consulting and CH2M HILL. 2001b. Water resources technical report. Montana statewide oil and gas environmental impact statement and amendment of the Powder River and Billings resource management plans. Prepared for the U.S. Dept. of Interior, Bureau of Land Management, Miles City Field Office. Miles City, MT.

Ayers, R.S., and D.W. Wescott. 1985. Water quality for agriculture. FAO irrigation and drainage paper 29, rev. 1. Food and Agriculture Organization of the United Nations, Rome.

Bauder, J.W., and T.A. Brock. 2001. Irrigation water quality, soil amendment, and crop effects on sodium leaching. Arid Land Res. Manage. 15:101-113.

Cai, L., S.A. Prathapar, and H.G. Beecher. 1994. Modelling leaching and recharge in a bare transitional red-brown earth ponded with low salinity water in summer. Aust. J. Exp. Agric. 24:1085-1092.

Chaudhari, S.K., and R.B. Somawanshi. 2004. Unsaturated flow of different quality irrigation waters through clay, clay loam and silt loam soils and its dependence on soil and solution parameters. Agric. Water Manage. 64: 69-90.

Coalbed methane development in Montana: Hearing, U.S. Senate, Committee on Appropriations, March 10, 2001. Hearing before a Subcommittee of the Committee on Appropriations. S.Hrg. 107-104 (Available online at http://www.access.gpo.gov/congress/senate) (Verified 6 Sept. 2004).

Crescimanno, G., M. Iovino, and G. Provenzano. 1995. Influence of salinity and sodicity on soil structural and hydraulic characteristics. Soil Sci. Soc. Am. J. 59:1701-1708.

Feddes, R.A., P.J. Kowalik, and H. Zaradny. 1978. Simulation of field water use and crop yield. John Wiley & Sons, New York.

Feng, G.L., A, Meiri, and J. Letey. 2003a. Evaluation of a model for irrigation management under saline conditions. I. Effects on plant growth. Soil Sci. Soc. Am. J. 67:71-76.

Feng, G.L., A, Meiri, and J. Letey. 2003b. Evaluation of a model for irrigation management under saline conditions. II. Salt distribution and rooting pattern effects. Soil Sci. Soc. Am. J. 67:77-80.

Levy, G.J. 1999. Sodicity. p. G27-G64. *In* Sumner, M.E. (ed.). Handbook of soil science. CRC Press, Boca Raton.

Levy, G.J., N. Sharshekeev, and G.L. Zhuravskaya. 2002. Water quality and sodicity effects on soil bulk density and conductivity in interrupted flow. Soil Sci. 167:692-700.

Lima, L.A., M.E. Grismer, and D.R. Nielsen. 1990. Salinity effects on Yolo loam hydraulic properties. Soil Sci. 150:451-458.

Lowry, M.E., and J.F. Wilson, Jr. 1986. Hydrology of area 50, northern Great Plains and Rocky Mountain coal provinces, Wyoming and Montana. U.S. Geological Survey Water Resources Investigations, 83-545. Cheyenne, WY.

Mace, J.E., and C. Amrhein. 2001. Leaching and reclamation of a soil irrigated with moderate SAR waters. Soil Sci. Soc. Am. J. 65:199-204.

McIntyre, D.S. 1979. Exchangeable sodicum, subplasticity and hydraulic conductivity of some Australian soils. Aust. J. Soi Res. 17:115-20.

McNeal, B.L., and N.T. Coleman. 1966. Effect of solution composition on soil hydraulic conductivity. Soil Sci. Soc. Am. Proc. 30:308-312.

Meshnick, J.C. 1977. Soil survey of Big Horn County, Montana. U.S. Soil Conservation Service, n.l.

Minhas, P.S., and D.R. Sharma. 1986. Hydraulic conductivity and clay dispersion as affected by application sequence of saline and simulated water. Irrig. Sci. 7:159-167.

Montana Board of Environmental Review March 2003. Coalbed methane discharge standards. Available at: http://waterquality.montana.edu/docs/methane/cbmstandards.shtml. (Verified 7 Sept. 2004).

Mulligan, M., and J. Wainwright. 2004. Modelling and model building. p. 7-73. *In* Wainwright, J., and M. Mulligan (eds.). Environmental modeling: Finding simplicity in complexity. John Wiley & Sons Ltd., West Sussex, England.

Oster, J.D. 1994. Irrigation with poor quality water. Agric. Water Manage. 25:271-297.

Quirk, J.P., and R.K. Schofield. 1955. The effect of electrolyte concentration on soil permeability. J. Soil Sci. 6:163-178.

Rice, C.A., T.T. Bartos, and M.S. Ellis. 2002. Chemical and isotopic composition of water in the Fort Union and Wasatch formations of the Powder River Basin, Wyoming and Montana: Implications for coalbed methane development. *In* S.D. Schwochow and V.F.

Nuccio (eds.) Coalbed methane of North America – II. Rocky Mountain Association of Geologists.

Shainberg, I., and J. Letey. 1984. Response of soils to sodic and saline conditions. Hilgardia 52:1-57.

Simunek, J., K. Huang, M. Sejna, and M.Th. van Genuchten. 1998b. Hydrus-1D for Windows. U.S. Salinity Laboratory, Riverside, CA. Available at: http://www.ussl.ars.usda.gov/MODELS/HYDR1D1.HTM (Verified 4 Nov. 2004).

Simunek, J., M. Sejna, and M. Th. van Genuchten. 1998a. The HYDRUS-1D software package for simulating the one-dimensional movement of water, heat, and multiple solutes in variably-saturated media. U.S. Salinity Laboratory, Riverside, CA. (Available online at http://www.pc-progress.cz/Fr_Services_Hydrus_Downloads.htm) (Verified 11 Oct. 2004).

Taylor, S. A., and G. L. Ashcroft. 1972. Physical edaphology. The physics of irrigated and nonirrigated soils. W. H. Freeman and Company. San Francisco.

Tedeschi, A., and M. Menenti. 2002. Simulation studies of long-term saline water use: model validation and evaluation of schedules. Agric. Water Manage. 54:123-157.

The Orderly Development of Coalbed Methane Resources from Public Lands, September 6, 2001. Oversight hearing before the Subcommittee on Mineral and Energy Resources, Committee on Resources, U.S. House of Representatives. Serial No. 107-58. (Available online at http://www.access.gpo.gov/congress/house) (Verified 6 Sept. 2004).

U.S. Bureau of Land Management, Buffalo Field Office. 2003. Final environmental impact statement and proposed plan amendment for the Powder River Basin Oil and Gas Project. WY-070.02-065. (Available online at http://www.wy.blm.gov/nepa/prb-feis/index.htm) (Verified 7 Sept. 2004).

U.S. Bureau of Reclamation. n.d. The Great Plains Cooperative Agricultural Weather Network [online]. Available at: http://www.usbr.gov/gp/agrimet/index.cfm (Verified 9 Nov. 2004).

van Genuchten, Th.M. 1980. A closed-form equation for predicting the hydraulic conductivity of unsaturated soils. Sci. Soc. Am. J. 44:892-898.

Van Voast, W.A. Chemical signature of formation waters associated with coalbed methane. AAPG Bull. 87:667-676.

Wraith, J.M., and D. Or. 1998. Nonlinear parameter estimation using spreadsheet software. J. Nat. Resour. Life Sci. Educ. 27:13-19.

SUMMARY AND CONCLUSIONS

A repacked soil columns experiment and a suite of soil water balance simulations were conducted to examine potential effects of the agricultural use of coalbed methane (CBM) product water on soils typical of irrigable soils in Montana's Powder River Basin (PRB).

In the soil columns study, sandy loam, silt loam, and clay loam soils were pre-treated with water having a salinity and sodicity typical of CBM water (EC=3.0 dS/m, SAR=30.7), or of Powder River water (EC=1.6 dS/m, SAR=4.9). Replicate tension infiltrometer measurements of water flux through the soil surface were obtained using the pre-treatment quality (CBM or PR) water, and these were compared with subsequent measurements on the same columns using deionized (DI) water to simulate rainfall or snowmelt.

Experimental results validated a hypothesis of greater mean infiltration water flux for PR than for CBM pre-treated soils using the pre-treatment water qualities for testing in the clay and sandy loam, but not in the higher-calcium silt loam soil. Results failed to fully support hypotheses based on EC-SAR combinations in the pre-treatment waters and on comparative texture, clay content and clay mineralogy of the soils, that the mean decline in flux rates between pre-treatment and DI water treatments would be greater in CBM-pre-treated soils, in the B horizons of all soils, and in soils with a higher smectite clay mineral content. The sandy loam was the only one of the three soils exhibiting a significant pre-treatment water quality effect, and there was no significant pre-treatment water quality effect of horizon or of soils. Results point to the need to examine soil baseline chemistry and level of aggregation in addition to texture and clay content when the use of CBM product water for

irrigation is considered. The A and B horizons of the three soils were similar in clay content. Soil aggregation was disrupted in the repacked soils used in this study and was not quantified.

In the soil water balance simulations, 48 scenarios were modeled to represent irrigation water covering a range of sodicities on different soil types. Soil water retention and hydraulic conductivity functions were estimated for four soils typical of those currently irrigated in the PRB: a fine sandy loam, silt loam, silty clay loam, and silty clay soil.

Baseline measured water retention functions were modified for each soil to approximate expected changes resulting from increasingly sodic irrigation waters, based on literature reports. The Hydrus-1D numerical code was used to simulate water flow and root water uptake for a single growing season in uniform 1 m deep soil materials under alfalfa crop. Flood and sprinkler irrigation simulations based on common and developing practices in the PRB were conducted for each soil.

The simulations did not include salt transport or salinity balance, and therefore did not address total salinity or specific ion effects on plant water uptake or physiology. Rather, they were intended to provide insight concerning potential impacts of changes in soil hydraulic properties only on the partitioning of water balance components during a single growing season. Inclusion of salt transport and salinity impacts on these processes requires substantially more knowledge of soil properties than was available and incurs additional model uncertainty beyond that involved in soil water flow. This would seem a fruitful avenue for follow-up on the investigations reported here.

Simulation results generally showed that flood irrigation created larger changes in soil water balance than did sprinkler irrigation under the more sodic scenarios, particularly decreases in transpiration and increases in runoff. The water balance of the coarser soils was less affected by the altered hydraulic properties than was that of the finer soils, although the silty clay loam soil exhibited smaller changes than did the more finely textured silt loam soil because of the specific imposed modification s to the soil hydraulic properties. The fine sandy loam appeared to maintain conditions favorable to root water uptake and deep drainage, whereas the silt loam soil appeared to reach a threshold at the 4th level of simulated sodicity, at which there were decreases in root water uptake under both irrigation methods, and increases in runoff with sprinkler irrigation. In this soil under sprinkler irrigation, decreased root water uptake was a result of slow drainage and therefore lack of aeration due to high wetness, while under flood irrigation, the decline in transpiration was likely attributable to decreases in surface infiltration and in plant-available water. Relatively high surface runoff and low infiltration values, becoming more notable across sodicity Scenarios 1-5, characterized the finest-textured silty clay soil.

Simulation results suggest that PRB landowners contemplating the use of CBM product water for irrigation may wish to consider that clay content and soil texture may not be proportionally related to susceptibility to adverse effects of sodic water, and that a lower-intensity, higher-frequency irrigation method such as sprinklers may allow soils to maintain hydraulic function more readily than less frequent, high-water-volume flood irrigations. However, low frequency, high-intensity sprinkler methods such as center pivot may result in runoff patterns more similar to the flood scenarios used here. Furthermore, enhancement of

infiltration during flood irrigation of fields may be accomplished by allowing water to remain ponded for longer periods, as long as soil aeration does not decline below critical levels. In the field, the salt concentrating effects of water droplet evaporation under sprinkler irrigation (not modeled in this study) could also merit consideration.

Based on both the experimental and computer simulation investigations, it appears that PRB CBM water might be productively used for irrigation under some conditions without adverse effects on soil water flow or on the partitioning of water in soils. Prudent use would involve not only examination of soil texture and clay fraction and of irrigation water salinity and sodicity, but also monitoring of soil salt balance, and application of water at a rate compatible with the soil's capacity for infiltration and hydraulic conductivity.

Reclamation and long-term management of sodic soils has been accomplished in some areas through the addition of calcium soil amendments such as gypsum, or acidifying agents such as sulfur, which help to dissolve calcium solids. Costs involved in amendment application may preclude their use in some instances. Fresh water supply is a key component of amendment use, as sufficient water must be moved through the soil profile to remove excess salts and sodium from the root zone. Soils in semiarid regions such as the PRB may contain large amounts of calcium solids because low annual rainfall limits wet-season dissolution and flushing of salts. Calcium added as an amendment under these circumstances will result in further precipitation of calcium and further SAR increases, counter to management objectives.

Great care must be taken in extrapolating observations or results from the present studies to specific situations on the ground. In addition to the need to consider longer-term

impacts of sodic water application on soils than were addressed in either the laboratory experiment or computer simulations, there are aspects of both of these projects that limit the direct transfer of results to the field. The conventional handling methods used in the repacked soil column study likely decreased the inter-soil variation in hydraulic behavior due to destruction of larger soil aggregates. The volume of pre-treatment water used in the experiments was assumed to have been sufficient to equilibrate the soils to the applied waters, but sodium exchange processes within the smaller (<1cm) aggregates that remained after sieving might require additional time. Due to the scenario simplifications and computing limitations inherent in any modeling effort, some relationships apparent in results from the model simulations may not be representative of trends observed under agronomic conditions. In fact, several potentially important field processes were identified that are not addressed by the simulation study.

It is informative to look at the results of these studies as illustrations of some cases where there may be fairly direct relationships between certain soil and water characteristics and a particular hydraulic response, and other cases where the same relationships are apparently mediated by other factors. The intent with these investigations has not been to necessarily draw definitive conclusions about any of the relationships investigated, but to contribute some insights to a complex ongoing scientific discussion on the effects of saline-sodic water on soil-water relationships.

APPENDICES

APPENDIX A

FIELD SOIL DESCRIPTIONS, SOIL COLUMNS EXPERIMENT

Field Soil Descriptions

Descriptions summarized from information provided by Dr. Thomas Keck, Soil Scientist, USDA Natural Resources Conservation Service, Whitehall, MT, personal communication 2003-2004.

Sandy Loam (Logan-Trident Rd.)

Map Unit: 35B, Kalsted sandy loam, 0-4 percent slopes.

Taxonomic class: Coarse-loam, mixed, superactive, frigid Aridic Calciustept.

A—0 to 3 inches; find sandy loam, strongly effervescent.

Bk1—3 to 10 inches (sampled); fine sandy loam, violently effervescent

Silt Loam

Taxonomic class: Coarse-silty, mixed, frigid, superactive Aridic Calciustoll.

Ap--0 to 5 inches; brown (10YR 5/3) silt loam, very dark grayish brown (10YR 3/2) moist; weak, find granular structure; estimated clay 20 percent; no rock fragments; strongly effervescent; mildly alkaline (pH 7.8); clear, irregular boundary due to mixing by worms.

Bk₁—5 to 18 inches; pale brown (10YR 6/3) silt loam, dark grayish brown (10YR 4/3) moist; weak, medium subangular blocky structure; estimated clay 18 percent; no rock fragments; violently effervescent; moderately alkaline (pH 8.2); clear, smooth boundary.

Bk₂—18 to 40 inches; very pale brown (10YR 7/3) silt loam, brown (10YR 5/3) moist; weak, coarse subangular blocky structure; estimated clay 14 percent; no rock fragments; violently effervescent; moderately alkaline (pH 8.2); gradual, smooth boundary.

Bk3—40 to 60+ inches; very pale brown (10YR 7/4) silt loam, yellowish brown (10YR 5/4) moist; massive; estimated clay 12 percent; no rock fragments; violently effervescent; moderately alkaline (pH 8.2).

Clay Loam (Bench Rd.)

Map Unit: 44C Varney clay loam, 4-8 percent slopes. Taxonomic class: Fine, smecitic, frigid Torrertic Haplustoll Silty clay textures throughout.

APPENDIX B

X-RAY DIFFRACTION CLAY MINERALOGY RESULTS, SOIL COLUMNS EXPERIMENT

X-ray Diffraction Clay Mineralogy Results

Single samples of A and B horizons for the study three soils were submitted to the Environmental and Soils Laboratory, North Dakota State University's Department of Soil Science (Fargo, ND) for analysis of clay mineralogy.

Procedures

Sample preparation for qualitative analysis of the clay-size particles by XRD involved preparing oriented slides using the Millipore filter transfer method (Moore and Reynolds, 1989). A Philips automated iffractometer, equipped with CuKa radiation, variable divergence theta-compensating slit, and a diffracted beam monochromator, was used to analyze the oriented slides. Phases were identified by comparison with in-house reference diffractograms, as well as by computer search-match procedures which employ the ICDD Powder Diffraction File.

After the initial scans were run, the oriented slides were placed overnight in a chamber and exposed to ethylene glycol vapor. This glycolation step aids in the identification ofsmectite group minerals, and in distinguishing smectite group from chlorite or vermiculite group minerals.

XRD analysis, combined with additional chemical and thermal treatments, can distinguish among the major groups of common soil clay minerals: smectite (S), mica-Illite (I), Kaolinite (K), Chlorite (C), and vermiculite. The analyses presented here aim only to qualitatively identify these clay mineral groups in the oriented slides made from the <2~m soil fraction. Individual minerals can sometimes be suggested by peak relative intensities, e.g., glauconite in the mica-illite group, or saponite from weathered basalt in the smectite group. Smectite can be separated into montmorillonite, beidellite, and others, with additional chemical tests. To achieve this level of identification would require one or more of the following: sample source information, chemical analyses, cation exchange capacity measurements, scanning electron microscopy.

Procedures: Moore, D.M., and R.C. Reynolds, Jr. 1989. X-ray diffraction and the identification and analysis of clay minerals. Oxford University Press, New York.

Summary of results from XRD analyses:

Clay loam – A and B horizons Clay minerals: Kaolinite, chlorite and illite. Smectite was confirmed by glycolation treatment. Other minerals: Quartz, feldspars and calcite.

Comments: Chlorite was identified by only one definitive peak at $\sim 220~2\theta$. Iron oxides could not be ruled out.

Silt Loam – A and B horizons Clay minerals: Kaolinite and illite.

Smectite was not confirmed by glycolation treatment.

Other minerals: Quartz, feldspars and calcite.

Comments: Chlorite could not be ruled out because of an apparent anomaly found at \sim 220 2θ . The anomaly is not large enough to qualify as a peak. Dolomite could not be ruled out because of an anomaly at \sim 31.50 2θ .

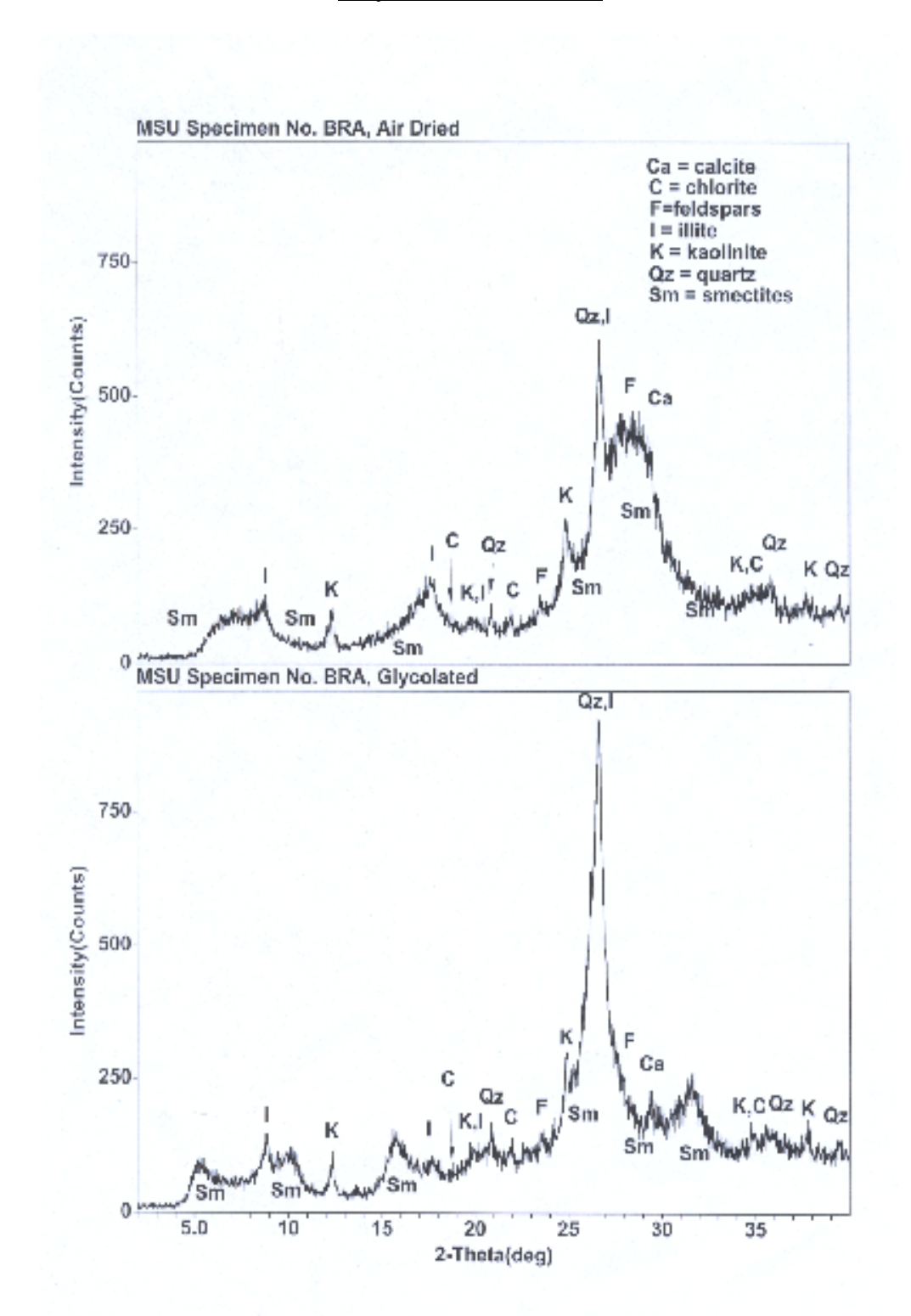
Sandy Loam – A and B horizons Clay minerals: Kaolinite and illite.

Smectite was not confirmed by glycolation treatment.

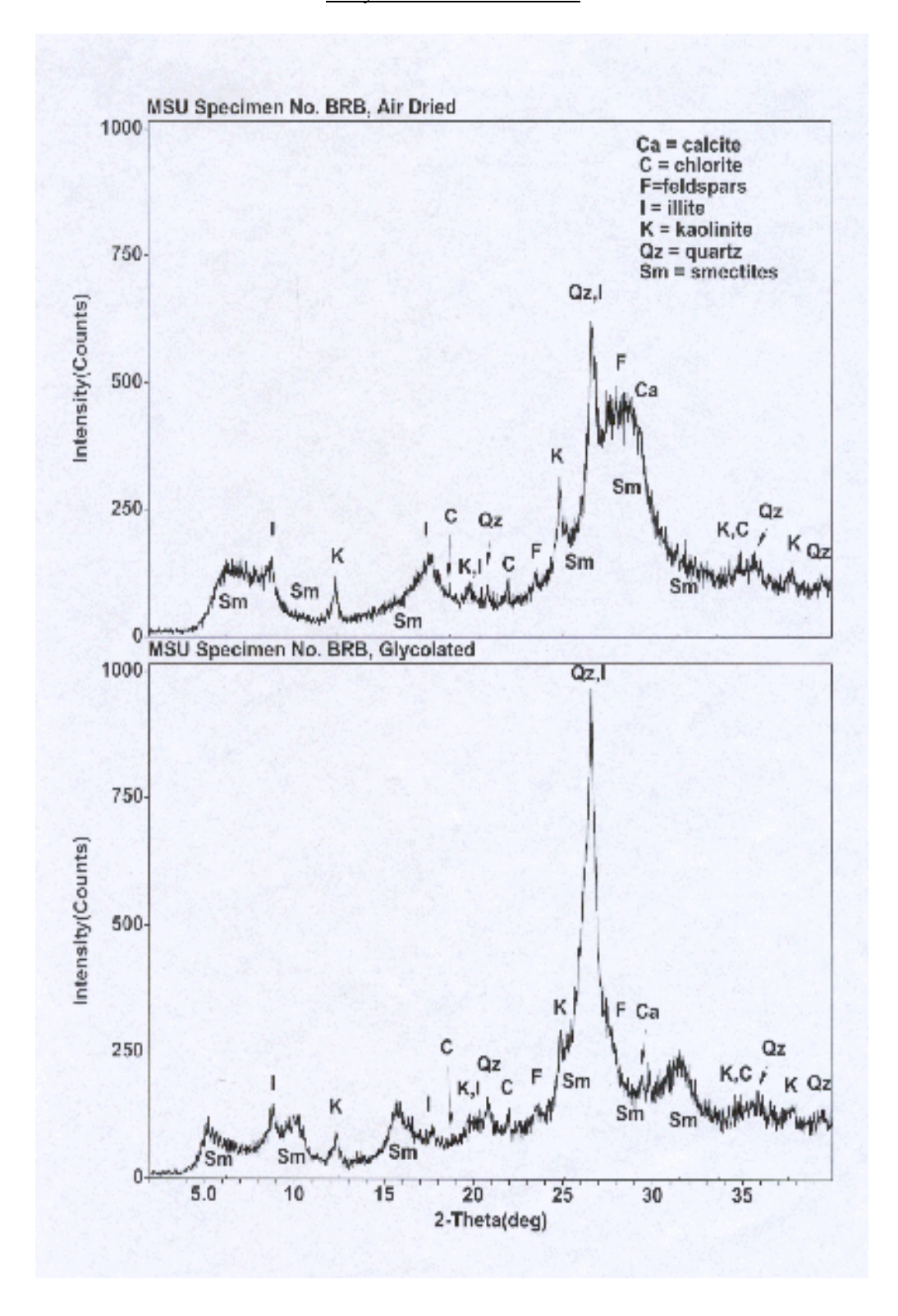
Other minerals: Quartz, feldspars and calcite.

Comments: Chlorite could not be ruled out because of an apparent anomaly found at ~ 220 20. Iron oxides could not be ruled out. Magnesian calcite cannot be ruled out because of an anomaly at ~ 300 2 θ .

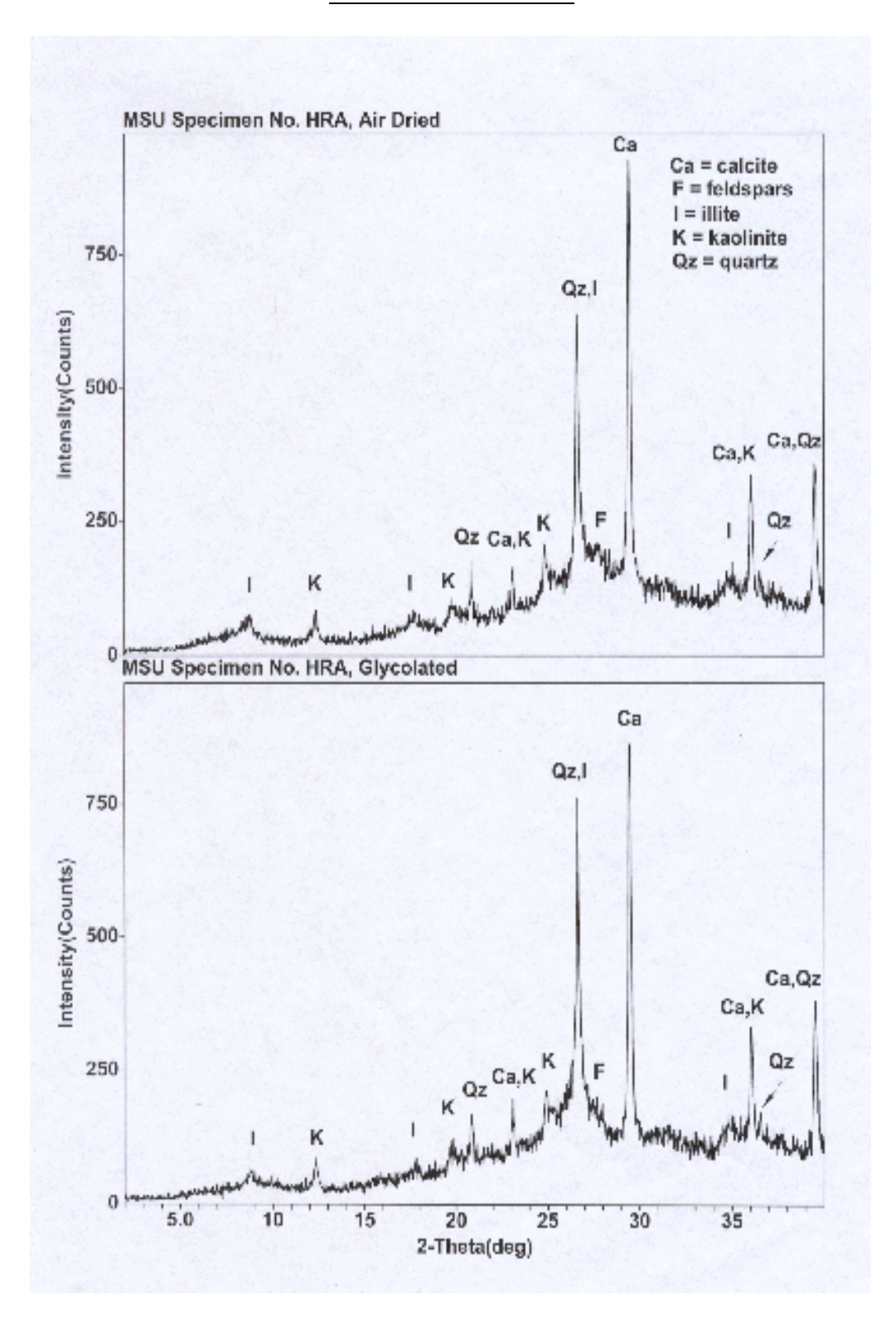
Clay Loam – A Horizon



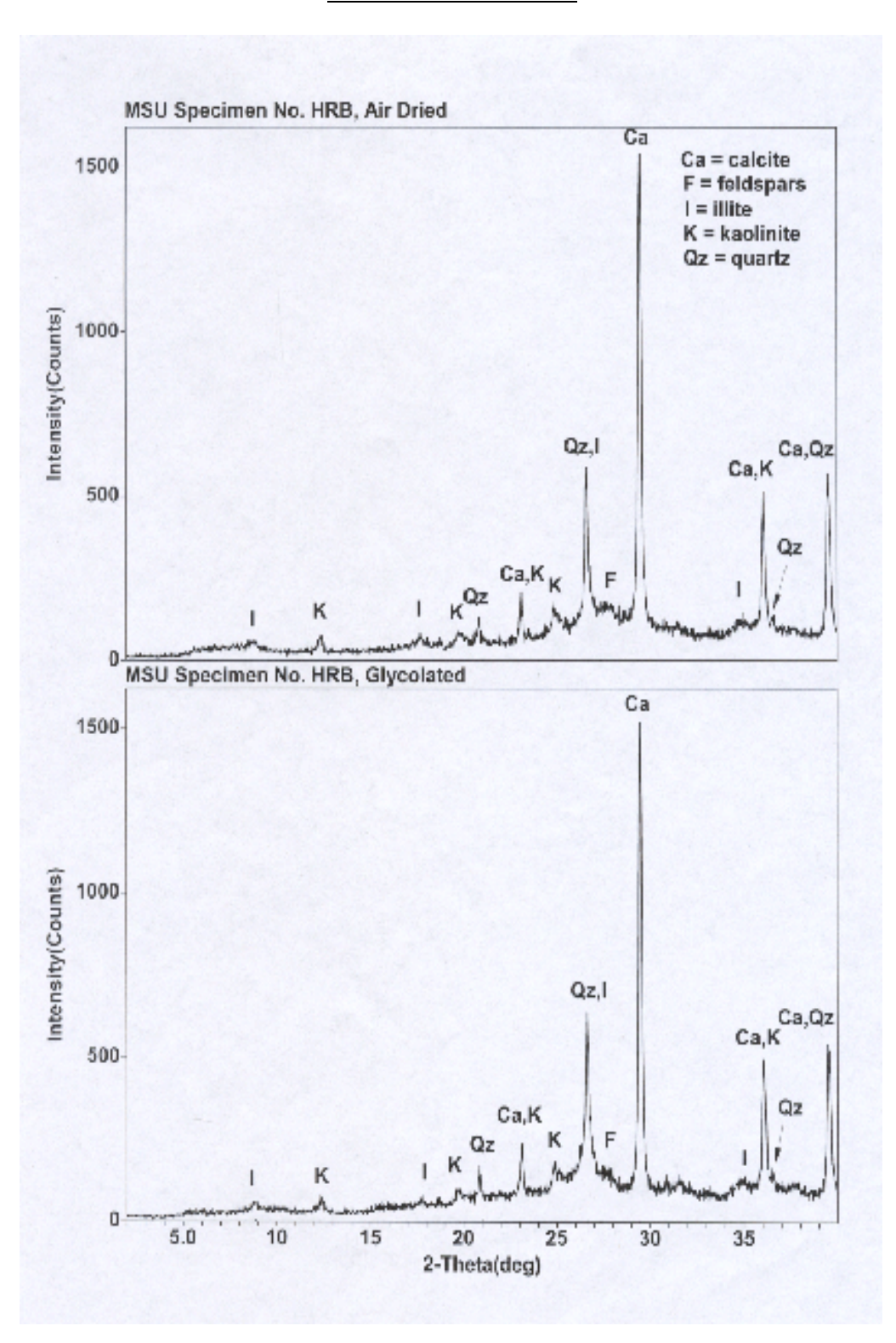
<u>Clay Loam – B Horizon</u>



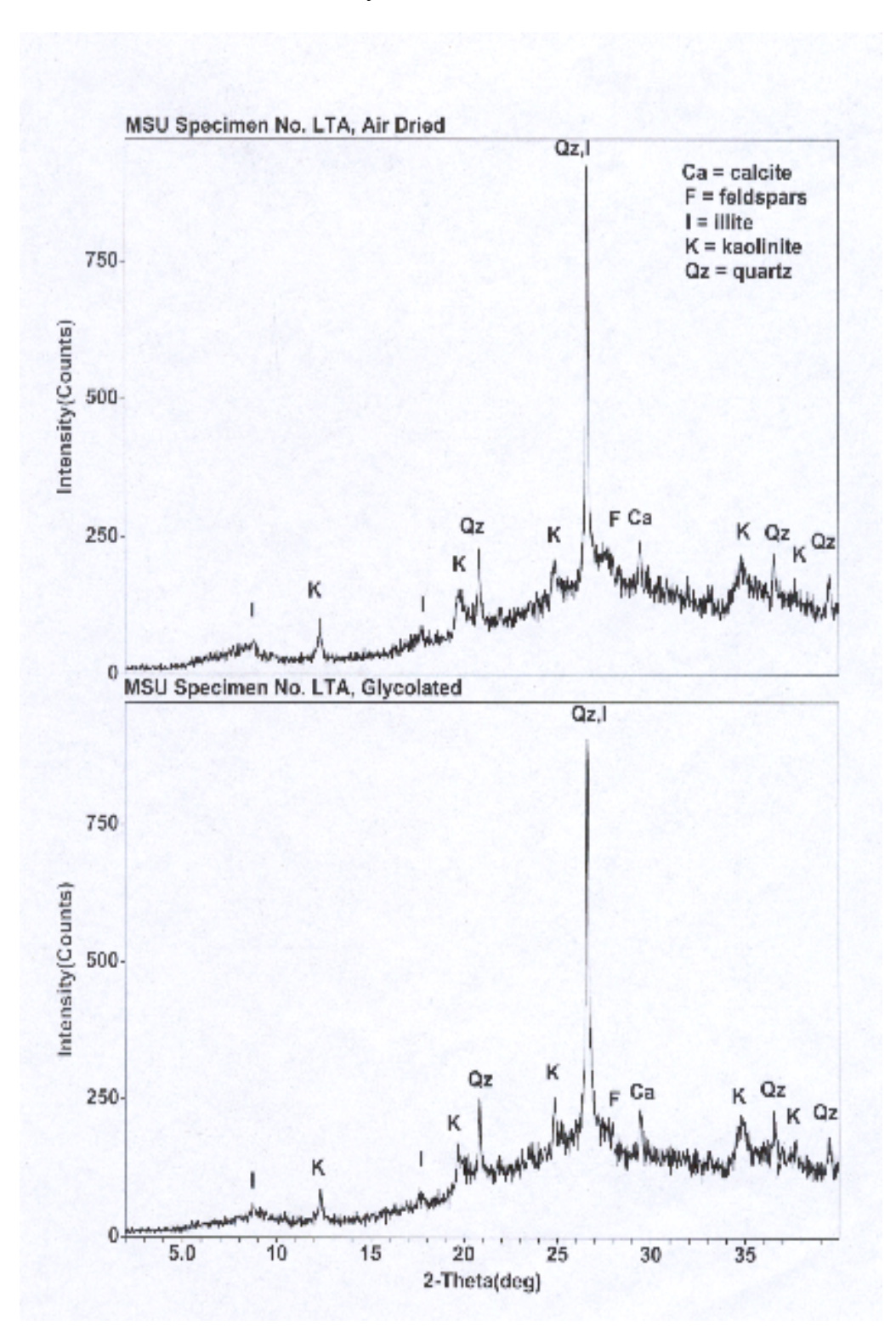
<u>Silt Loam – A Horizon</u>



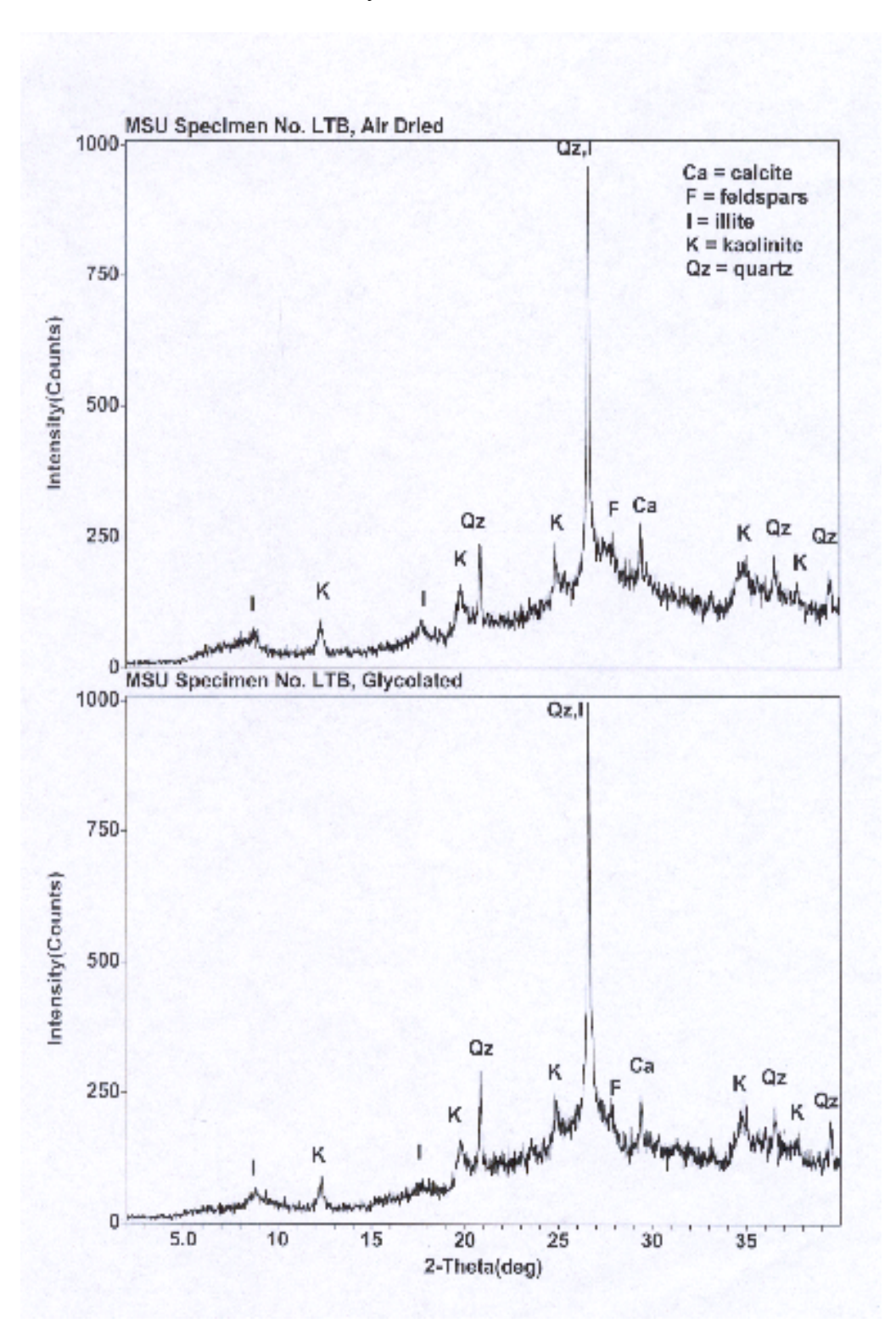
<u>Silt Loam – B Horizon</u>



Sandy Loam – A Horizon



Sandy Loam – B Horizon



APPENDIX C

BASELINE AND TREATED SOIL CHEMISTRY, SOIL COLUMNS EXPERIMENT

Baseline and Treated Soil Chemistry

Three untreated samples and 2 treated (with CBM or PR water) samples of the A and B horizons of the three soil columns study soils were sent to MDS Harris laboratories (Lincoln, NE) for analysis of organic matter, cation composition, and soluble nutrients.

Table C1. Soil organic matter and cation composition, baseline and treated (CBM or PR water) samples.

Soil	Horizon	Status	OM	K	Mg	Ca	Na	Н	Total CEC
			%	%CEC	%CEC	%CEC	%CEC	%CEC	mmolc/g
CL	A	Baseline	2.9	3.7	9.2	83.2	3.8	0.0	34.6
		CBM	2.4	4.2	8.2	70.3	17.4	0.0	41.8
		PR	2.4	5.6	10.3	79.4	4.9	0.0	45.8
	В	Baseline	2.3	3.4	9.3	79.0	8.3	0.0	33.3
		CBM	2.1	3.6	8.6	69.5	18.4	0.0	45.4
		PR	2.3	5.5	10.7	78.2	5.7	0.0	42.2
SiL	A	Baseline	2.8	9	11.0	79.3	0.7	0.0	26.5
		CBM	3	8.1	10.0	69.3	12.6	0.0	33.8
		PR	2.5	8.9	11.9	76.2	3.1	0.0	29.7
	В	Baseline	1.7	4.9	9.7	84.4	1.0	0.0	26.0
		CBM	1.7	4.8	9.1	70.3	15.8	0.0	31.0
		PR	1.6	6.1	11.6	78.6	3.8	0.0	29.3
SL	A	Baseline	2.5	5	7.1	87.8	0.1	0.0	19.6
		CBM	2.4	5.9	6.5	67.0	20.7	0.0	23.7
		PR	2.4	8.6	10.5	76.5	4.5	0.0	23.8
	В	Baseline	1.8	4.8	8.3	86.7	0.1	0.0	22.0
		CBM	1.8	5.3	7.1	69.2	18.4	0.0	26.7
		PR	1.9	7.9	10.8	77.5	3.9	0.0	25.0

132

Table C2. Soluble soil nutrients, baseline samples

Clay Loam – A horizon Baseline

1 Soluble Nutrient Test 0.8 Hg Electrical Conductivity 0.89 mmhos/cm Saturation % 46.39 Sodium (Na) 3.3 Meq/L Calcium (Ca) 3.4 Meq/L Magnesium (Mg) 0.4 Meq/L Potassium (K) 0.5 Meg/L Ammonium-N (NH4) 40.6 ppm Phosphate (PO4) 1.0 ppm Nitrate-N (NO3) 6.9 ppm Bicarbonate (HCO3) 103.7 ppm Sulfate (SO4) 52.8 ppm Chloride (Cl) 138.9 ppm Boron (B03) 0.4 ppm SAR 2.39

2 Soluble Nutrient Test pH 8.3 Electrical Conductivity 0.69 mmhos/cm Saturation % 48.35 Sodium (Na) 3.0 Meg/L Calcium (Ca) 2.7 Meg/L Magnesium (Mg) 0.3 Meg/L Potassium (K) 0.3 Meg/L Ammonium-N (NH4) 12.6 ppm Phosphate (PO4) 1.0 ppm Nitrate-N (NO3) 6.2 ppm Bicarbonate (HCO3) 97.6 ppm Sulfate (SO4) 43.2 ppm Chloride (Cl) 86.5 ppm Boron (B03) 0.7 ppm SAR 2.45

3 Soluble Nutrient Test pH 8.2 Electrical Conductivity 0.77 mmhos/cm Saturation % 51.19 Sodium (Na) 2.7 Meg/L Calcium (Ca) 3.2 Meg/L Magnesium (Mg) 0.4 Meg/L Potassium (K) 0.4 Meg/I, Ammonium-N (NH4) 4.2 ppm Phosphate (PO4) 1.0 ppm Nitrate-N (NO3) 10.8 ppm Bicarbonate (HCO3) 109.8 ppm Sulfate (SO4) 48.0 ppm Chloride (Cl) 103.3 ppm Boron (B03) 0.4 ppm SAR 2.01

Clay Loam - B Horizon Baseline

1 Soluble Nutrient Test pH 8.2 Electrical Conductivity 2.18 mmhos/cm Saturation % 53.33 Sodium (Na) 9.4 Meq/L Calcium (Ca) 7.1 Meg/L Magnesium (Mg) 1.0 Meq/L Potassium (K) 0.6 Meg/L Ammonium-N (NH4) 7.0 ppm Phosphate (PO4) 1.0 ppm Nitrate-N (NO3) 13.9 ppm Bicarbonate (HCO3) 109.8 ppm Sulfate (SO4) 302.4 ppm Chloride (Cl) 395.5 ppm Boron (B03) 0.7 ppm SAR 4.67

2 Soluble Nutrient Test pH 8.2 Electrical Conductivity 2.28 mmhos/cm Saturation % 53.41 Sodium (Na) 9.9 Meq/L Calcium (Ca) 7.6 Meg/L Magnesium (Mg) 1.1 Meg/L Potassium (K) 0.6 Meg/L Ammonium-N (NH4) 12.6 ppm Phosphate (PO4) 1.0 ppm Nitrate-N (NO3) 13.9 ppm Bicarbonate (HCO3) 97.6 ppm Sulfate (SO4) 340.8 ppm Chloride (Cl) 402.5 ppm Boron (B03) 0.4 ppm SAR 4.75

3 Soluble Nutrient Test pH 8.1 Electrical Conductivity 2.57 mmhos/cm Saturation % 42.86 Sodium (Na) 10.8 Meq/L Calcium (Ca) 9.0 Meg/L Magnesium (Mg) 1.2 Meq/L Potassium (K) 0.7 Meq/L Ammonium-N (NH4) 5.6 ppm Phosphate (PO4) 1.0 ppm Nitrate-N (NO3) 18.3 ppm Bicarbonate (HCO3) 103.7 ppm Sulfate (SO4) 374.4 ppm Chloride (Cl) 427.0 ppm Boron (B03) 0.4 ppm SAR 4.78

133

Table C2 (cont.)

Silt Loam – A horizon Baseline

1 Soluble Nutrient Test pH 7.4 Electrical Conductivity 2.79 mmhos/cm Saturation % 43.96 Sodium (Na) 1.1 Meg/L Calcium (Ca) 16.3 Meg/L Magnesium (Mg) 3.7 Meq/L Potassium (K) 3.1 Meg/L Ammonium-N (NH4) 18.2 ppm Phosphate (PO4) 7.2 ppm Nitrate-N (NO3) 376.6 ppm Bicarbonate (HCO3) 97.6 ppm Sulfate (SO4) 105.6 ppm Chloride (Cl) 13.8 ppm Boron (B03) 0.4 ppm **SAR 0.35**

SAR 0.35

2 Soluble Nutrient Test
pH 7.4
Electrical Conductivity 3.01 mmhos/cm
Saturation % 56.58
Sodium (Na) 1.1 Meq/L
Calcium (Ca) 16.4 Meq/L
Magnesium (Mg) 3.9 Meq/L
Potassium (K) 3.2 Meq/L
Ammonium-N (NH4) 14.0 ppm
Phosphate (PO4) 7.2 ppm
Nitrate-N (NO3) 393.4 ppm
Bicarbonate (HCO3) 109.8 ppm
Sulfate (SO4) 110.4 ppm
Chloride (Cl) 12.6 ppm

Boron (B03) 0.4 ppm

SAR 0.35

3 Soluble Nutrient Test pH 7.4 Electrical Conductivity 2.92 mmhos/cm Saturation % 49.43 Sodium (Na) 1.1 Meq/L Calcium (Ca) 17.1 Meg/L Magnesium (Mg) 4.1 Meg/L Potassium (K) 3.5 Meg/L Ammonium-N (NH4) 23.8 ppm Phosphate (PO4) 8.2 ppm Nitrate-N (NO3) 390.6 ppm Bicarbonate (HCO3) 97.6 ppm Sulfate (SO4) 110.4 ppm Chloride (Cl) 12.0 ppm Boron (B03) 0.4 ppm SAR 0.34

Silt Loam-B horizon Baseline

1 Soluble Nutrient Test pH 8.1 Electrical Conductivity 0.88 mmhos/cm Saturation % 50.00 Sodium (Na) 1.3 Meg/L Calcium (Ca) 4.7 Meg/L Magnesium (Mg) 1.0 Meq/L Potassium (K) 0.8 Meq/L Ammonium-N (NH4) 1.4 ppm Phosphate (PO4) 1.0 ppm Nitrate-N (NO3) 83.9 ppm Bicarbonate (HCO3) 103.7 ppm Sulfate (SO4) 33.6 ppm Chloride (Cl) 10.5 ppm Boron (B03) 0.4 ppm SAR 0.77

2 Soluble Nutrient Test 0.8 Hg Electrical Conductivity 1.25 mmhos/cm Saturation % 52.78 Sodium (Na) 1.4 Meq/L Calcium (Ca) 8.5 Meg/L Magnesium (Mg) 1.4 Meq/L Potassium (K) 1.0 Meg/L Ammonium-N (NH4) 5.6 ppm Phosphate (PO4) 2.1 ppm Nitrate-N (NO3) 95.5 ppm Bicarbonate (HCO3) 109.8 ppm Sulfate (SO4) 67.2 ppm Chloride (Cl) 8.8 ppm Boron (B03) 0.4 ppm SAR 0.63

3 Soluble Nutrient Test pH 7.8 Electrical Conductivity 1.12 mmhos/cm Saturation % 52.58 Sodium (Na) 1.4 Meg/L Calcium (Ca) 8.0 Meq/L Magnesium (Mg) 1.3 Meg/L Potassium (K) 0.9 Meq/L Ammonium-N (NH4) 11.2 ppm Phosphate (PO4) 2.1 ppm Nitrate-N (NO3) 73.6 ppm Bicarbonate (HCO3) 97.6 ppm Sulfate (SO4) 67.2 ppm Chloride (Cl) 8.4 ppm Boron (B03) 0.4 ppm SAR 0.65

Table C2 (cont.)

Sandy Loam - A horizon Baseline

1. Soluble Nutrient Test pH 7.9 Electrical Conductivity 0.77 mmhos/cm Saturation % 46.05 Sodium (Na) 0.3 Meg/L Calcium (Ca) 7.9 Meg/L Magnesium (Mg) 1.0 Meq/L Potassium (K) 0.6 Meq/L Ammonium-N (NH4) 16.8 ppm Phosphate (PO4) 4.1 ppm Nitrate-N (NO3) 23.1 ppm Bicarbonate (HCO3) 109.8 ppm Sulfate (SO4) 52.8 ppm Chloride (Cl) 12.7 ppm Boron (B03) 0.4 ppm **SAR 0.14**

2 Soluble Nutrient Test pH 7.9 Electrical Conductivity 0.74 mmhos/cm Saturation %47.73 Sodium (Na) 0.3 Meq/L Calcium (Ca) 7.6 Meg/L Magnesium (Mg) 1.0 Meq/L Potassium (K) 0.6 Meg/L Ammonium-N (NH4) 9.8 ppm Phosphate (PO4) 4.1 ppm Nitrate-N (NO3) 22.3 ppm Bicarbonate (HCO3) 97.6 ppm Sulfate (SO4) 57.6 ppm Chloride (Cl) 16.2 ppm Boron (B03) 0.4 ppm SAR 0.14

3 Soluble Nutrient Test pH 7.8 Electrical Conductivity 0.78 mmhos/cm Saturation % 38.61 Sodium (Na) 0.3 Meq/L Calcium (Ca) 7.8 Meg/L Magnesium (Mg) 1.0 Meq/L Potassium (K) 0.6 Meg/L Ammonium-N (NH4) 16.8 ppm Phosphate (PO4) 4.1 ppm Nitrate-N (NO3) 25.5 ppm Bicarbonate (HCO3) 91.5 ppm Sulfate (SO4) 52.8 ppm Chloride (Cl) 11.6 ppm Boron (B03) 0.4 ppm SAR 0.14

Sandy Loam – B horizon Baseline

1 Soluble Nutrient Test pH 8.2 Electrical Conductivity 0.61 mmhos/cm Saturation % 42.11 Sodium (Na) 0.2 Meq/L Calcium (Ca) 6.2 Meg/L Magnesium (Mg) 0.9 Meq/L Potassium (K) 0.6 Meg/L Ammonium-N (NH4) 8.4 ppm Phosphate (PO4) 3.1 ppm Nitrate-N (NO3) 9.9 ppm Bicarbonate (HCO3) 91.5 ppm Sulfate (SO4) 52.8 ppm Chloride (Cl) 7.6 ppm Boron (B03) 0.4 ppm SAR 0.11

2 Soluble Nutrient Test pH 8.1 Electrical Conductivity 0.48 mmhos/cm Saturation % 38.89 Sodium (Na) 0.3 Meq/L Calcium (Ca) 5.4 Meg/L Magnesium (Mg) 1.0 Meq/L Potassium (K) 0.5 Meg/L Ammonium-N (NH4) 9.8 ppm Phosphate (PO4) 3.1 ppm Nitrate-N (NO3) 7.2 ppm Bicarbonate (HCO3) 91.5 ppm Sulfate (SO4) 43.2 ppm Chloride (Cl) 15.3 ppm Boron (B03) 0.4 ppm SAR 0.17

3 Soluble Nutrient Test pH 8.1 Electrical Conductivity 0.61 mmhos/cm Saturation % 43.48 Sodium (Na) 0.3 Meq/L Calcium (Ca) 6.2 Meq/L Magnesium (Mg) 0.9 Meq/L Potassium (K) 0.6 Meg/L Ammonium-N (NH4) 9.8 ppm Phosphate (PO4) 4.1 ppm Nitrate-N (NO3) 9.9 ppm Bicarbonate (HCO3) 97.6 ppm Sulfate (SO4) 57.6 ppm Chloride (Cl) 10.2 ppm Boron (B03) 0.4 ppm SAR 0.16

Table C3. Soluble soil nutrients, pre-treated samples

Clay Loam - A horizon CBM

1 Soluble Nutrient Test pH 8.0 Electrical Conductivity 3.54 mmhos/cm Saturation % 72.84 Sodium (Na) 18.3 Meg/L Calcium (Ca) 3.9 Meq/L Magnesium (Mg) 0.7 Meg/L Potassium (K) 0.8 Meg/L Ammonium-N (NH4) 12.6 ppm Phosphate (P04) 1.0 ppm Nitrate-N (N03) 61.3 ppm Bicarbonate (HC03) 109.8 ppm Sulfate (S04) 86.4 ppm Chloride (Cl) 591.5 ppm Boron (B03) 0.4 ppm SAR 12.07

2 Soluble Nutrient Test pH 7.9 Electrical Conductivity 2.89 mmhos/cm Saturation % 72.73 Sodium (Na) 15.5 Meg/L Calcium (Ca) 4.2 Meg/L Magnesium (Mg) 0.7 Meq/L Potassium (K) 0.9 Meg/L Ammonium-N (NH4) 11.2 ppm Phosphate (P04) 1.0 ppm Nitrate-N (N03) 55.0 ppm Bicarbonate (HC03) 103.7 ppm Sulfate (S04) 72.0 ppm Chloride (Cl) 584.5 ppm Boron (B03) 0.4 ppm SAR 9.90

Clay Loam - B horizon CBM

1 Soluble Nutrient Test pH 8.4 Electrical Conductivity 2.66 mmhos/cm Saturation % 75.71 Sodium (Na) 15.6 Meg/L Calcium (Ca) 3.0 Meq/L Magnesium (Mg) 0.5 Meg/L Potassium (K) 0.6 Meg/L Ammonium-N (NH4) 8.4 ppm Phosphate (P04) 1.0 ppm Nitrate-N (N03) 67.2 ppm Bicarbonate (HC03) 122.0 ppm Sulfate (S04) 816 ppm Chloride (Cl) 619.5 ppm Boron (B03) 0.4 ppm SAR 11.79

2 Soluble Nutrient Test pH 8.7 Electrical Conductivity 1.19 mmhos/cm Saturation % 81.58 Sodium (Na) 12.0 Meg/L Calcium (Ca) 2.2 Meg/L Magnesium (Mg) 0.4 Meq/L Potassium (K) 0.5 Meg/L Ammonium-N (NH4) 11.2 ppm Phosphate (P04) 2.1 ppm Nitrate-N (N03) 10.3 ppm Bicarbonate (HC03) 128.1 ppm Sulfate (S04) 67.2 ppm Chloride (Cl) 315.0 ppm Boron (B03) 0.4 ppm SAR 10.52

Silt Loam - A horizon - CBM

1 Soluble Nutrient Test pH 8.3 Electrical Conductivity 2.91 mmhos/cm Saturation % 64.63 Sodium (Na) 13.4 Meg/L Calcium (Ca) 5.9 Meq/L Magnesium (Mg) 1.5 Meg/L Potassium (K) 1.9 Meg/L Ammonium-N (NH4) 11.2 ppm Phosphate (P04) 7.2 ppm Nitrate-N (N03) 22.0 ppm Bicarbonate (HC03) 115.9 ppm Sulfate (S04) 81.6 ppm Chloride (Cl) 208.9 ppm Boron (B03) 0.4 ppm SAR 6.97

2 Soluble Nutrient Test pH 8.3 Electrical Conductivity 1.10 mmhos/cm Saturation % 60.26 Sodium (Na) 8.4 Meq/L Calcium (Ca) 4.1 Meg/L Magnesium (Mg) 0.9 Meq/L Potassium (K) 1.1 Meg/L Ammonium-N (NH4) 11.2 ppm Phosphate (P04) 9.3 ppm Nitrate-N (N03) 22.4 ppm Bicarbonate (HC03) 122.0 ppm Sulfate (S04) 62.4 ppm Chloride (Cl) 577.5 ppm Boron (B03) 0.4 ppm SAR 5.31

Silt Loam B horizon CBM

L Soluble Nutrient Test PH 8.2 Electrical Conductivity 2.79 mmhos/cm Saturation % 53.16 Sodium (Na) 15.2 Meg/L Calcium (Ca) 6.6 Meq/L Magnesium (Mg) 1.2 Meg/L Potassium (K) 0.8 Meg/L Ammonium-N (NH4 8.4 ppm Phosphate (P04) 2.1 ppm Nitrate-N (N03) 24.4 ppm Bicarbonate (HC03) 128.1 ppm Sulfate (S04) 67.2 ppm Chloride (Cl) 612.5 ppm Boron (B03) 0.4 ppm SAR 7.70

2 Soluble Nutrient Test pH 8.0 Electrical Conductivity 2.79 mmhos/cm Saturation % 51.96 (Na) 16.1 Meq/L Sodium Calcium (Ca) 5.1 Meg/L Magnesium (Mg) 1.0 Meg/L Potassium (K) 0.8 Meg/L Ammonium-N (NH4) 8.4 ppm Phosphate (P04) 2.1 ppm Nitrate-N (N03) 82.7 ppm Bicarbonate (HC03) 122.0 ppm Sulfate (S04) 81.6 ppm Chloride (Cl) 80.5 ppm Boron (B03) 0.4 ppm SAR 9.22

Table C3 (cont.)

Sandy Loam - A horizon CBM

1 Soluble Nutrient Test pH 8.6 Electrical Conductivity 2.23 mmhos/cm Saturation % 45.31 Sodium- (Na) 13.2 Meg/L Calcium (Ca) 1.9 Meq/L Magnesium (Mg) 0.4 Meg/L Potassium (K) 0.5 Meq/L Ammonium-N (NH4) 11.2 ppm Phosphate (P04) 7.2 ppm Nitrate-N (N03) 9.4 ppm Bicarbonate (HC03) 152.5 ppm Sulfate (S04) 72.0 ppm Chloride (Cl) 518.0 ppm Boron (B03) 0.4 ppm SAR 12.31

2 Soluble Nutrient Test pH 8.7 Electrical Conductivity 2.39 mmhos/cm Saturation % 41.79 Sodium (Na) 14.2 Meg/L Calcium (Ca) 2.6 Meg/L Magnesium (Mg) 1.0 Meq/L Potassium (K) 0.8 Meg/L Ammonium-N (NH4) 12.6 ppm Phosphate (P04) 8.2 ppm Nitrate-N (N03) 16.2 ppm Bicarbonate (HC03) 183.0 ppm Sulfate (S04) 72.0 ppm Chloride (Cl) 518.0 ppm Boron (B03) 0.4 ppm SAR 10.58

Sandy Loam - B horizon CBM

1 Soluble Nutrient Test pH 9.1 Electrical Conductivity 2.63 mmhos/cm Saturation % 38.55 Sodium (Na) 14.1 Meq/L Calcium (Ca) 2.8 Meq/L Magnesium (Mg) 0.8 Meg/L Potassium (K) 0.6 Meq/L Ammonium-N (NH4) 8.4 ppm Phosphate (P04) 5.2 ppm Nitrate-N (N03) 7.7 ppm Bicarbonate (HC03) 140.3 ppm Sulfate (S04) 72.0 ppm Chloride (Cl) 651.0 ppm Boron (B03) 0.4 ppm SAR 10.51

2 Soluble Nutrient Test pH 9.0 Electrical Conductivity 2.82 mmhos/cm Saturation % 39.51 Sodium (Na) 15.9 Meg/L Calcium (Ca) 2.3 Meg/L Magnesium (Mg) 0.6 Meq/L Potassium (K) 0.6 Meg/L Ammonium-N (NH4) 9.8 ppm Phosphate (P04) 4.1 ppm Nitrate-N (N03) 23.5 ppm Bicarbonate (HC03) 122.0 ppm Sulfate (S04) 72.0 ppm Chloride (Cl) 591.5 ppm Boron (B03) 0.4 ppm SAR 13.20

Clay Loam – A horizon PR

I Soluble NutrientTest PH 8.2 Electrical Conductivity 1.22 mmhos/cm Saturation % 71.88 Sodium (Na) 4.5 Meq/L Calcium (Ca) 5.3 Meq/L Magnesium (Mg) 1.1 Meq/L Potassium (K) 1.4 Meq/L Ammonium-N (NH4) 15.4 ppm Phosphate (P04) 3.1 ppm Nitrate-N (N03) 45.5 ppm Bicarbonate (HC03) 97.6 ppm Sulfate (S04) 177.6 ppm Chloride (Cl) 105.0 ppm Boron (B03) 0.4 ppm SAR 2.52

2 Soluble Nutrient Test pH 8.2 Electrical Conductivity 1.43 mmhos/cm Saturation % 66.67 Sodium (Na) 5.3 Meq/L Calcium (Ca) 7.0 Meg/L Magnesium (Mg) 1.3 Meq/L Potassium (K) 1.6 Meg/L Ammonium-N (NH4) 15.4 ppm Phosphate (P04) 3.1 ppm Nitrate-N (N03) 39.2 ppm Bicarbonate (HC03) 85.4 ppm Sulfate (S04) 230.4 ppm Chloride (Cl) 107.8 ppm Boron (B03) 0.4 ppm SAR 2.60

Clay Loam – B horizon PR

1 Soluble Nutrient Test pH 8.1 Electrical Conductivity 1.55 mmhos/cm Saturation % 66.67 Sodium (Na) 6.4 Meg/L Calcium (Ca) 5.9 Meq/L Magnesium (Mg) 1.3 Meg/L Potassium (K) 1.4 Meq/L Ammonium-N (NH4) 14.0 ppm Phosphate (P04) 3.1 ppm Nitrate-N (N03) 56.6 ppm Bicarbonate (HC03) 91.5 ppm Sulfate (SO4) 225.6 ppm Chloride (Cl) 88.5 ppm Boron (B03) 0.4 ppm **SAR 3.37**

2 Soluble Nutrient Test pH 8.0 Electrical Conductivity 1.51 mmhos/cm Saturation % 59.46 Sodium (Na) 5.7 Meg/L Calcium (Ca) 6.7 Meq/L Magnesium (Mg) 1.3 Meg/L Potassium (K) 1.6 Meg/L Ammonium-N (NH4) 18.2 ppm Phosphate (P04) 4.1 ppm Nitrate-N (N03) 68.0 ppm Bicarbonate (HC03) 122.0 ppm Sulfate (S04) 206.4 ppm Chloride (Cl) 556.5 ppm Boron (B03) 0.4 ppm SAR 2.85

Table C3 (cont.)

Silt Loam - A horizon PR

1 Soluble Nutrient Test PH 7.8 Electrical Conductivity 3.09 mmhos/cm Saturation % 54.76 Sodium ' (Na) 4.2 Meg/L Calcium (Ca) 8.6 Meq/L Magnesium (Mg) 2.5 Meg/L Potassium (K) 2.8 Meq/L Ammonium-N (NH4) 22.4 ppm Phosphate (P04) 10.3 ppm Nitrate-N (N03) 59.4 ppm Bicarbonate (HC03) 91.5 ppm Sulfate (S04).187.2 ppm Chloride (Cl) 630.5' ppm Boron (B03) 0.4 ppm SAR 1.78

2 Soluble Nutrient Test pH 8.2 Electrical Conductivity 1.73 mmhos/cm Saturation % 48.65 Sodium (Na) 5.0 Meg/L Calcium (Ca) 10.6 Meq/L Magnesium (Mg) 3.1 Meq/L Potassium (K) 3.2 Meq/L Ammonium-N (NH4) 22.4 ppm Phosphate (P04) 11.3 ppm Nitrate-N (N03) 94.5 ppm Bicarbonate (HC03) 91.5 ppm Sulfate (S04) 216.0 ppm Chloride (Cl) 107.8 ppm Boron (B03) 0.4 ppm SAR 1.91

Silt Loam B horizon PR

1 Soluble NutrientTest pH 8.3 Electrical Conductivity 1.97 mmhos/cm Saturation % 39.53 Sodium (Na) 5.8 Meg/L Calcium (Ca) 10.2 Meq/L Magnesium (Mg) 2.7 Meq/L Potassium (K) 1.9 Meg/L Ammonium-N (NH4) 15.4 ppm Phosphate (P04) 4.1 ppm Nitrate-N (N03) 48.3 ppm Bicarbonate (HC03) 97.6 ppm Sulfate (S04) 278.4 ppm Chloride (Cl) 160.7 ppm Boron (B03) 0.4 ppm **SAR 2.28**

2 Soluble Nutrient Test pH 8.2 Electrical Conductivity 1.54 mmhos/cm Saturation % 43.90 Sodium (Na) 4.8 Meg/L Calcium (Ca) 8.7 Meg/L Magnesium (Mg) 2.0 Meq/L Potassium (K) 1.6 Meg/L Ammonium-N (NH4) 12.6 ppm Phosphate (P04) 3.1 ppm Nitrate-N (N03) 34.3 ppm Bicarbonate (HC03) 91.5 ppm Sulfate (S04) 230.4 ppm Chloride (Cl) 107.4 ppm Boron (B03) 0.4 ppm **SAR 2.08**

Sandy Loam – A horizon PR

1 Soluble Nutrient Test pH 8.3 Electrical Conductivity 0.94 mmhos/cm Saturation %49.18 Sodium (Na) 3.1 Meg/L Calcium (Ca) 3.0 Meq/L Magnesium (Mg) 0.8 Meg/L Potassium (K) 1.1 Meg/L Ammonium-N (NH4) 22.4 ppm Phosphate (P04) 3.1 ppm Nitrate-N (N03) 10.0 ppm Bicarbonate (HC03) 140.3 ppm Sulfate (S04) 129.6 ppm Chloride (Cl) 102.9 ppm Boron (B03) 0.4 ppm SAR 2.25

2 Soluble Nutrient Test pH 8.3 Electrical Conductivity 1.18 mmhos/cm Saturation % 40.85 Sodium (Na) 3.9 Meq/L Calcium (Ca) 3.8 Meg/L Magnesium (Mg) 1.1 Meq/L Potassium (K) 1.3 Meg/L Ammonium-N (NH4) 18.2 ppm Phosphate (P04) 3.1 ppm Nitrate-N (N03) 8.8 ppm Bicarbonate (HC03) 109.8 ppm Sulfate (S04) 172.8 ppm Chloride (Cl) 129.2 ppm Boron (B03) 0.4 ppm SAR 2.49

Sandy Loam – B horizon PR

1 Soluble Nutrient Test pH 8.5 Electrical Conductivity 1.03 mmhos/cm Saturation % 37.21 Sodium (Na) 3.4 Meg/L Calcium (Ca) 3.7 Meq/L Magnesium (Mg) 1.2 Meq/L Potassium (K) 1.3 Meq/L Ammonium-N (NH4) 15.4 ppm Phosphate (P04) 3.1 ppm Nitrate-N (N03) 8.4 ppm Bicarbonate (HC03) 122.0 ppm Sulfate (S04) 144.0 ppm Chloride (Cl) 123.2 ppm Boron (B03) 0.4 ppm SAR 2.17

2 Soluble Nutrient Test pH 8.5 Electrical Conductivity 1.19 mmhos/cm Saturation % 32.97 Sodium (Na) 3.9 Meg/L Calcium (Ca) 3.8 Meg/L Magnesium (Mg) 1.2 Meq/L Potassium (K) 1.5 Meg/L Ammonium-N (NH4) 15.4 ppm Phosphate (P04) 3.1 ppm Nitrate-N (N03) 8.0 ppm Bicarbonate (HC03) 122.0 ppm Sulfate (S04) 187.2 ppm Chloride (Cl) 136.2 ppm Boron (B03) 0.4 ppm **SAR 2.4**

APPENDIX D

STATISTICAL TABLES FROM SPSS, SOIL COLUMNS EXPERIMENT

Table D1. ANOVA results for water flux measured using pre-treatment quality (CBM or PR) water for a) sandy loam, B) silt loam, c) clay loam soils.

a) Dependent Variable: lnFluxPreTreatmentWaterQuality

Source	Type III Sum of Squares	df	Mean Square	F	Sig.
Corrected Model	12.129(a)	15	.809	55.301	.000
Intercept	14.648	1	14.648	1001.813	.000
Horizon	4.686	1	4.686	320.467	.000
PreTreatmentWaterQuality	2.363	1	2.363	161.636	.000
SupplyPressure	4.805	3	1.602	109.544	.000
Horizon * PreTreatmentWaterQuality	.251	1	.251	17.177	.000
Horizon * SupplyPressure	.001	3	.000	.029	.993
PreTreatmentWaterQuality * SupplyPressure	.022	3	.007	.502	.682
Horizon * PreTreatmentWaterQuality * SupplyPressure	.000	3	8.18E-005	.006	.999
Error	.936	64	.015		
Total	27.713	80			
Corrected Total	13.065	79			

a R Squared = 0.928 (Adjusted R Squared = 0.912)

b) Dependent Variable: lnFluxPreTreatmentWaterQuality

	Type III Sum		Mean		
Source	of Squares	df	Square	F	Sig.
Corrected Model	110.520(a)	15	7.368	57.187	.000
Intercept	160.699	1	160.699	1247.287	.000
Horizon	.013	1	.013	.103	.749
PreTreatmentWaterQuality	.037	1	.037	.285	.595
SupplyPressure	104.035	3	34.678	269.161	.000
Horizon * PreTreatmentWaterQuality	2.955	1	2.955	22.939	.000
Horizon * SupplyPressure	1.486	3	.495	3.845	.014
PreTreatmentWaterQuality * SupplyPressure	1.233	3	.411	3.189	.029
Horizon * PreTreatmentWaterQuality * SupplyPressure	.760	3	.253	1.967	.128
Error	8.246	64	.129		
Total	279.465	80			
Corrected Total	118.765	79			

a R Squared = 0.931 (Adjusted R Squared = 0.914)

Table D1 (cont.)

c) Dependent Variable: lnFluxPreTreatmentWaterQuality

Source	Type III Sum of Squares	df	Mean Square	F	Sig.
Corrected Model	119.961(a)	15	7.997	34.821	.000
Intercept	231.668	1	231.668	1008.686	.000
Horizon	.226	1	.226	.985	.325
PreTreatmentWaterQuality	5.321	1	5.321	23.168	.000
SupplyPressure	108.110	3	36.037	156.905	.000
Horizon * PreTreatmentWaterQuality	3.133	1	3.133	13.640	.000
Horizon * SupplyPressure	1.248	3	.416	1.811	.154
PreTreatmentWaterQuality * SupplyPressure	1.486	3	.495	2.157	.102
Horizon * PreTreatmentWaterQuality * SupplyPressure	.437	3	.146	.634	.596
Error	14.699	64	.230		
Total	366.328	80			
Corrected Total	134.661	79			

a R Squared = 0.891 (Adjusted R Squared = 0.865)

Table D2. ANOVA results for relative mean difference in water flux measured using pretreatment (CBM or PR) and DI water for a) sandy loam, b) silt loam, c) clay loam soils.

a) Dependent Variable: 1/FractionFluxDiff

Course	Type III Sum	4t	Mean	E	Cia
Source	of Squares	df	Square	F	Sig.
Corrected Model	.045(a)	16	.003	7.878	.000
Intercept	7.496	1	7.496	21195.638	.000
Horizon	.030	1	.030	84.097	.000
PreTreatmentWaterQuality	.004	1	.004	12.006	.001
SupplyPressure	.008	4	.002	5.940	.000
Horizon * PreTreatmentWQ	6.62E-005	1	6.62E-005	.187	.667
Horizon * SupplyPressure	5.21E-005	3	1.74E-005	.049	.985
PreTreatmentWQ * SupplyPressure	.001	3	.000	.628	.599
Horizon * PreTreatmentWQ * SupplyPressure	.000	3	8.34E-005	.236	.871
Error	.022	63	.000		
Total	13.854	80			
Corrected Total	.067	79			

a R Squared = 0.667 (Adjusted R Squared = 0.582)

Table D2 (cont.)

b) Dependent Variable: 1/FractionFluxDiff

	Type III Sum of	10	Mean	Б	a:
Source	Squares	df	Square	F	Sig.
Corrected Model	2.266(a)	15	.151	.914	.553
Intercept	19.880	1	19.880	120.354	.000
Horizon	.374	1	.374	2.263	.137
PreTreatmentWaterQuality	.066	1	.066	.401	.529
SupplyPressure	.447	3	.149	.901	.446
Horizon * PreTreatmentWQ	.067	1	.067	.405	.527
Horizon * SupplyPressure	.259	3	.086	.522	.669
PreTreatmentWQ * SupplyPressure	.507	3	.169	1.023	.388
Horizon * PreTreatmentWQ * SupplyPressure	.547	3	.182	1.103	.354
Error	10.572	64	.165		
Total	32.717	80			
Corrected Total	12.837	79			

a R Squared = 0.177 (Adjusted R Squared = -0.017)

c) Dependent Variable: 1/FractionFluxDiff

	Type III Sum of		Mean		
Source	Squares	df	Square	F	Sig.
Corrected Model	1.077(a)	15	.072	1.983	.031
Intercept	18.023	1	18.023	497.552	.000
Horizon	.026	1	.026	.710	.403
PreTreatmentWaterQuality	.009	1	.009	.247	.621
SupplyPressure	.243	3	.081	2.236	.093
Horizon * PreTreatmentWQ	.245	1	.245	6.765	.012
Horizon * SupplyPressure	.302	3	.101	2.779	.048
PreTreatmentWQ * SupplyPressure	.196	3	.065	1.807	.155
Horizon * PreTreatmentWQ * SupplyPressure	.056	3	.019	.519	.671
Error	2.318	64	.036		
Total	21.418	80			
Corrected Total	3.396	79			

a R Squared = 0.317 (Adjusted R Squared = 0.157)

Table D3. Multiple comparisons results for relative mean flux decrease measured using DI water, by horizon-pre-treatment water quality pairs in the clay loam.

Dependent Variable: 1/(2+FractionDiffFlux)

Tamhane

(I) Horizon*PreTrtWQ	(J) Horizon*PreTrtWQ	Mean Difference (I-J)	Std. Error	Sig.
A-CBM	A-PR	090	.055	.527
	B-CBM	147	.071	.282
	B-PR	015	.019	.969
A-PR	A-CBM	.090	.055	.527
	B-CBM	057	.089	.988
	B-PR	.075	.056	.721
B-CBM	A-CBM	.147	.071	.282
	A-PR	.057	.089	.988
	B-PR	.132	.072	.401
B-PR	A-CBM	.015	.019	.969
	A-PR	075	.056	.721
	B-CBM	132	.072	.401

Based on observed means.

Table D4. ANOVA results among soils comparing mean flux decrease measured using DI water.

Dependent Variable: 1/(2+FractionDiffFlux)

	Type III Sum of		Mean		
Source	Squares	df	Square	F	Sig.
Corrected Model	3.682(a)	47	.078	1.165	.236
Intercept	51.394	1	51.394	764.192	.000
Soil	.295	2	.147	2.193	.114
Horizon	.131	1	.131	1.954	.164
PreTreatmentWQ	.017	1	.017	.252	.616
SupplyPressure	.374	3	.125	1.853	.139
Soil * Horizon	.299	2	.150	2.225	.111
Soil * PreTreatmentWQ	.062	2	.031	.462	.631
Horizon * PreTreatmentWQ	.192	1	.192	2.855	.093
Soil * Horizon * PreTreatmentWQ	.120	2	.060	.892	.411
Soil * SupplyPressure	.324	6	.054	.802	.569
Horizon * SupplyPressure	.203	3	.068	1.006	.391
Soil * Horizon * SupplyPressure	.358	6	.060	.887	.506
PreTreatmentWQ * SupplyPressure	.100	3	.033	.497	.685
Soil * PreTreatmentWQ * SupplyPressure	.604	6	.101	1.496	.181
Horizon * PreTreatmentWQ * SupplyPressure	.232	3	.077	1.151	.330
Soil * Horizon * PreTreatmentWQ * SupplyPressure	.371	6	.062	.920	.482
Error	12.913	192	.067		
Total	67.989	240			
Corrected Total	16.595	239			

a R Squared = 0.222 (Adjusted R Squared =0.031)

Table D5. Jonckheere-Terpstra non-parametric test results comparing mean relative water

flux measurements by soil type.

	Soil#		N	Mean Rank
SL	1.00		80	107.65
SiL	2.00		80	130.89
CL	3.00		80	122.96
	Total	I	240	

Jonckheere-Terpstra Test(a)

	1/(2+FractionDiffFlux)
Number of Levels in Soil#	3
N	240
Observed J-T Statistic	10442.000
Mean J-T Statistic	9600.000
Std. Deviation of J-T Statistic	585.605
Std. J-T Statistic	1.438
Asymp. Sig. (2-tailed)	.150

a Grouping Variable: Soil#

Table D6. Jonckheere-Terpstra non-parametric test results comparing mean relative water flux measurements by soil type, by pre-treatment water quality interaction.

	SoilPreTrtWQ#	N	Mean Rank
SiL-CBM	1.00	40	140.58
SiL-PR	2.00	40	121.20
CL-CBM	3.00	40	111.88
CL-PR	4.00	40	134.05
SL-CBM	5.00	40	96.10
SL-PR	6.00	40	119.20
	Total	240	

Jonckheere-Terpstra Test(a)

1 \(\frac{1}{2}\)	
	1/(2+FractionDiffFlux)
Number of Levels in SoilPreTrtWQ#	6
N	240
Observed J-T Statistic	10988.000
Mean J-T Statistic	12000.000
Std. Deviation of J-T Statistic	612.644
Std. J-T Statistic	-1.652
Asymp. Sig. (2-tailed)	.099

a Grouping Variable: SoilPreTrtWQ#

Table D7. Means and standard errors for relative mean infiltration flux (cm/h) for clay loam, silt loam, and sandy loam soils. Statistics are for untransformed measurements.

Soil	Mean	Std. Error
CL	0.285	0.052
SiL	0.254	0.050
SL	0.420	0.018

Table D8. Means and standard errors for relative mean infiltration flux (cm/h) for clay loam, silt loam and sandy loam soils at four soil-supply pressures. Statistics are for untransformed measurements.

Soil-Supply Pressure	Mean	Std. Error
CL-0.5	0.589	0.052
CL-2	0.335	0.096
CL-6	0.111	0.098
CL-12	0.105	0.120
SiL-0.5	0.448	0.091
SiL-2	0.245	0.107
SiL-6	0.161	0.114
SiL-12	0.162	0.072
SL-0.5	0.475	0.032
SL-2	0.462	0.035
SL-6	0.412	0.037
SL-12	0.331	0.034

APPENDIX E HYDRUS-1D INPUT DATA, MODEL SIMULATION STUDY

Table E1. Soil hydraulic parameter values (van Genuchten 1980) used for Hydrus-1D simulations

Soil	Scenario	θr	θs	α	n	Ks
				(1/cm)		(cm/h)
Fine Sandy Loam	Baseline	0.0350	0.4700	0.0120	2.0361	4.4208
	1	0.0347	0.4747	0.0108	2.0564	3.9787
	2	0.0315	0.4935	0.0036	2.1379	3.3156
	3	0.0280	0.5170	0.0042	2.2397	2.6525
	4	0.0245	0.5405	0.0048	2.3415	2.2104
	5	0.0210	0.6110	0.0060	2.4433	1.3262
Silt Loam	Baseline	0.0766	0.5300	0.0164	1.6335	0.4500
	1	0.0758	0.5353	0.0181	1.6498	0.4050
	2	0.0689	0.5565	0.0246	1.6743	0.3375
	3	0.0460	0.5830	0.0288	1.7152	0.2700
	4	0.0306	0.6095	0.0575	1.7968	0.1665
	5	0.0153	0.6890	0.0657	1.9602	0.1125
Silty Clay Loam	Baseline	0.0950	0.5500	0.0138	1.7125	0.4161
	1	0.0979	0.5555	0.0124	1.7143	0.3745
	2	0.1093	0.5775	0.0134	1.7160	0.2913
	3	0.1235	0.6050	0.0130	1.7177	0.2080
	4	0.1378	0.6325	0.0125	1.7194	0.1373
	5	0.1520	0.7150	0.0121	1.7211	0.0624
Silty Clay	Baseline	0.1150	0.5700	0.0127	1.5885	0.0200
-	1	0.1185	0.5757	0.0114	1.5901	0.0180
	2	0.1323	0.5985	0.0123	1.5917	0.0150
	3	0.1495	0.6270	0.0119	1.5933	0.0100
	4	0.1668	0.6555	0.0116	1.5949	0.0050
	5	0.2185	0.7410	0.0112	1.5981	0.0010

Table E2. Simulated water balance components for baseline soil conditions and for five scenarios of increasing sodicity in fine sandy loam, silt loam, silty clay loam, and silty clay soils. All values, excluding the RWU/ET ratio, are in cm.

soils. All values, excluding the RWU/ET ratio, are in cm.							
Soil	Irrig. Method						
Fine Sandy Loam	Sprinkler	Baseline	1	2	3	4	5
Precip. + Irrig. =	135.8 cm						
Root Water Uptake		43.1	43.1	43.1	43.1	43.1	43.1
Deep Drainage		40.2	40.3	49.7	47.0	44.6	37.6
Change in Soil Water Storage		9.9	9.8	0.4	3.0	5.4	12.4
Runoff		0.0	0.0	0.4	0.0	0.0	0.0
		42.8	42.8	42.8	42.8	42.8	42.8
Evaporation	T-4-1						
	Total	135.9	135.9	135.9	133.9	135.9	133.9
ET		85.9	85.9	85.9	85.9	85.9	85.9
RWU/ET		0.50	0.50	0.50	0.50	0.50	0.50
Infiltration			135.8	135.8		135.8	
Fine Sandy Loam	Flood	Baseline	1	2	3	4	5
Precip. + Irrig. =	63.6.cm						
Root Water Uptake		28.4	28.9	32.5	33.2	33.3	34.0
•		18.4	18.4	20.8	19.1	18.0	13.9
Deep Drainage		-1.9			-10.9	-8.9	-4.7
Change in Soil Water Storage Runoff			-2.3	-12.7			
		0.0	0.0	0.0	0.0	0.0	0.0
Evaporation	T . 1	18.0	18.3	22.7	21.9	21.0	20.2
	Total	62.9	63.3	63.4	63.4	63.3	63.4
Cum ET (cm)		46.4	47.2	55.2	55.1	54.3	54.3
RWU/ET		0.61	0.61	0.59	0.60	0.61	0.63
Infiltration		63.6	63.6	63.6	63.6	63.6	63.6
(Table continued)							

(Table continued)

Table E2 (cont.)

Table E2 (cont.) Soil	Irrig. Method Simulated Conditions						
Silt Loam	Sprinkler	Baseline	1	2	3	4	5
Precip. + Irrig. =	1	Duscime	1		3	•	5
Treesp. Tilig.	133.0 c m						
Root Water Uptake		43.1	43.1	42.9	42.1	11.9	4.3
Deep Drainage		24.3	23.0	19.2	14.9	36.7	33.6
Change in Soil Water Storage		25.7	27.0	31.0	34.7	45.1	52.8
Runoff		0.0	0.0	0.0	0.0	0.0	0.0
Evaporation		42.8	42.8	42.8	42.8	42.4	42.4
	Total	135.8	135.8	135.8	134.5	136.1	133.1
ET		85.9	85.9	85.7	84.9	54.3	46.7
RWU/ET		0.50	0.50	0.50	0.50	0.22	0.09
T. (71)		1250	1250	1250	1050	1250	1250
Infiltration	721 1		135.8			135.8	
Silt Loam	Flood	Baseline	1	2	3	4	5
Precip. + Irrig. =	63.6.cm						
Root Water Uptake		31.5	31.3	30.8	30.6	24.3	20.6
Deep Drainage		0.8	0.1	0.0	0.0	0.0	0.0
Change in Soil Water Storage		5.2	4.8	3.3	1.2	-1.2	-1.4
Runoff		8.1	9.8	12.6	15.3	24.9	27.2
Evaporation		18.0	17.6	16.8	16.5	15.6	17.1
-	Total	63.6	63.6	63.6	63.6	63.6	63.6
ET		49.5	48.8	47.6	47.1	39.9	37.7
RWU/ET		0.64	0.64	0.65	0.65	0.61	0.55
Infiltration (Table 2 anti-man 4)		55.1	53.1	49.0	46.0	39.0	35.9

(Table continued)

Table E2 (cont.)

Table E2 (cont.)							
Soil	Irrig. Method					<u> </u>	
Silty Clay Loam	Sprinkler	Baseline	1	2	3	4	5
Precip. + Irrig. =	135.8 cm						
Root Water Uptake		42.8	43.1	43.1	43.0	43.0	41.0
Deep Drainage		23.6	23.5	21.2	18.5	15.6	8.2
Change in Soil Water Storage		26.3	26.6	28.9	31.5	34.5	44.0
Runoff		0.0	0.0	0.0	0.0	0.0	0.0
Evaporation		42.8	42.8	42.8	42.8	42.8	42.8
	Total	135.6	135.9	135.9	135.9	135.9	135.9
Cum ET (cm)		85.6	85.9	85.9	85.8	85.8	83.8
Cum RWU/ET		0.50	0.50	0.50	0.50	0.50	0.49
Infiltration		135.8	135.8	135.8	135.8	135.8	135.6
Silty Clay Loam	Flood	Baseline	1	2	3	4	5
Precip. + Irrig. =	63.6.cm						
Root Water Uptake		31.1	31.8	31.8	32.1	32.7	34.3
Deep Drainage		3.9	5.0	3.8	2.2	0.9	0.0
Change in Soil Water Storage		8.5	8.7	10.1	11.1	12.0	11.4
Runoff		0.0	0.0	0.0	0.0	0.0	0.0
Evaporation		18.3	18.6	18.5	18.6	18.6	19.0
	Total	61.8	64.1	64.1	64.0	64.2	64.7
ET		49.4	50.4	50.2	50.7	51.3	53.3
RWU/ET		0.63	0.63	0.63	0.63	0.64	0.64
Infiltration		45.4	45.4	44.8	43.8	42.4	40.3
(T. 1.1 1)							

(Table continued)

Table E2 (cont.)

Soil	Irrig. Method	Simulated Conditions					
Silty Clay	Sprinkler	Baseline	1	2	3	4	5
Precip. + Irrig. =	135.8 cm						
Root Water Uptake		16.3	18.9	16.9	19.8	24.5	17.6
Deep Drainage		8.7	4.6	0.0	0.0	0.0	0.0
Change in Soil Water Storage		40.8	40.7	40.2	27.8	12.8	6.9
Runoff		30.8	32.8	40.4	50.9	62.8	79.5
Evaporation		39.2	38.9	38.4	37.4	35.7	31.8
	Total	135.8	135.8	135.8	135.8	135.8	135.8
ET		55.5	57.7	55.3	57.1	60.2	49.4
RWU/ET		0.29	0.33	0.31	0.35	0.41	0.36
Infiltration		93.9	92.0	84.2	73.6	62.1	44.7
Silty Clay	Flood	Baseline	1	2	3	4	5
Precip. + Irrig. =	63.6.cm						
Root Water Uptake		31.5	31.8	31.8	32.1	28.5	24.3
Deep Drainage		0.0	0.0	0.0	0.0	0.0	0.0
Change in Soil Water Storage		8.5	7.9	6.9	4.5	2.9	2.8
Runoff		5.6	6.0	7.4	9.8	14.8	20.5
Evaporation		18.0	18.0	17.5	17.2	17.4	15.9
	Total	63.6	63.6	63.6	63.6	63.6	63.6
ET		49.5	49.7	49.3	49.3	45.9	40.2
RWU/ET		0.64	0.64	0.64	0.65	0.62	0.60
Infiltration		36.2	35.8	34.3	32.1	28.4	22.8